TRIBHUVAN UNIVERSITY

INSTITUTE OF ENGINEERING

PULCHOWK CAMPUS

THESIS NO: 076/MSPSE/16

The Optimal Placement of a Photovoltaic-integrated Dynamic Voltage Restorer for the enhancement of Power Quality within the Distribution System.

A Case Study of 11kV Tanahusur Radial Distribution Feeder and 11kV Simara Industrial Feeder

By

Prabin Dhakal

076 MSPSE 016

Submitted to

A THESIS

SUBMITTED TO THE DEPARTMENT OF ELECTRICAL ENGINEERING

IN PARTIAL FULFILLMENT OF THE REQUIREMENTS FOR

THE DEGREE OF MASTER OF SCIENCE IN

POWER SYSTEM ENGINEERING

DEPARTMENT OF ELECTRICAL ENGINEERING

LALITPUR, NEPAL

December 2023

The Optimal Placement of a Photovoltaic-integrated Dynamic Voltage Restorer for the enhancement of Power Quality within the Distribution System.

A Case Study of 11kV Tanahusur Radial Distribution Feeder and 11kV Simara Industrial Feeder

By
Prabin Dhakal

076 MSPSE 016

Thesis Supervisors:

Associate Professor Basanta Gautam (Ph.D)

Institute of Engineering, Pulchowk Campus

A thesis submitted to the Department of Electrical Engineering in partial fulfillment of the requirements for the degree of

Master of Science in Power System Engineering

Department of Electrical Engineering

Institute of Engineering, Pulchowk Campus

Tribhuvan University

Lalitpur, Nepal

December 2023

COPYRIGHT©

Accredited by University Grants Commission (UGC) Nepal 2020

त्रिभुवन विश्वविद्यालय
TRIBHUVAN UNIVERSITY
इन्जिनियरिङ्ग अध्ययन संस्थान
INSTITUTE OF ENGINEERING
पुल्चोक क्याम्पस
PULCHOWK CAMPUS
DEPARTMENT OF ELECTRICAL ENGINEERING
Pulchowk, Lalitpur

CERTIFICATE OF APPROVAL

The undersigned, certify that they have reviewed and hereby recommend to the esteemed Institute of Engineering for acceptance , a thesis titled "***The Optimal Placement of a Photovoltaic-integrated Dynamic Voltage Restorer for the Enhancement of Power Quality within the Distribution System: A Case Study of the 11kV Tanahusur Radial Distribution Feeder and 11kV Simara Industrial Feeder***" submitted by **Mr.Prabin Dhakal** in partial fulfillment of the requirements for the degree of Master in Power System Engineering.

Assoc. Prof. Dr. Basanta Kumar Gautam
Supervisor
Department of Electrical Engineering

Kedar Raj Silwal
Manager, External Examiner
Nepal Electricity Authority

Assoc. Prof. Dr. Basanta Kumar Gautam
Program Co-ordinator
Power System Engineering

Asst. Prof. Yubaraj Adhikari
Head of Department
Department of Electrical Engineering

December 2023

ABSTRACT

In the context of power distribution, maintaining high Power Quality (PQ) is crucial. Voltage fluctuations like sags, swells, and harmonics can disrupt PQ. To address these issues, a sophisticated solution involving a Dynamic Voltage Restorer (DVR) has been devised. The DVR serves as a dynamic energy store, utilizing solar energy from Photovoltaic (PV) cells. To optimize this process, a smart algorithm called Maximum Power Point Tracking (MPPT) is integrated with Incremental Conductance method. This algorithm ensures that solar energy is harnessed efficiently and the system operates at its peak performance. To manage reactive power generation, a Voltage Source Inverter (VSI) is introduced. This component utilizes Pulse Width Modulation (PWM) techniques for precise control, enabling it to inject reactive power into the grid. For improved control precision, a Space Vector Pulse Width Modulation (SVPWM) strategy is implemented. This enhances the synchronization of voltage injection, mitigating phase angle mismatches and reducing harmonic distortions. Ensuring synchronization and power factor correction is achieved through a Proportional Resonant (PR) controller. This controller, when cascaded with a harmonic compensator, effectively minimizes undesirable harmonic components in the system's output current. This aids in maintaining a consistent power factor and a higher quality power output. The overall system's performance and effectiveness are evaluated through simulation using MATLAB 2023a software. This comprehensive solution not only tackles PQ issues but also harnesses solar energy optimally, contributing to a more stable and efficient power distribution system. In this thesis, an IEEE-13 Node Test Feeder, a section of 11kV Tanahusur feeder of Tanahu District as well as 11 kV industrial feeder of Simara distribution center is modeled and analyzed in MATLAB programming environment to get the optimized results. The optimization for the placement of DVR is done using System Average RMS variation Frequency index (SARFI) method. Simulation results with DVR placed in the optimal location for all three systems show a consequential enhancementin voltage profile of systems with DVR being able to restore the voltage at neighboring buses to more than 98% of the nominal rated voltage at each bus.

ACKNOWLEDGEMENT

I would like to extend my heartfelt gratitude to my esteemed thesis supervisor, Prof. Dr. Basanta Kumar Gautam, for his exceptional guidance, invaluable mentorship, and unwavering encouragement throughout the entirety of this research endeavor. Prof. Gautam's dedication to my academic and personal growth has been a source of inspiration and motivation.

I would also like to express my sincere appreciation to the entire faculty and staff of the Department of Electrical Engineering at the Institute of Engineering (IOE), Pulchowk. Their support and contributions have been instrumental in shaping the quality of this work.

I am deeply indebted to the dedicated team at the NEA Simara distribution center, NEA Tanahu Distribution Centre and the Parwanipur 132kV/11kV Sub-station for their generous assistance in data collection. Their collaboration has been pivotal in ensuring the accuracy and comprehensiveness of this research.

Last but certainly not least, I wish to convey my profound gratitude to my cherished friends and loving family for their unwavering support and boundless love throughout this academic journey. Their encouragement has been my pillar of strength, and I am truly thankful for their presence in my life.

TABLE OF CONTENTS

LIST OF FIGURES AND TABLES

LIST OF ABBREVIATIONS

SYMBOLS	DEFINITION
PQ	Power Quality
DVR	Dynamic Voltage Restorer
PV	Photo Voltaic
THD	Total Harmonic Distortion
DSTATCOM	Distribution Static Compensator
PI	Proportional Integral
PWM	Pulse Width Modulated
SVPWM	Space Vector Pulse width Modulation
PR	Proportional Resonant
FACTS	Flexible AC Transmission Systems
VSC	Voltage Source Converter
BIPV	Building Integrated Photovoltaics
BESS	Battery Energy Storage System
SRF	Synchronous Reference Frame
VPCC	Source Voltage
VDVR	Injection Voltage
VDC	DC Link Voltage
IEEE	Institute of Electrical and Electronics Engineers

CPDs	Custom Power Devices
SARFI	System Average RMS Variation Frequency Index
SSSC	Static Synchronous Series Compensator

CHAPTER 1: INTRODUCTION

1.1 Background

In the contemporary era, there has been a notable surge of interest and concern regarding power quality and reliability within distribution systems, driven by the integration of advanced manufacturing systems, industrial drives, and precision electronic equipment into modern industrial and commercial applications. This evolving landscape demands a higher level of power supply quality and reliability in distribution networks than ever before. Power quality issues encompass a broad spectrum of phenomena, including voltage sag, voltage swell, flicker, harmonics distortion, impulse transients, and interruptions. These disturbances have gained significance due to the proliferation of sensitive and critical equipment in power systems, spanning from communication systems to process industries and precision manufacturing processes. The repercussions of these disturbances range from equipment malfunctions and errors to complete plant shutdowns, resulting in a loss of manufacturing capability. Voltage sag and voltage swell are particularly prominent among power quality problems in distribution systems. Voltage sag, often referred to as voltage dip, is characterized by a decrease in the RMS voltage level to a range of 10% to 90% of nominal voltage at the power frequency. These dips are typically short in duration, ranging from half a cycle to one minute, as defined by the International Electro-Technical Commission (IEC). Voltage sags are often associated with system faults but can also be triggered by the energization of heavy loads or the startup of large motors, which can draw 6 to 10 times their full load current during startup. Sag durations are further categorized into three types: instantaneous, momentary, and temporary, each corresponding to utility device operation times. On the other hand, voltage swell, sometimes-referred to as momentary overvoltage, is defined by IEEE 1159 as an increase in the RMS voltage level to a range of 110% to 180% of nominal voltage at the power frequency. Swells are also of short duration, typically lasting from half a cycle to one minute. They can result from temporary voltage rises on healthy phases during a single-line-to-ground fault or be caused by actions such as switching off a large load or energizing a large capacitor bank. The severity of a voltage swell depends on factors such as fault location, system impedance, and grounding.

It is imperative to assess power quality from the perspective of economic consequences associated with equipment, taking into consideration the viewpoint of customers. Consequently, there is a growing need for tailored solutions for individual customers with highly sensitive loads, necessitating swift voltage regulation responses. Moreover, there is a need to comprehensively characterize voltage sag and swell phenomena in both domestic and industrial settings, including variations in magnitudes and phase angle changes, commonly referred to as phase angle jumps. These phase angle jumps represent variations in phase angle before and during voltage sag or swell events and are calculated as arguments of the complex voltage. Addressing these challenges requires a device capable of injecting minimal energy to regulate load voltage at predetermined values. The Dynamic Voltage Restorer (DVR) emerges as a prominent solution for mitigating power quality problems associated with voltage sags and swells. DVRs are strategically placed between the power supply and sensitive loads, enabling them to inject voltage of the required magnitude and frequency into the distribution feeder. The DVR operates in a manner that maintains a constant magnitude of load voltage, with an average real power of zero in steady-state conditions. Voltage sags and swells, being the most prevalent power quality issues, are effectively rectified by DVRs, making them a vital asset in modern industrial applications.

To further enhance the capabilities of DVRs, there are innovative approaches such as utilizing photovoltaic (PV) technology for DVRs, accompanied by advanced control techniques. These advancements, implemented through tools like MATLAB/SIMULINK and Space Vector Pulse Modulation Technique (PSVT) with Proportional Resonant (PR)-Controllers, offer self-sufficient control schemes for mitigating voltage sag, swell, and harmonics, providing a holistic solution to power quality challenges. This progressive approach ensures the continued reliability and quality of power supply, safeguarding the operations of sensitive equipment and industries.

1.2 Problem Statement

Power quality is the combination of voltage quality and current quality. Thus, power quality is concerned with deviations of voltage and/or current from the ideal. Power distribution systems, ideally, should provide their customers with an uninterrupted flow of energy at smooth sinusoidal voltage at the contracted magnitude level and frequency. However, in practice, power systems, especially the distribution systems have numerous nonlinear loads, which significantly affect the quality of power supplies. Because of the nonlinear loads, the purity of the waveform of supplies is lost. This ends up producing many Power quality problems. While power disturbances occur on

all electrical systems, the sensitivity of today's sophisticated electronic devices makes them more susceptible to the quality of power supply. For some sensitive devices, a momentary disturbance can cause scrambled data, interrupted communications, a frozen mouse, system crashes and equipment failure etc. A power voltage spike can damage valuable components. Power Quality problems encompass a wide range of disturbances such as voltage sags/swells, flicker, harmonics distortion, impulse transient, and interruptions.

1.2.1 Power Quality Concern

The variation in the definitions of power quality as given here are much wider than the general interpretation of power quality. This has to do with the fact that power quality in most cases is an issue due to the phrase "bad power quality". A power quality disturbance is only seen as an issue when it causes problems, either for the customer or for the network operator. Voltage sags, Voltage dips and harmonics are the problems encountered which makes power quality, a matter of concern. This is due to the presence of nonlinear elements in the power system (i.e. either in the network or in the loads). The main distortion is due to power-electronic loads like computers, televisions, energy- saving lamps. Such loads can be found in increasing numbers with domestic and commercial customers in a run to increase efficiency & productivity leading to increased distortion in the network. The effect is especially severe for lower-order voltage harmonics at the terminals of rotating machines & higher-order harmonics for capacitor banks.

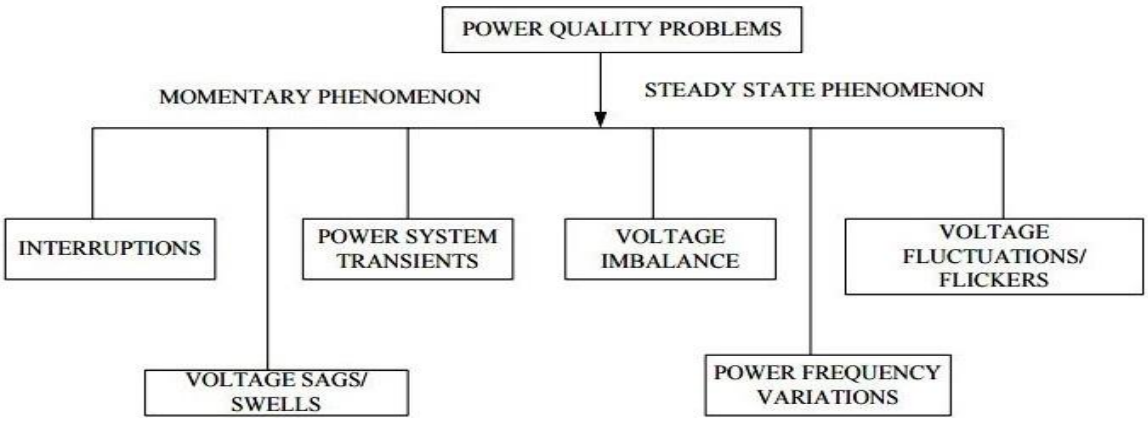

Fig 1.2.1: Classification of Power Quality Problems

1.2.2 Power Quality Problems

Voltage dip: A voltage dip is used to refer to short-term reduction in voltage of less than half a second.

Voltage sag: Voltage sags can occur at any instant of time, with amplitudes ranging from 10% to 90% and duration lasting for half a cycle to one minute.

Voltage swell: Voltage swell is defined as an increase in RMS voltage or current at the power frequency for durations from 0.5 cycles to 1 min.

Voltage 'spikes', 'impulses' or 'surges': These are terms used to describe abrupt, very brief increases in voltage value.

Voltage transients: They are temporary, undesirable voltages that appear on the power Supply line. Transients are high over-voltage disturbances (up to 20KV) that last for a very short time.

Harmonics: The fundamental frequency of the AC electric power distribution system is 50 Hz. A harmonic frequency is any sinusoidal frequency, which is a multiple of the fundamental frequency.

Flickers: Visual irritation and introduction of many harmonic components in the supply power and their associated ill effects.

Causes of Dips, Sags and Surges:

- Rural location remote from power source.
- Unbalanced load on a three phase system.
- Switching of heavy loads.
- Long distance from a distribution transformer with interposed loads Unreliable grid systems.
- Equipment not suitable for local supply.

Causes of Transients and Spikes:

- Lightening.
- Arc welding.
- Switching on heavy or reactive equipment such as motors, transformers, motor drives.
- Electric grade switching.

1.2.3 Solutions to Power Quality Problems

There are two approaches to the mitigation of power quality problems. The solution to the power quality can be done from customer side or from utility side First approach is called load conditioning, which ensures that the equipment is less sensitive to power disturbances, allowing the operation even under significant voltage distortion. The other solution is to install line-conditioning systems that suppress or counteracts the power system disturbances. Currently they are based on PWM converters and connect to low and medium voltage distribution system in shunt or in series. Series active power filters must operate in conjunction with shunt passive filters in order to compensate load current harmonics. Shunt active power filters operate as a controllable current source and series active power filters operates as a controllable voltage source. Both schemes are implemented preferable with voltage source PWM inverters, with a dc bus having a reactive element such as a capacitor. However, with the restructuring of power sector and with shifting trend towards distributed and dispersed generation, the line conditioning systems or utility side solutions will play a major role in improving the inherent supply quality; some of the effective and economic measures can be identified as following:

Lightening and Surge Arresters:

Arresters are designed for lightening protection of transformers, but are not sufficiently voltage limiting for protecting sensitive electronic control circuits from voltage surges.

Thyristor Based Static Switches:

The static switch is a versatile device for switching a new element into the circuit when the voltage support is needed. It has a dynamic response time of about one cycle. To correct quickly for voltage spikes, sags or interruptions, the static switch can used to switch one or more of devices such as capacitor, filter, alternate power line, energy storage systems etc. The static switch can be used in the alternate power line applications.

Energy Storage Systems:

Storage systems can be used to protect sensitive production equipment from shutdowns caused by voltage sags or momentary interruptions. These are usually DC storage systems such as UPS, batteries, superconducting magnet energy storage (SMES), storage capacitors or even flywheels driving DC generators .The output of these devices can be supplied to the system through an

inverter on a momentary basis by a fast acting electronic switch. Enough energy is fed to the system to compensate for the energy that would be lost by the voltage sag or interruption.
However, there are many different methods to mitigate voltage sags and swells, but the use of a custom Power device is considered to be the most efficient method. For example, Flexible AC Transmission Systems (FACTS) for transmission systems, the term custom power pertains to the use of power electronics controllers in a distribution system, specially, to deal with various power quality problems. Just as FACTS improves the power transfer capabilities and stability margins, custom power makes sure customers get pre-specified quality and reliability of supply.
Some of these devices include: Active Power Filters (APF), Battery Energy Storage Systems (BESS), Distribution Static synchronous Compensators (DSTATCOM), Distribution Series Capacitors (DSC), Dynamic Voltage Restorer (DVR), Surge Arresters (SA), Super conducting Magnetic Energy Systems (SMES), Static Electronic Tap Changers (SETC), Solid-State Transfer Switches (SSTS), Solid State Fault Current Limiter (SSFCL), Static VAR Compensator (SVC), Thyristor Switched Capacitors (TSC), and Uninterruptible Power Supplies (UPS).

1.2.4 Voltage Sag

Voltage sags and momentary power interruptions are probably the most important PQ problem affecting industrial and large commercial customers. These events are usually associated with a fault at some location in the supplying power system. Interruptions occur when the fault is on the circuit supplying the customer. However, voltage sags occur even if the faults happen to be far away from the customer's site.

Voltage sags lasting only 4-5 cycles can cause a wide range of sensitive customer equipment to drop out. To industrial customers, voltage sag and a
momentary interruption are equivalent if both shut their process down. A typical example of voltage sag is shown in fig 1.2.2

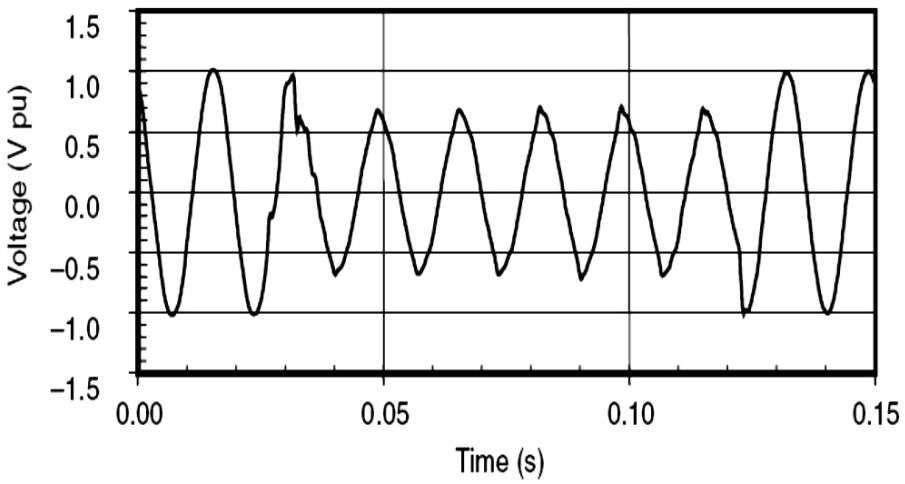

Fig 1.2.2 Typical Voltage Sag

Characteristics of Voltage Sags:

Voltage sags, which can cause equipment impacts, are caused by faults on the power system. Motor starting also results in voltage sags but the magnitudes are usually not severe enough to cause equipment disoperation.

How a fault results in voltage sag?

The one-line diagram given below in fig. 1.2.3 can be used to explain this phenomenon.

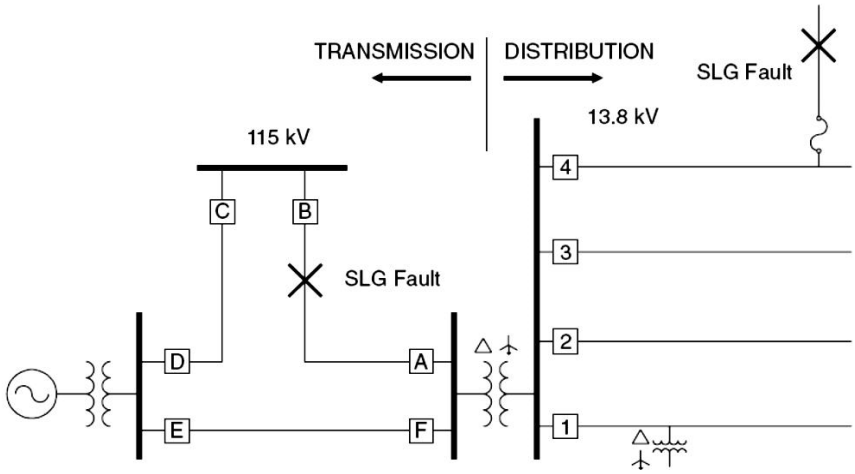

Fig 1.2.3 Example of Power System

Consider a customer on the feeder controlled by breaker 1. In the case of a fault on this feeder, the customer will experience voltage sag during the fault and an interruption when the breaker

opens to clear the fault. For temporary fault, enclosure may be successful.

Anyway, sensitive equipment will almost surely trip during this interruption. Another kind of likely event would be a fault on one of the feeders from the substation or a fault somewhere on the transmission system, in either of these cases, the customer will experience a voltage sag during the actual period of fault. As soon as breakers open to clear the fault, normal voltage will be restarted at the customer's end. Fig. 1.2.4 is a plot of rms voltage versus time and the waveform characteristics at the customer's location for one of these fault conditions.

This waveform is typical of the customer voltage during a fault on a parallel feeder circuit that is cleared quickly by the substation breaker. The total duration of fault is 150m sec. The voltage during a fault on a parallel feeder will depend on the distance from the substation to fault point. A fault close to substation will result in much more significant sag than a fault near the end of feeder. Fig 1.2.4 shows the voltage sag magnitude at the plant bus as a function of fault location for an example system.

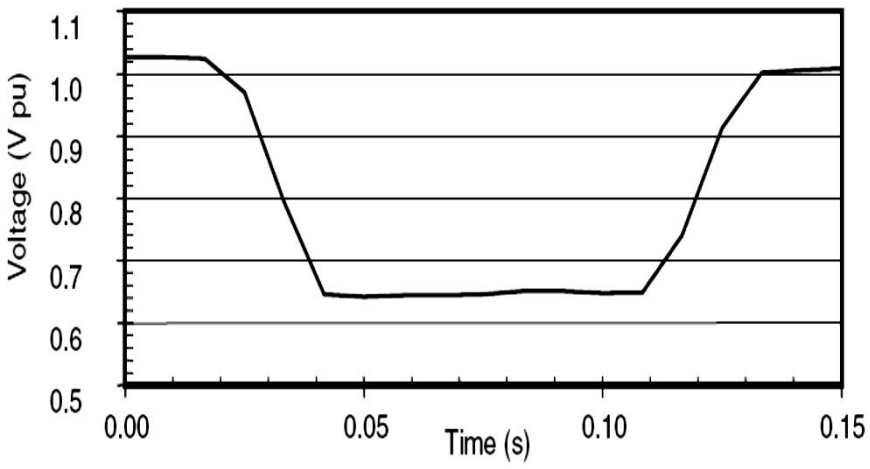

Fig 1.2.4 Voltage Sag Magnitude

1.2.5 Voltage Swell

A swell is the reverse form of a Sag, having an increase in AC Voltage for a duration of 0.5 cycles to 1 minute's time. For swells, high-impedance neutral connections, sudden large load reductions, and a single-phase fault on a three-phase system are common sources. Swells can cause data errors, light flickering, electrical contact degradation, and semiconductor damage in

electronics causing hard server failures. Our power conditioners and UPS Solutions are common solutions for swells.

It is important to note that, much like sags, swells may not be apparent until results are seen. Having your power quality devices monitoring and logging your incoming power will help measure these events.

Over-voltage

Over-voltages can be the result of long-term problems that create swells. Think of an overvoltage as an extended swell. Over-voltages are also common in areas where supply transformer tap settings are set incorrectly and loads have been reduced. Over-voltage conditions can create high current draw and cause unnecessary tripping of downstream circuit breakers, as well as overheating and putting stress on equipment. Since an overvoltage is a constant swell, the same UPS and Power Conditioners will work for these. Please note however that if the incoming power is constantly in an overvoltage condition, the utility power to your facility may need correction as well. The same symptoms apply to the over-voltages and swells however since the overvoltage is more constant you should expect some excess heat. This excess heat, especially in data center environments, must be monitored.

If you are experiencing any of these power quality problems, we have solutions ranging from Power Conditioners / Voltage Regulators to traditional UPS Systems and Flywheel UPS Solutions.

Swell causes

Swells are less common than voltage sags, but also usually associated with system fault conditions. A swell can occur due to a single line-to ground fault on the system, which can also result in a temporary voltage rise on the unfaulted phases. This is especially true in ungrounded or floating ground delta systems, where the sudden change in ground reference result in a voltage rise on the ungrounded phases. On an ungrounded system, the line-to ground voltages on the ungrounded phases will be 1.73 pu during a fault condition. Close to the substation on a grounded system, there will be no voltage rise on unfaulted phases because the substation transformer is usually connected delta-wye, providing a low impedance path for the fault current. Swells can also be generated by sudden load decreases. The abrupt interruption of current can generate a large voltage, per the formula: $v = L\, di/dt$, where L is the inductance of the line, and di/dt is the change in current flow. Switching on a large capacitor bank can also cause a swell, though it

more often causes an oscillatory transient

1.2.6 Custom Power Devices (CPDs)

The introduction of power electronic loads has raised much concern about power quality problems caused by harmonics, distortions, interruptions, and surges. The use of electronic devices increases the power quality problems. Equipment such as large industrial drives (e.g., cyclo-converters) generate significantly high voltage and current harmonics and create extensive voltage fluctuation.

The application of harmonic filters and SVCs to radial transmission systems can offer partial solution to high THD levels and voltage fluctuations. Yet, the lack of dynamic capabilities of these devices limits them to bulk correction. In addition, they might be effective in one application but fail to correct other power quality issues.

FACTS controllers improve the reliability and quality of power transmission by simultaneously enhancing both power transfer capacity and stability whereas custom power devices enhance the quality and reliability of power delivered to the customer. With a custom power device, a customer (e.g., a sensitive load) will be able to receive a pre-specified quality of electric power with a combination of specifications including but not limited to:

- Magnitude and duration of over and under voltages with specified limits,
- Low harmonic distortion in the supply, load voltages, and currents.
- Small phase imbalance
- Low flicker in the supply voltage
- Control of power interruptions, and
- Control of supply voltage frequency within specified limits.

Classification of Custom power devices are based on their power electronic controllers, which can be either of the network reconfiguration type or of the compensation type. The network reconfiguration devices also called switchgear include the solid state and or static versions or current limiting, current breaking, and current transferring components. The compensation type custom power devices either compensate a load (e.g., correct its power factor, imbalance) or improve the quality for the supply voltage (e.g., eliminate its harmonics). They are connected either in shunt or in series or a combination of both. Custom power devices are classified as follows:

Network – reconfiguration custom power devices includes

- Solid state current limiter (SSCL),
- Solid–state breaker (SSB), and
- Solid state transfer switch (SSTS)

Compensation-custom power devices includes

- Distribution STATCOM,
- Dynamic voltage restorer / regulator (DVR), and
- Unified power quality conditioner (UPQC).

Custom power devices are designed to improve the quality of power at their point of installation of the power distribution system. They are not primarily designed to improve the power quality of the entire system.

1.3 Rationale of the Study

Numerous studies have explored the deployment of Custom Power Devices (CPDs) in diverse systems to enhance power system efficiency, reduce losses, improve voltage stability, and save energy costs. However, research on optimizing CPD placement, particularly using Space Vector Pulsed Width Modulation with PR Controller, remains limited. Furthermore, most existing research focuses on high-voltage transmission systems, neglecting medium-voltage distribution networks.

To address this gap, our study proposes a SARFI (System Average RMS Frequency Index) based technique for strategically locating Dynamic Voltage Restorers (DVRs) in radial distribution systems. We evaluate the impact of various faults on power quality in radial distribution networks and design a PV Integrated DVR to restore load-node voltage to its pre-fault state, ensuring minimal operational disruptions. We assess the effectiveness of the PV Integrated DVR under different load and line length uncertainties.

Utilizing electric networks optimally is crucial for economic viability and system reliability. Therefore, we employ the SARFI-based approach to minimize voltage deviations from pre-fault levels and determine the optimal DVR placement. This analysis contributes to the reliable and stable operation of DVRs, enhancing overall system performance by deploying them in strategically optimal locations.

1.4 Objectives

1.4.1 Main Objective

The main objective of this thesis is to determine the optimal location to place a PV (Photovoltaic) integrated DVR in radial distribution systems in order to restore the pre-fault operating voltage at the buses affected by voltage sag and swell during fault using Space Vector pulse width Modulation with Proportional Resonant (PR) Controller. Also, to minimize the Total Harmonic Distortion of the system

1.4.2 Specific Objectives

The study was carried out to meet the following specific objectives:

- To develop a SIMULINK model of PV based DVR and integrate it in a radial distribution system to investigate its effectiveness.
- To find the location for the optimal placement of DVR in the IEEE 13 Node Test system and a study it with 11kV Simara Industrial Feeder and 11kV Tanahusur Feeder.
- To find optimal location of DVR using SARFI (System Average RMS Frequency Index) approach.

CHAPTER 2: LITERATURE REVIEW

Dynamic Voltage Restorers (DVRs) have been widely studied in the literature as an effective solution for mitigating voltage disturbances in power systems. Voltage sags, swells, and interruptions can cause severe damage to electrical equipment and disrupt the operation of critical loads, such as data centers, hospitals, and manufacturing plants. DVRs are power electronics-based devices that are connected in parallel with the load to compensate for voltage deviations and maintain the load voltage within the allowable limits.

The design of DVRs involves selecting the appropriate converter topology, selecting the rating of the converter components, and determining the control strategy. Several converter topologies, such as the voltage source converter (VSC), current source converter (CSC), and hybrid converter. The VSC topology is the most widely used converter topology for DVRs due to its high power density, fast dynamic response, and easy controllability. The rating of the converter components, such as the DC-link capacitor, inductors, and semiconductor devices, is another crucial factor in the design of DVRs. The rating of these components affects the cost, size, and performance of the DVR.

Various control strategies have also been proposed for DVRs, including PI control, fuzzy logic control, and Space vector Transformation and model predictive control (MPC). PI control is the simplest control strategy that can regulate the output voltage of the DVR by adjusting the duty cycle of the converter switches. However, PI control has limited performance under highly nonlinear and time-varying conditions. Fuzzy logic control is a more advanced control strategy that can handle nonlinear and uncertain systems by using linguistic variables and fuzzy rules. Fuzzy logic control has been shown to be effective in regulating the output voltage of DVRs under various operating conditions. MPC is a predictive control strategy that uses a mathematical model of the system to predict the future behavior of the system and optimize the control inputs. MPC has been shown to be effective in regulating the output voltage of DVRs under highly nonlinear and time-varying conditions.

Various studies have evaluated the performance of DVRs under different operating conditions, including various load impedances, fault locations, and fault types. The effectiveness of DVRs in compensating for voltage sags, swells, and interruptions has been demonstrated in several studies. The development of advanced control strategies and optimization techniques is expected to further enhance the performance and efficiency of

DVRs in the future.

Photovoltaic-based Dynamic Voltage Restorer (DVR) is a technology that uses solar panels to provide power to the grid during voltage dips or sags. This system combines two technologies: the DVR and the photovoltaic (PV) system, which offers a sustainable and environmentally friendly way to improve power quality. The main objective of the PV-based DVR is to protect sensitive loads from voltage sags and keep the voltage at a constant level. This literature review will focus on the recent developments and research on PV-based DVR.PV-based DVR is an innovative solution for power quality improvement. It is an ideal solution for remote areas where power quality is poor and grid connectivity is weak. In recent years, many researchers have been working on improving the performance of PV-based DVR. PV-based DVR system that uses a hybrid MPPT algorithm to improve the performance of the system. The proposed system was tested on a MATLAB Simulink, and the results showed that the system was effective in mitigating voltage sags/swells and providing a stable voltage to the load. The Space Vector Pulse width Modulation with PR controller was found to be effective in reducing the voltage sag and maintaining a stable voltage to the load. PV-based DVR system that uses a cascaded H-bridge multilevel inverter. The proposed system also reduced the THD and improved the power factor of the system.

PV-based DVR is an innovative solution for power quality improvement. It offers a sustainable and environmentally friendly way to improve power quality. The recent developments and research on PV-based DVR have shown promising results in mitigating voltage sags and restoring the voltage to the pre-fault value. The proposed systems have also reduced the THD and improved the power factor of the system. However, there is still a need for more research on PV-based DVR to improve its performance and make it more feasible for real-world applications.

2.1 Dynamic Voltage Restorer (DVR)

The Dynamic Voltage Restorer (DVR) is a series connected device analogous to a SSSC. The main function of a DVR is to eliminate or reduce voltage sags seen by sensitive loads such as semiconductor manufacturing plant or IT industry. DVR that have been installed so far are modular with ratings of 2 MVA per module. They have been designed to compensate three phase voltage sags up to 35% for duration of time less than half a second (depending on the

requirement). If the voltage sag occurs only in one phase (caused by SLG faults) then the DVR may be designed to provide compensation for sags exceeding 50%. The energy storage required in capacitors is typically in the range of 0.2 to 0.4 MJ per MW of load served.

A DVR is connected in series with the feeder using a transformer. The low voltage winding is connected to the converter. If the objective of a DVR is mainly to regulate the voltage at the load bus, it remains for most of the time in stand-by mode during which the converter is bypassed (no voltage is injected). Only when sag is detected, the DVR injects a series voltage of the required magnitude. It is necessary to protect a DVR against the fault currents (as in the case of a SSSC). A DVR with IGBT/IGCT devices can be controlled to act as a series active filter to isolate the load from voltage harmonics on the source side. It is also possible to balance the voltage on the load side by injecting negative and/or zero sequence voltages in addition to harmonic voltages.

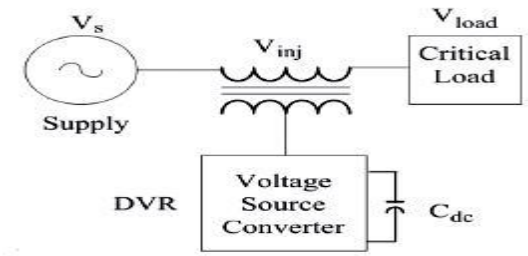

Fig 2.1 Basic circuit of DVR

Among the power quality problems (sags, swells, harmonics…) voltage sags are the most severe disturbances. In order to overcome these problems the concept of custom power devices is introduced recently. One of those devices is the Dynamic Voltage Restorer (DVR), which is the most efficient and effective modern custom power device used in power distribution networks. DVR is a recently proposed series connected solid state device that injects voltage into the system in order to regulate the load side voltage. It is normally installed in a distribution system between the supply and the critical load feeder at the point of common coupling (PCC). Other than voltage sags and swells compensation, DVR can also added other features like: line voltage harmonics compensation, reduction of transients in voltage and fault current limitations.

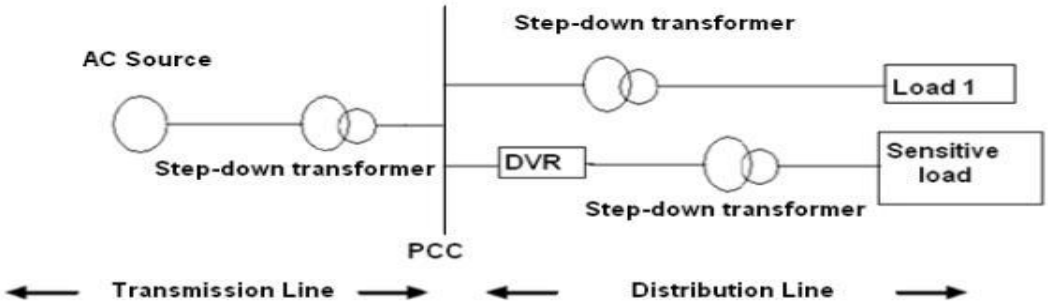

Fig 2.2 Location of DVR

2.2 Basic Configuration of DVR

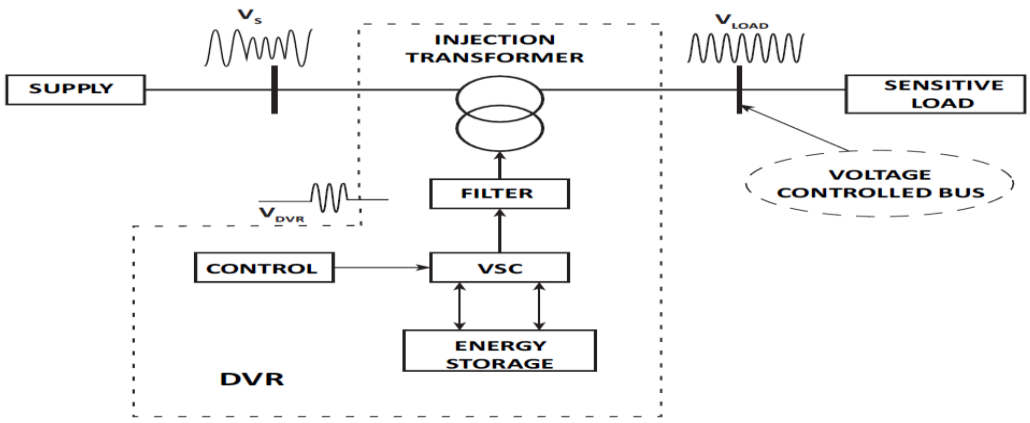

Fig 2.3 Schematic Diagram of DVR

The general configuration of the DVR consists of:

- An Injection/ Booster transformer.
- A Harmonic filter.
- Storage Devices.
- A Voltage Source Converter (VSC).
- DC charging circuit.
- A Control and Protection system.

2.2.1 Injection/ Booster Transformer

The Injection / Booster transformer is a specially designed transformer that attempts to limit the coupling of noise and transient energy from the primary side to the secondary side. Its main tasks are:

1. It connects the DVR to the distribution network via the HV-windings and transforms and couples the injected compensating voltages generated by the voltage source converters to the I incoming supply voltage
2. In addition, the Injection / Booster transformer serves the purpose of isolating the load from the system (VSC and control mechanism).

2.2.2 Harmonic Filter

The main task of harmonic filter is to keep the harmonic voltage content generated by the VSC to the permissible level.

2.2.3 Voltage Source Converter:

A VSC is a power electronic system consists of a storage device and switching devices, which can generate a sinusoidal voltage at any required frequency, magnitude, and phase angle. In the DVR application, the VSC is used to temporarily replace the supply voltage or to generate the part of the supply voltage which is missing. There are four main types of switching devices:

- Metal Oxide Semiconductor Field Effect Transistors (MOSFET),
- Gate Turn-Off Thyristors (GTO),
- Insulated Gate Bipolar Transistors(IGBT), and
- Integrated Gate Commutated Thyristors (IGCT).

Each type has its own benefits and drawbacks. The IGCT is a recent compact device with enhanced performance and reliability that allows building VSC with very large power ratings. Because of the highly sophisticated converter design with IGCTs, the DVR can compensate dips which are beyond the capability of the past DVRs using conventional devices. The purpose of storage devices is to supply the necessary energy to the VSC via a dc link for the generation of injected voltages. The different kinds of

energy storage devices are Superconductive Magnetic energy storage (SMES), batteries and capacitance.

2.2.4 DC Charging Circuit

The dc charging circuit has two main tasks

- The first task is to charge the energy source after a sag compensation event.
- The second task is to maintain dc link voltage at the nominal dc link voltage.

2.2.5 Energy Storage

The energy storage device serves as an essential component for the DVR as it serves asthe power bank to supply voltage support during voltage sags and absorbs the excess power from the grid during voltage swell.

2.2.6 Control and Protection:

The control technique to be adopted depends on the type of load as some loads are sensitive to only magnitude change whereas some other loads are sensitive to both magnitude and phase angle shift. Control techniques that utilize real and reactive power compensation are generally classified as pre- sag compensation, in-phase compensation and energy optimization technique. For our study, pre-sag compensation was used where the load voltage is restored to its pre-sag magnitude and phase. Therefore, this method is suitable for loads which are sensitive to magnitude and also phase angle shift. Differential current protection of the transformer, or short circuit current on the customer load side are only two examples of many protection functions possibility.

2.3 Equations Related to DVR

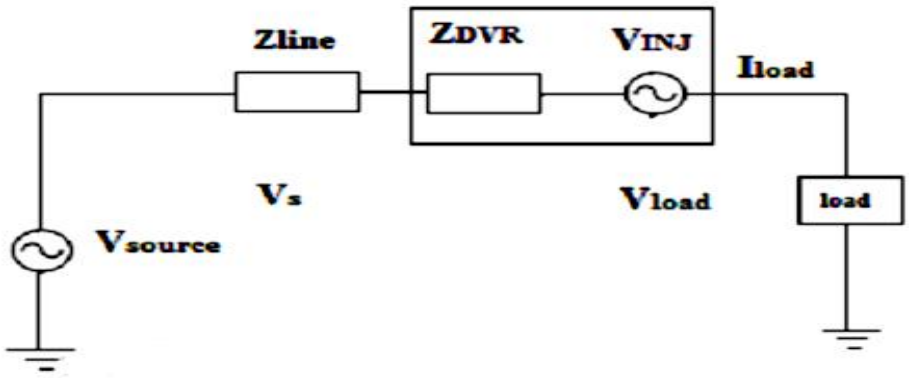

Fig 2.4 Equivalent Circuit diagram of DVR

The system impedance Zth depends on the fault level of the load bus. When the system voltage (Vsource) drops, the DVR injects a series voltage VDVR through the injection transformer so that the desired load voltage magnitude VL can be maintained. The series injected voltage of the DVR can be written as

$$\boldsymbol{V_{DVR} = V_L + Z_{source} I_L - V_{source}} \quad (2.3$$

Where,

$\boldsymbol{V_L}$: The desired load voltage magnitude

$\mathbf{Z_{source}}$: The load impedance.

$\mathbf{I_L}$: The load current.

$\boldsymbol{V_{source}}$: the system voltage during fault condition.

The load current I_L is given by,

$$\mathbf{I_L = \frac{[P_L + jQ_L]}{V}}$$

(2.4)

When V_L is considered as a reference equation can be rewritten as,

$$\boldsymbol{V_{DVR} < 0 = V_L < 0 + Z_{Source} < (\beta - \theta) - V_{source} < \delta}$$

(2.5)

 , β, δ are angles of V_{DVR}, Z_{source}, V_{source} respectively and θ is Load power angle

$$\boldsymbol{\theta = \tan^{-1}(\frac{\theta_L}{P_L})} \quad (2.6)$$

The complex power injection of the DVR can be written as,

$$\mathbf{S_{DVR} = V_{DVR} I_L} \quad (2.7)$$

It requires the injection of only reactive power and the DVR itself is capable of generating the reactive power.

2.4 Operating Modes of DVR

The basic function of the DVR is to inject a dynamically controlled voltage V_{DVR} generated by a forced commutated converter in series to the bus voltage by means of a booster transformer. The momentary amplitudes of the three injected phase voltages are controlled such as to eliminate any detrimental effects of a bus fault to the load voltage V_L. This means that any differential voltages caused by transient disturbances in the ac feeder will be compensated by an equivalent voltage generated by the converter and injected on the medium voltage level through the booster transformer.

The DVR has three modes of operation which are: protection mode, standby mode, injection/boost mode.

2.4.1 Protection Mode

If the over current on the load side exceeds a permissible limit due to short circuit on the load or large inrush current, the DVR will be isolated from the systems by using the bypass switches (S2 and S3 will open) and supplying another path for current (S1 will be closed).

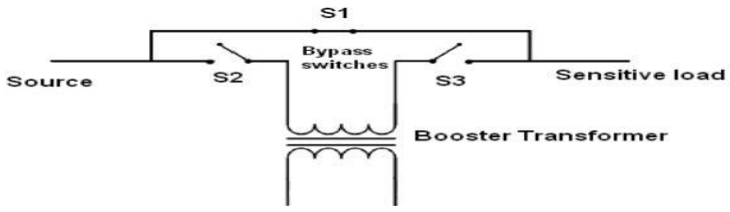

Fig. 2.5 Protection Mode

2.4.2 Standby Mode: (VDVR= 0)

In the standby mode the booster transformer's low voltage winding is shorted through the converter. No switching of semiconductors occurs in this mode of operation and the full load current will pass through the primary.

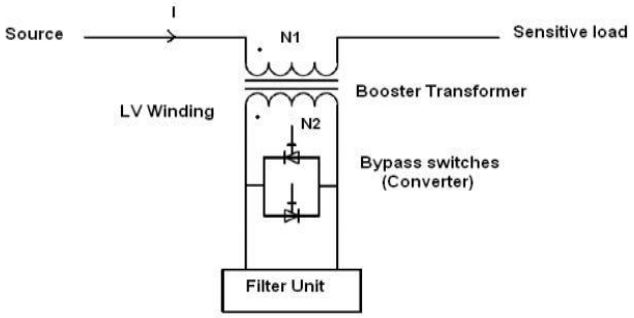

Fig.2.6 Standby Mode

2.4.3 Injection/Boost Mode: (VDVR>0)

In the Injection/Boost mode the DVR is injecting a compensating voltage through the booster transformer due to the detection of a disturbance in the supply voltage.

2.5 Voltage Injection Methods of DVR

Voltage injection or compensation methods by means of a DVR depend upon the limiting factors such as: DVR power ratings, various conditions of load, and different types of voltage sags. Some loads are sensitive towards phase angel jump and some are sensitive towards change in magnitude and others are tolerant to these. Therefore the control strategies depend upon the type of load characteristics.

There are four different methods of DVR voltage injection which are

- Pre-sag compensation method
- In-phase compensation method
- In-phase advanced compensation method
- Voltage tolerance method with minimum energy injection

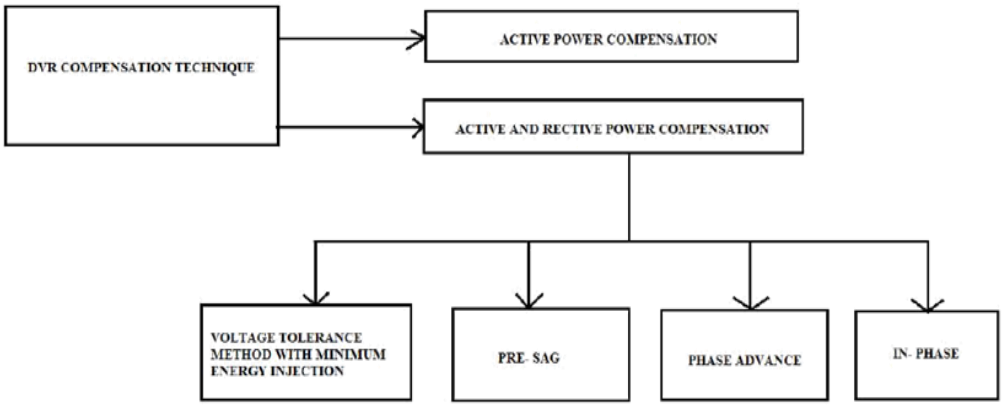

Figure 2.7: Compensation techniques of a DVR

2.5.1 Pre-Sag/Dip Compensation Method

The pre-sag method tracks the supply voltage continuously and if it detects any disturbances in supply voltage it will inject the difference voltage between the sag or voltage at PCC and pre-fault condition, so that the load voltage can be restored back to the pre-fault condition. Compensation of voltage sags in the both phase angle and amplitude sensitive loads would be achieved by pre-sag compensation method. In this method the injected active power cannot be controlled and it is determined by external conditions such as the type of faults and load conditions.

$$\mathbf{V_{DVR} = V_{prefault} - V_{sag}} \qquad (2.8)$$

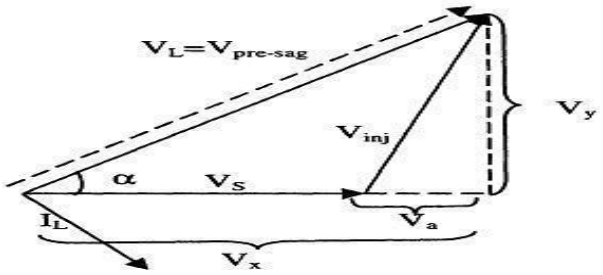

Fig 2.8 Pre-sag compensation

2.5.2 In-Phase Compensation Method

This is the most straight forward method. In this method the injected voltage is in phase with the supply side voltage irrespective of the load current and pre-fault voltage. The phase angles of the pre-sag and load voltage are different but the most important criteria for power quality that is the constant magnitude of load voltage are satisfied.

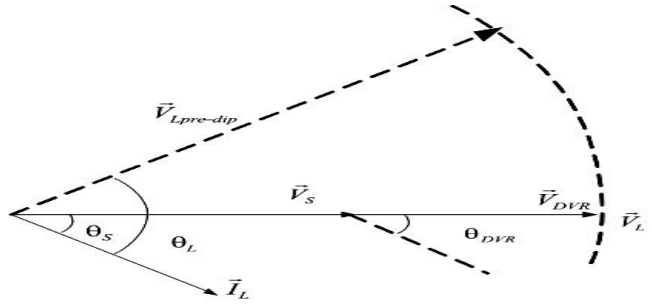

Fig 2.9 In-Phase Compensation Method

$$|V_L|=|V_{prefault}| \quad (2.9)$$

One of the advantages of this method is that the amplitude of DVR injection voltage is minimum for certain voltage sag in comparison with other strategies. Practical application of this method is in non-sensitive loads to phase angle jump.

2.5.3 In-Phase Advanced Compensation Method

In this method, the real power spent by the DVR is decreased by minimizing the power angle between the sag voltage and load current. In case of pre-sag and in-phase compensation method, the active power is injected into the system during disturbances. The active power supply is limited stored energy in the DC links and this part is one of the most expensive parts of DVR. The minimization of injected energy is achieved by making the active power component zero by having the injection voltage phasor perpendicular to the load current phasor.

In this method the values of load current and voltage are fixed in the system so we can change only the phase of the sag voltage. IPAC method uses only reactive power and unfortunately, not al1 the sags can be mitigated without real power, as a consequence, this

method is only suitable for a limited range of sags.

2.5.4 Voltage Tolerance Method with Minimum Energy Injection

A small drop in voltage and small jump in phase angle can be tolerated by the load itself. If the voltage magnitude lies between 90%-110% of nominal voltage and 5%-10% of nominal state that will not disturb the operation characteristics of loads. Both magnitude and phase are the control parameter for this method, which can be achieved by small energy injection.

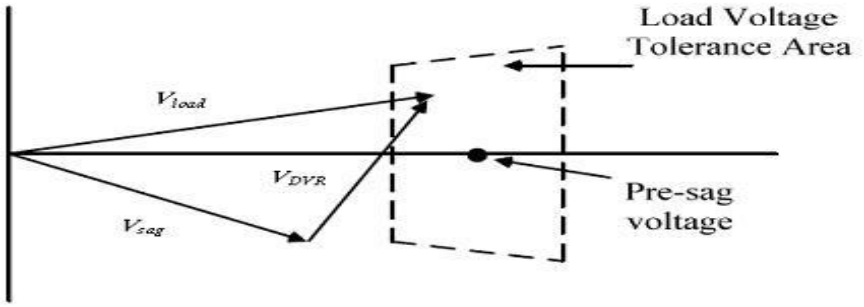

Fig. 2.10: Voltage tolerance method with minimum energy injection

2.6 Block Diagram of DVR-Connected System

The control strategy of the DVR is to achieve these two components of the injection voltage and this is achieved by controlling the supply current. The currents are sensed and the two components of currents, one is the component to maintain the dc bus voltage of DVR and the second one is to maintain the load terminal voltages, are added with the sensed load current to estimate the reference supply current.

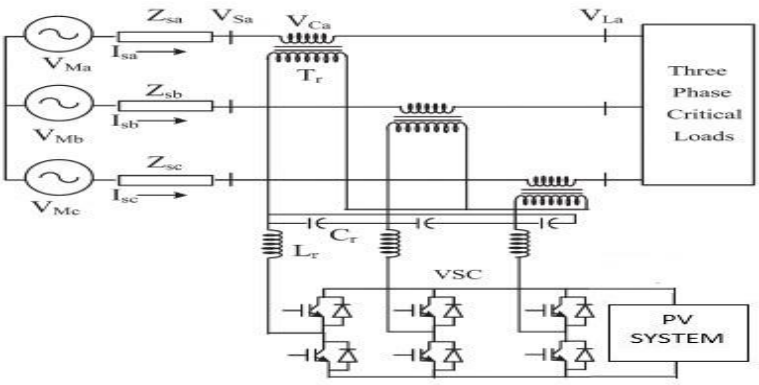

Fig.2.11: Schematic of the PV based DVR-connected system

2.7 Power Circuit Topologies for DVR

Power circuit topologies for DVR are broadly classified into two; one uses stored energy and the other uses no significant energy storage. The system topologies are;

1. Topologies with stored energy
    - Constant DC-link voltage
    - Variable DC-link voltage
2. Topologies with power from the supply
    - Supply side connected passive shunt converter
    - Load side connected passive shunt converter

Among these, the DVR configuration with stored energy is discussed in this paper. The topologies with constant DC link voltage as well as variable DC link voltage.

2.7.1 Constant DC-link voltage

A DVR with constant DC-link voltage illustrated in fig 2.12 is expected to have superior performance and an effective utilization of the energy storage. An additional converter is expected to convert energy from the main storage to a small DC-link and thereby control and stabilize the DC-link voltage. The stored energy can be delivered from different kinds of energy storage systems such as batteries, flywheel storage or SMES. The DVR with a constant voltage is here considered to be a reference topology by which the other DVR topologies are evaluated. It offers a constant DC-link voltage at all times and does not increase the current drawn from the supply. This configuration is also known as Battery

Supported DVR as the DC link voltage is always constant. The performance of this system is improved compared to the variable DC link solution, but the equipment costs are higher as energy storage is needed and a separate high-rated power converter is necessary.

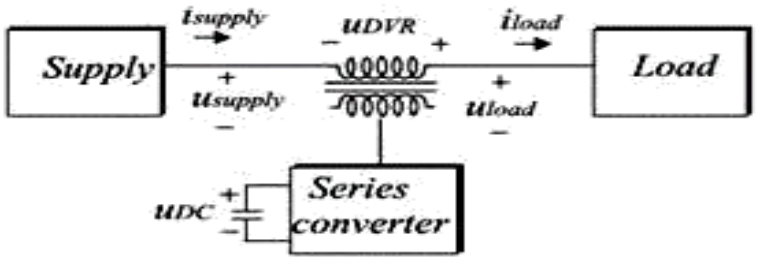

Fig.2.12 DVR with constant DC link voltage

2.7.2 Variable DC link voltage

The DVR with variable DC-link voltage is illustrated in fig.2.13. It offers benefits in simplicity due to only one high rated converter and only DC-link capacitors as the energy storage. The voltage injection capacity depends on the actual level of the DC-link voltage and energy saving control strategies are urgent to fully utilize the energy storage system. As this DVR configuration is capable of compensating power quality problems with the help of its self-supporting DC bus, this type is generally referred to as Self Supported DVR. The DC-link voltage can be utilized only down to a certain DC-link voltage level. Hence, the range of power disturbances that can be compensated by this type of DVR configuration is limited.

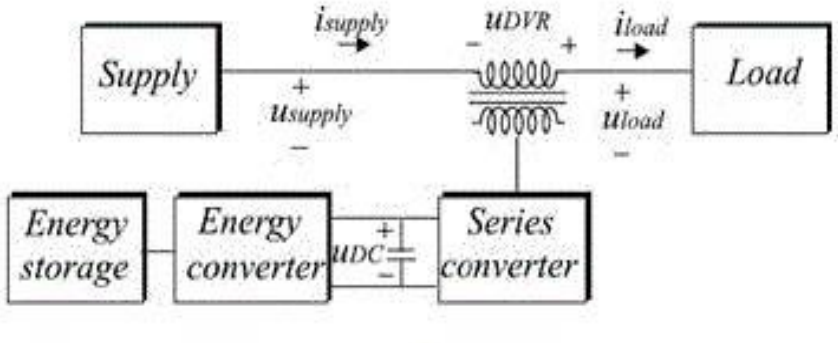

Fig. 2.13 DVR with Variable DC link voltage

2.8 Photovoltaic System and Modelling

Photovoltaic (PV) is a method of generating electrical power by converting solar radiation into direct current electricity using semiconductors that exhibit the photovoltaic effect. Photovoltaic power generation employs solar panels comprising a number of cells containing a photovoltaic material. Materials presently used for photovoltaic include mono crystalline silicon, polycrystalline silicon, amorphous silicon, cadmium telluride, and copper indium selenide/sulfide. Due to the growing demand for renewable energy sources, the manufacturing of solar cells and photovoltaic arrays has advanced considerably in recent years.

2.8.1 Solar Cell

A solar cell is a solid state device that converts the energy of sunlight directly into electricity by the photovoltaic effect. Assemblies of cells are used to make solar modules, also known as solar panels. The energy generated from these solar modules, referred to as solar power, is an example of solar energy.

The origin of the PV potential is the difference in the chemical potential, called the Fermi level, of the electrons in the two isolated materials. When they are joined, the junction approaches a new thermodynamic equilibrium. Such equilibrium can be achieved only when the Fermi level is equal in the two materials. This occurs by the flow of electrons from one material to the other until a voltage difference is established between them, which have a potential just equal to the initial difference of the Fermi level. This potential drives the photocurrent in the PV circuit.

Photovoltaics is the field of technology and research related to the practical application of photovoltaic cells in producing electricity from light, though it is often used specifically to refer to the generation of electricity from sunlight.

Cells are described as photovoltaic cells when the light source is not necessarily sunlight. These are used for detecting light or other electromagnetic radiation near the visible range, for example infrared detectors), or measurement of light intensity.

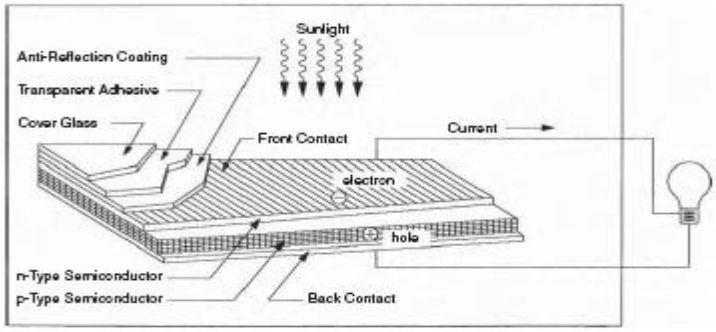

Fig 2.14: Basic construction of PV cell

The diagram above illustrates the operation of a basic photovoltaic cell, also called a solar cell. Solar cells are made of the same kinds of semiconductor materials used in microelectronics, such as silicon (melted sand) or cadmium telluride. For solar cells, a thin semiconductor wafer is specially treated to form an electric field, positive on one side and negative on the other. When light energy strikes the solar cell, electrons are knocked loose from the atoms in the semiconductor material. If electrical conductors are attached to the positive and negative sides, forming an electrical circuit, the electrons can be captured in the form of an electric current. This electricity can then be used to power a load, such as a light or a tool. Each PV cell converts about 5 to 15 percent of the sunlight that hits it into electrical current. Photovoltaic cells are modular. That is, one can be used to make a very small amount of electricity, or many can be used together to make a large amount of electricity.

Photovoltaic cell produces only about one-half volt of electricity, cells are often mounted together in groups called modules. Each module holds about forty photovoltaic cells. By being put into modules, the current from a number of cells can be combined. PV cells can be strung together in a series of modules or strung together in a parallel placement to increase the electrical output.

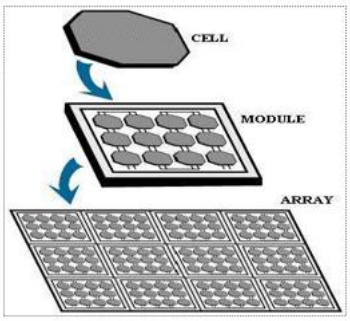

Fig 2.15: The PV array set up

When multiple PV cell modules are put together, they can form an arrangement called an array or array field. In general, the larger the area of a module or array, the more electricity that will be produced. Photovoltaic modules and arrays produce direct current (dc) electricity. They can be connected in both series and parallel electrical arrangements to produce any required voltage and current combination.

2.8.2 Main Operation

Photons in sunlight hit the solar panel and are absorbed by semiconducting materials, such as silicon. Electrons (negatively charged) are knocked loose from their atoms, allowing them to flow through the material to produce electricity. Due to the special composition of solar cells, the electrons are only allowed to move in a single direction. An array of solar cells converts solar energy into a usable amount of direct current (DC) electricity.

2.8.3 Equivalent Circuit

The complex physics of the PV cell can be represented by the equivalent electrical circuit. The circuit parameters are as follows. The current I at the output terminals is equal to the light-generated current I_L, less the diode current I_d and the shunt-leakage current I_{sh}. The series resistance R_s represents the internal resistance to the current flow, and depends on the pn junction depth, impurities, and contact resistance. The shunt resistance R_{sh} is inversely related to the leakage current to ground. In an ideal PV cell, $R_s = 0\Omega$ (no series loss), and $R_{sh} = \infty$(no leakage to ground). In a typical high-quality 1 in.2 silicon cell, Rs varies from 0.05 to 0.10 Ω and R_{sh} from 200 to 300 Ω. The PV conversion efficiency is sensitive to small variations in Rs, but is insensitive to variations in R_{sh}. A small increase in Rs can decrease the PV output significantly. In the equivalent circuit, the current delivered to the external load equals the current I_L generated by the illumination, less the

diode current Id and the shunt leakage current I_{sh}. The open-circuit voltage Voc of the cell is obtained when the load current is zero, i.e., when I = 0, and is given by the following:

$$V_{oc}=V+IR_{sh} \quad (2.9)$$

The shunt resistance (R_{sh}) is very large and the series resistance (Rs) is very small. Therefore, it is common to neglect these resistances in order to simplify the solar cell model. The resultant ideal voltage-current characteristic of a photovoltaic cell is given by the relation below and illustrated by the figure above.

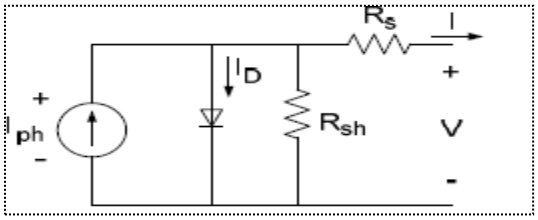

Fig 2.16: PV cell equivalent circuit

$$I = I_{PH} - I_D \quad (2.10)$$

$$I = I_{PH} - I_0\left[\exp\left(\frac{q(V+R_sI)}{AK_BT}\right)-1\right]-\frac{V+R_sI}{R_{sh}} \quad (2.11)$$

Where,

I_{ph} = photocurrent,
I_D = diode current,
I_0 = saturation current,
A = ideality factor,
q = electronic charge $1.6x10^{-9}$,
k_B = Boltzmann's gas constant ($1.38x10^{-23}$),
T = cell temperature,
R_s = series resistance,
R_{sh} = shunt resistance,
I = cell current,
V = cell voltage

The power output of a solar cell is given by

$$P_{PV} = V_{PV} * I_{PV} \quad (2.12)$$

Where,

I_{PV} = Output current of solar cell (A).
V_{PV} = Solar cell operating voltage (V).
P_{PV} =Output power of solar cell (W).

The power-voltage (P-V) characteristic of a photovoltaic module operating at a standard irradiance of 1000 W/m^2 and temperature of 25^{o}C is shown below.

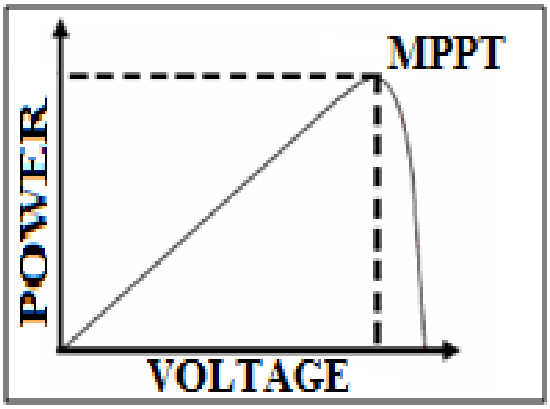

Fig: 2.17: Power-Voltage (PV) Characteristic of a Photovoltaic Module.

It can be seen from the characteristics, that there is a unique point on the characteristics at which the photovoltaic power is maximum. This point is termed as the maximum power point (MPP). The power corresponding to this point is termed as power at maximum power point (P_{mpp}) and the voltage as voltage at maximum power point (V_{mpp}). Due to high cost of solar cells, it must be ensured that the photovoltaic array operates at all time to provide maximum power output. Hence a maximum power point tracker must be used to track the maximum power of the system. This is commonly known as maximum power point tracking (MPPT). Now if the irradiance level of the photovoltaic system is changed from the standard 1000 W/m^2 to say 600 W/m^2 or 400 W/m^2 then the P-V characteristic will change as shown in the figure below.

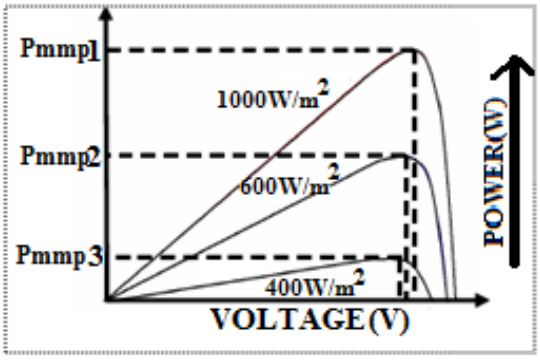

Fig 2.18: Variation of P-V Characteristics of Photovoltaic Module

The above graph shows that, the maximum power of the PV system also reduces accordingly. The maximum power point tracker must now track the new maximum power point for the changed irradiance level. In this thesis, Incremental Conductance and Integral Regulator method is used for the MPPT of the PV system.

2.8.4 Equivalent PV system

In the proposed system PV system with MPPT control (DC/DC boost Converter) which charges the Energy storage system (Battery Bank) of DVR. Reactive Power for the system in generated by VSI, which is controlled by SVT and PR Controller. The DVR system is connected to the Grid system via Injection Transformer.

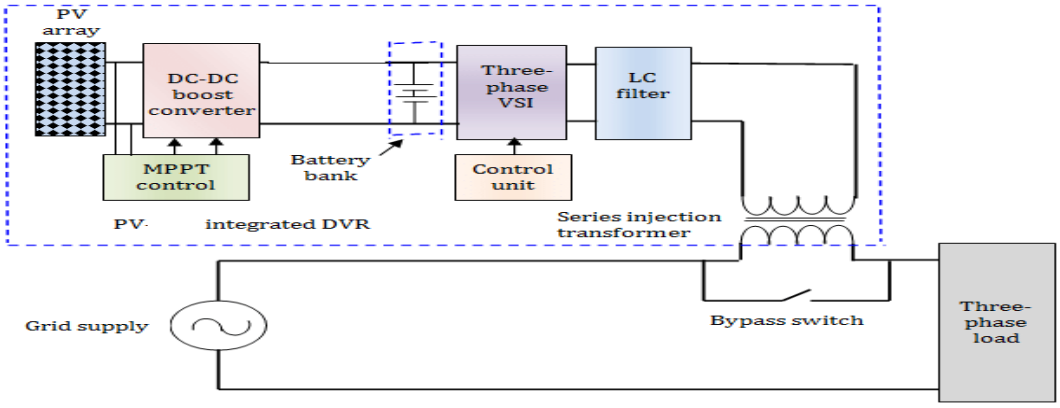

Fig 2.19: Equivalent block diagram of the System with PV System.

2.9 Photovoltaic System integrated with DVR

The integration of photovoltaic (PV) systems into the power grid has gained significant attention due to its potential to provide clean and sustainable energy. To maximize the energy output from PV systems, maximum power point tracking (MPPT) algorithms are essential. Among these, the Incremental Conductance (IncCond) and Integral Regulator (IR) methods have shown promise. Additionally, PV systems can be integrated with Dynamic Voltage Regulators (DVRs) to enhance grid operation and support energy storage.

2.9.1 Maximum Power Point Tracking (MPPT) Algorithms for PV System

Hybrid Incremental Conductance and Integral Regulator (HIC+IR) is a technique used in Maximum Power Point Tracking (MPPT) for photovoltaic (PV) systems. MPPT is crucial for optimizing the energy output of a solar panel by continuously adjusting the operating point to extract the maximum available power from the PV array. HIC+IR combines two popular MPPT algorithms, Incremental Conductance (IncCond) and Integral Regulator (IR), to improve tracking accuracy.

Incremental Conductance (IncCond): This algorithm tracks the MPP by comparing the instantaneous change in power with the instantaneous change in voltage. When the ratio of these changes approaches zero, the algorithm identifies that the system is operating at or near the MPP. IncCond is good at quickly tracking the MPP when the irradiance changes rapidly. The MPPT controller continuously measures both the voltage (V) and current (I) output of the PV array and finds out instantaneous Power (P=V*I). The Incremental Conductance (dI/dV) is then compared with zero. When dI/dV is zero, it means the system is operating at the MPP. When dI/dV is positive, it indicates that the operating point is to the left of the MPP, and when it's negative, it indicates the operating point is to the right of the MPP. To track the MPP, the controller adjusts the duty cycle of a DC-DC converter (typically a buck or boost converter) that connects the PV array to the load or battery. The direction of the duty cycle adjustment (increase or decrease) depends on the sign of dI/dV.

- If $dI/dV > 0$, indicating the operating point is to the left of the MPP, the duty cycle is increased to move towards the MPP.
- If $dI/dV < 0$, indicating the operating point is to the right of the MPP, the duty cycle is decreased to move towards the MPP.
- If $dI/dV \approx 0$, indicating that the system is close to the MPP, the duty cycle remains unchanged to fine-tune and maintain the MPP.

Above steps are performed iteratively, continuously adjusting the duty cycle to track changes in environmental conditions, such as sunlight intensity and temperature. This ensures that the PV system operates at or near its maximum power output.

The Incremental Conductance MPPT method is effective in quickly and accurately tracking the MPP of a PV system under varying conditions.

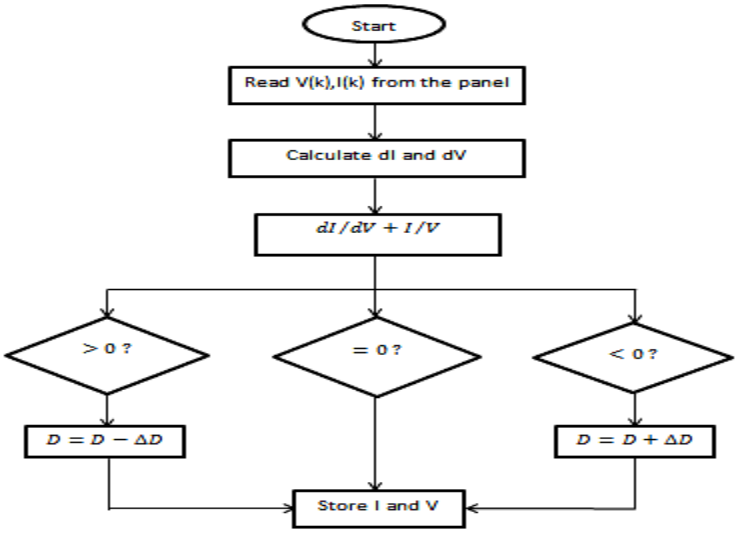

Fig 2.20: Flowchart of Incremental Conductance Method

Integral Regulator (IR): The IR algorithm uses an integral control loop to continuously adjust the duty cycle (in a PWM-based MPPT system) or the voltage reference (in a voltage-controlled MPPT system) to ensure that the system operates at the MPP. IR is known for its accuracy in steady-state conditions and its ability to handle noise and disturbances. The Integral Regulator Method is often combined with the Perturbation and Observation (P&O) method. In the P&O method, the system periodically perturbs (changes) the operating voltage or current and observes how the power output changes. It determines whether the power increases or decreases and adjusts the operating point accordingly. This process continues until the MPP is reached.The Integral Regulator Method adds an integral control component to the P&O method. This component helps in reducing oscillations around the MPP and fine-tunes the tracking process.

Hybrid Approach: HIC+IR combines the strengths of both IncCond and IR to provide a robust MPPT solution for PV systems. Here's how the hybrid approach typically works:

- Initially, the IncCond algorithm is used to quickly estimate the direction in which the MPP lies. It monitors the change in power and voltage and makes a preliminary adjustment.

- Once the IncCond algorithm identifies that the system is approaching the MPP, the IR algorithm takes over. IR uses its integral control loop to fine-tune the operating point and ensure that the PV system operates precisely at the MPP.
- The combination of these algorithms allows for fast tracking under changing conditions and precise tracking under steady-state conditions, leading to higher energy extraction efficiency.

The HIC+IR approach is effective in dealing with the dynamic nature of solar irradiance and temperature, making it a popular choice for MPPT in PV systems. It strikes a balance between speed and accuracy, resulting in improved energy yield compared to using either IncCond or IR alone.

2.9.2 Integration of PV Systems with DVR

DVRs are power quality devices used to regulate voltage fluctuations and maintain a stable grid voltage. They are particularly valuable in mitigating voltage sags and swells, which can lead to disruptions in sensitive loads. The integration of PV systems with DVRs allows for improved voltage regulation and enhanced grid stability.

Voltage Regulation

The integration of PV systems with DVRs enhances the grid's voltage regulation capabilities. DVRs can quickly respond to voltage sags and swells, while the PV system can provide additional reactive power support, helping to maintain voltage stability within the grid.

Grid Support during Faults

During grid faults, DVRs can inject compensating voltage to mitigate the impact of the fault on sensitive loads. Simultaneously, the PV system can continue to supply power, contributing to uninterrupted energy supply to critical loads.

2.9.3 Energy Storage System for DVR

Energy Management

PV systems integrated with DVRs can serve as a supplementary energy source for the DVR's energy storage system. During periods of excess PV generation, energy can be stored in the DVR's battery bank, ensuring a reliable power source during grid disturbances.

Backup Power Supply

In the event of prolonged grid outages or critical faults, the combined PV and DVR system can act as a backup power supply, providing continuous energy to critical loads and preventing costly downtime.

The integration of PV systems with MPPT algorithms like Incremental Conductance and Integral Regulator, combined with Dynamic Voltage Regulators using Space Vector Pulse Width Modulation and PR Controllers, offers numerous benefits for grid operation and energy storage. These integrated systems enhance voltage regulation, support grid stability, and provide backup power during grid disturbances. Future research should focus on optimizing the control strategies and assessing the economic viability of these integrated systems for widespread adoption in power distribution networks.

The key benefits of such an integration:

Improved Power Quality

One of the primary advantages is the improvement in power quality. The DVR can quickly respond to voltage sags and swells caused by grid disturbances, ensuring that the connected loads receive a stable and high-quality power supply. This is especially important for sensitive equipment and industrial processes.

Enhanced Voltage Support

The PV system can provide voltage support during normal operating conditions by injecting power into the grid. This can help maintain voltage levels within acceptable limits, reducing the likelihood of voltage sags and ensuring a more stable supply.

Efficient Energy Utilization

By mitigating voltage disturbances, the DVR prevents unnecessary interruptions and shutdowns of critical loads. This leads to more efficient energy utilization and minimizes production downtime, which can result in significant cost savings.

Grid Stability and Reliability

The integration of PV and DVR systems can contribute to grid stability and reliability. By mitigating voltage fluctuations, the grid becomes more resilient to disturbances, benefiting not only the connected facility but also neighboring consumers.

Optimal Utilization of PV Generation

The DVR helps maintain grid voltage within acceptable limits, allowing the PV system to operate optimally. During voltage sags, the DVR can compensate for the reduced grid voltage, ensuring that the PV system continues to generate electricity at its rated capacity.

Reduced Energy Costs

With improved power quality and reliability, businesses can reduce energy costs associated with downtime, equipment damage, and production inefficiencies. This can lead to significant savings in the long run.

Environmental Benefits

The integration of a PV system with a DVR promotes the use of renewable energy sources (solar power) while simultaneously enhancing the grid's stability. This contributes to reducing greenhouse gas emissions and supporting sustainability goals.

Regulatory Compliance

In some regions, grid operators have strict requirements regarding power quality and voltage stability. Integrating a DVR with a PV system can help meet these regulatory requirements, avoiding penalties and ensuring compliance.

Operational Flexibility

The integrated system provides operational flexibility, allowing for the seamless transition between grid-connected and islanded (standalone) modes of operation. This flexibility can be valuable in situations where grid reliability is a concern.

Long-Term Investment Protection

By safeguarding sensitive equipment and processes from voltage disturbances, the integrated PV-DVR system helps protect long-term investments in both the PV system and critical loads.

In summary, integrating a PV system with a Dynamic Voltage Restorer can provide a more stable and reliable power supply, reduce operational costs, enhance grid stability, and support the use of renewable energy sources—all of which contribute to improved energy sustainability and efficiency.

2.10 Control Strategy of DVR

2.10.1 Space Vector Transformation (SVT)

The DVR has a series injection transformer, VSI, solar-based DC link, and control circuit. The three-phase series trans- former is linked at the point of common coupling (PCC) with the transmission system to compensate for the grid voltage fluctuations. The main purpose of DVR is to retain the base-phase voltage. The reference voltage waveform is used for this purpose, which is similar to the development of the power. supply voltage. The required phase voltage is offset by the DVR system compared to the actual voltage pattern of the voltage difference. The actual voltage is compared to the voltage difference between the patterns of the phase shift of the voltage required by the DVR system. A block diagram of the proposed control scheme is shown in Figure 2.21.

The VSI is utilized to adjust the DVR power flow to provide appropriate reactive power to the transmission sys- tem. The DVR efficiency depends on the maximum voltage compensation capacity, actual injection direct current (DC) power transmission, and solar power connection system. The voltage applied from the DVR inverter converts the solid-state electronics and the PWM technique. Accordingly, the voltage applied is the phase angle of the controlled amplitude and the supply voltage. The DC connection of solar energy with the DVR input is provided for reactive power generation to create a steady output.

The proposed SVT method minimizes power losses and improves the voltage profile of the grid system. The measuring unit analyzes the voltage profile on the load side and signals the SVT optimizer. Based on the PWM feedback, the DVR inverter creates required voltage that feeds the distribution line through the PCC, optimizing power on the load side. This PWM technique also minimizes the harmonic content in the system.

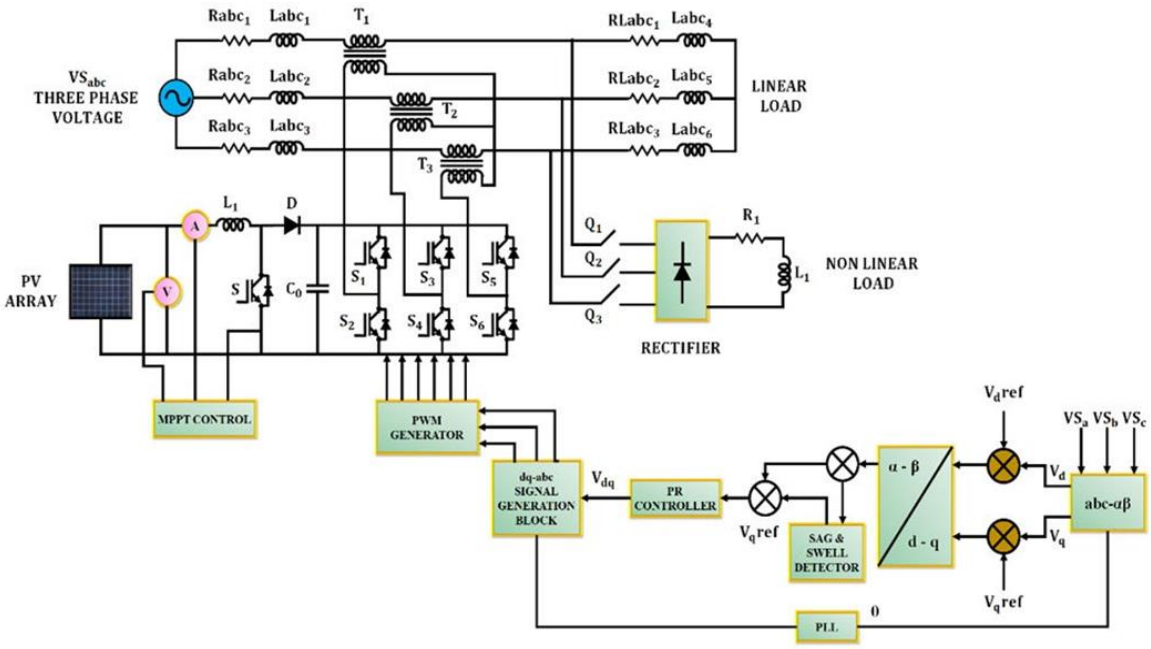

Fig. 2.21 A block diagram of the proposed control scheme

The control block diagram of PV supported DVR is shown in fig. 2.20. The system employs Space Vector transformations and method of unit vectors for reference signal estimation. The voltages at the PCC, V_S and load terminal V_L are sensed for deriving the IGBT gate signals. The reference load voltage V_L* is extracted using the derived unit vector.

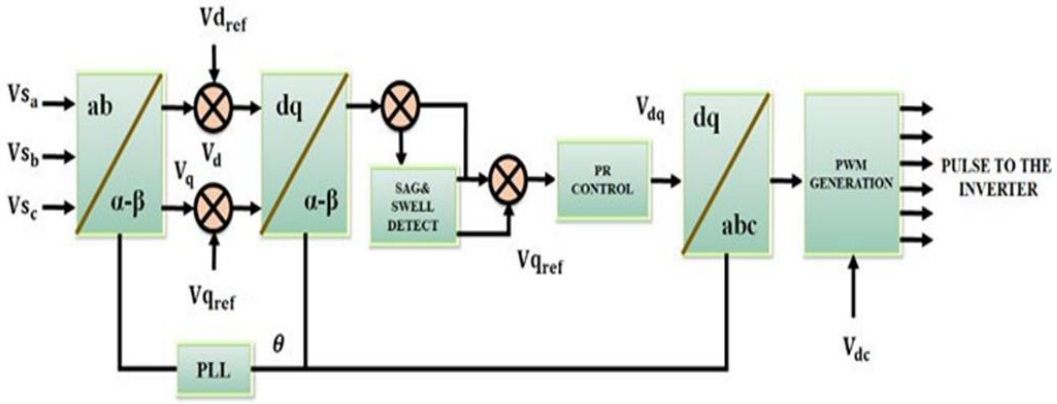

Fig. 2.22 SVT based-Control block diagram of PV supported DVR

Space vector modulation (SVM) is an algorithm for the control of pulse-width modulation (PWM). It is used for the creation of alternating current (AC) waveforms; most commonly to drive 3 phase AC powered motors at varying speeds from DC using multiple class-D amplifiers. There are variations of SVM that result in different quality and computational requirements. One active area of development is in the reduction of total harmonic distortion (THD) created by the rapid switching inherent to these algorithms.

A three-phase inverter as shown to the right converts a DC supply, via a series of switches, to three output legs which could be connected to a three-phase motor.

The switches must be controlled so that at no time are both switches in the same leg turned on or else the DC supply would be shorted. This requirement may be met by the complementary operation of the switches within a leg. i.e. if A+ is on then A− is off and vice versa. This leads to eight possible switching vectors for the inverter, V0 through V7 with six active switching vectors and two zero vectors.

Vector	A^+	B^+	C^+	A^-	B^-	C^-	V_{AB}	V_{BC}	V_{CA}	
V_0 = {000}	OFF	OFF	OFF	ON	ON	ON	0	0	0	zero vector
V_1 = {100}	ON	OFF	OFF	OFF	ON	ON	$+V_{dc}$	0	$-V_{dc}$	active vector
V_2 = {110}	ON	ON	OFF	OFF	OFF	ON	0	$+V_{dc}$	$-V_{dc}$	active vector
V_3 = {010}	OFF	ON	OFF	ON	OFF	ON	$-V_{dc}$	$+V_{dc}$	0	active vector
V_4 = {011}	OFF	ON	ON	ON	OFF	OFF	$-V_{dc}$	0	$+V_{dc}$	active vector
V_5 = {001}	OFF	OFF	ON	ON	ON	OFF	0	$-V_{dc}$	$+V_{dc}$	active vector
V_6 = {101}	ON	OFF	ON	OFF	ON	OFF	$+V_{dc}$	$-V_{dc}$	0	active vector
V_7 = {111}	ON	ON	ON	OFF	OFF	OFF	0	0	0	zero vector

Table. 2.22 Switching Vectors of SVT

To implement space vector modulation, a reference signal Vref is sampled with a frequency

fs (Ts = 1/fs). The reference signal may be generated from three separate phase references using the αβγ transform. The reference vector is then synthesized using a combination of the two adjacent active switching vectors and one or both of the zero vectors. Various strategies of selecting the order of the vectors and which zero vector(s) to use exist. Strategy selection will affect the harmonic content and the switching losses

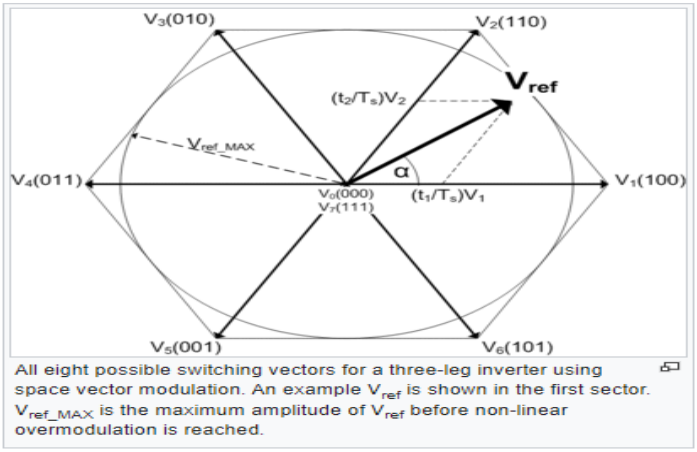

All eight possible switching vectors for a three-leg inverter using space vector modulation. An example V_{ref} is shown in the first sector. V_{ref_MAX} is the maximum amplitude of V_{ref} before non-linear overmodulation is reached.

Fig. 2.23 Switching Vectors of SVT

2.10.2 Proportional-Resonant (PR) Controller Based DVR

In comparison to traditional schemes, the PR controller not only achieves improved frequency domain stability, but also contributes to superior current tracking behavior and limits the THD in the proposed strategy. An ideal PR controller, which is mathematically attained by converting an ideal synchronous frame PI controller to a stationary frame that has infinite gain at resonant frequency ω_0.

$$G_C(s) = K_p + \frac{2K_i s}{s^2 + \omega_0^2} \qquad \text{…….. (2.13)}$$

Where,

ω_0=Resonant Frequency

K_p=Proportional Gain

K_i= Integral Gain

$S^2+ \omega_0^2$= produces infinite gain at reference frequency

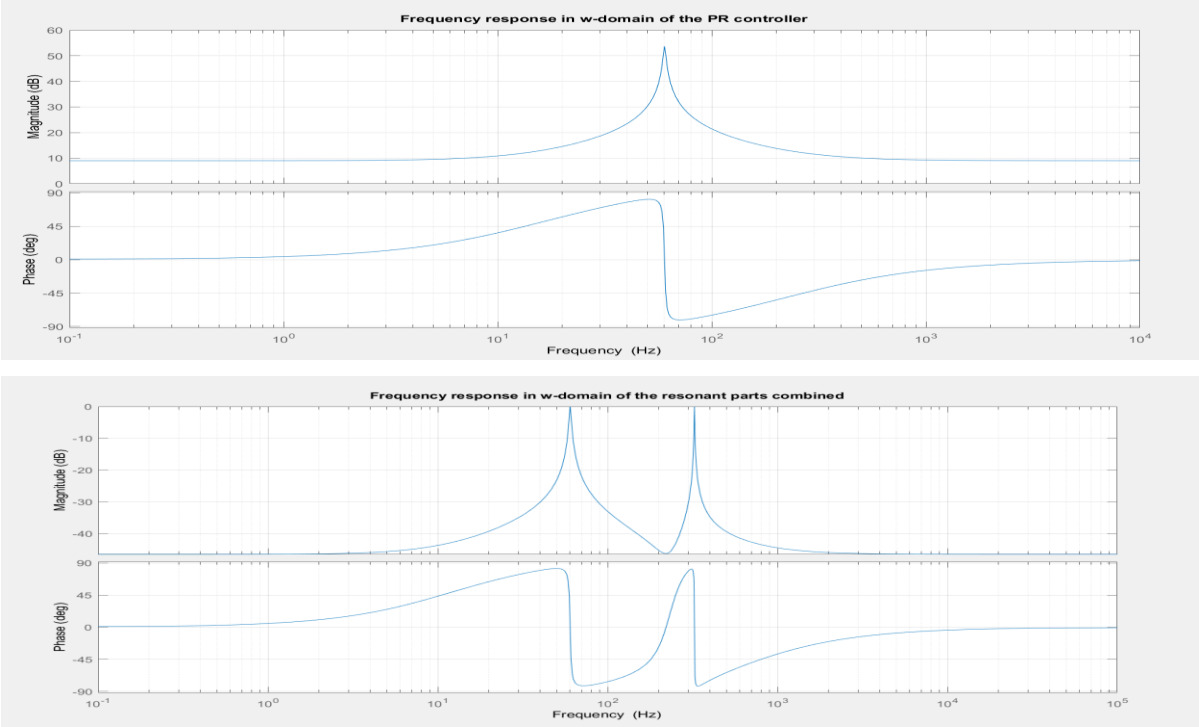

Fig. 2.24 Bode Plots of frequency response in w-domain of PR controller (Matlab)

CHAPTER 3: PROPOSED METHDOLOGY

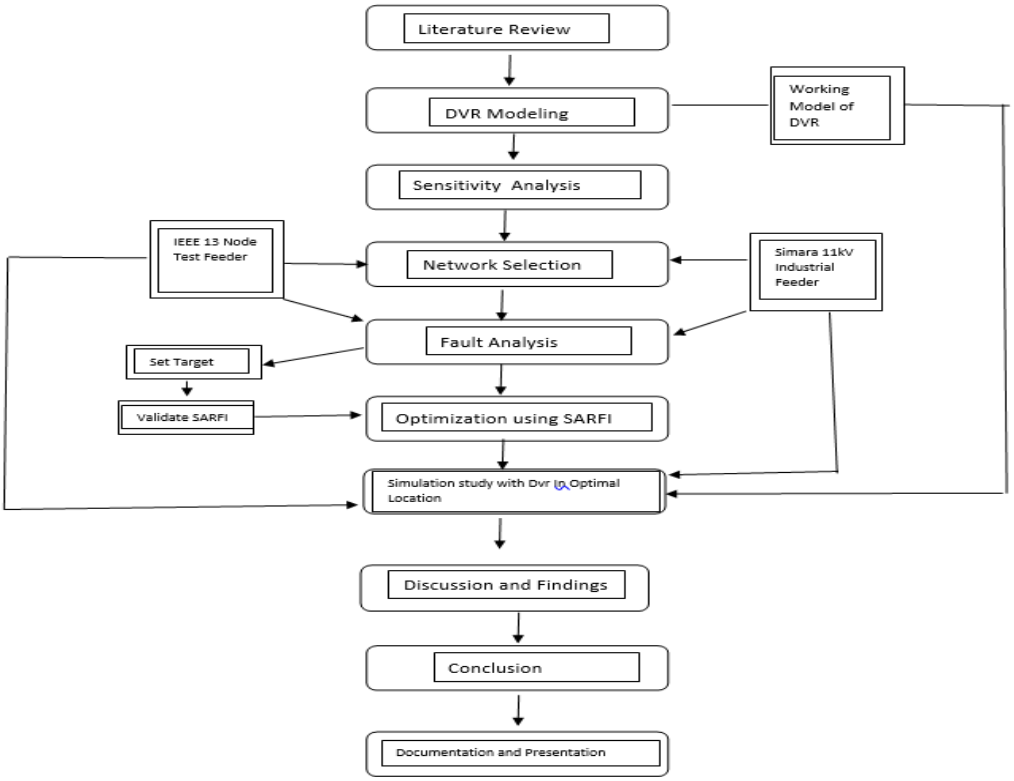

Fig 3.1: Flow diagram of Methodology

3.1 Literature Review

A significant portion of the research was covered by the literature review. Books, journals, papers, articles, and standard regulations were thoroughly studied and reviewed throughout the project. The literature review mainly focuses on finding out the effect of voltage disturbances on power quality and grid operation as a whole, different types of CPDs, mitigating voltage sag using CPDs, the working mechanism of DVR, and optimization techniques were extremely prioritized to obtain the required background for the study. Moreover, in this process, the required assumptions and theories were noted so that to be used in the project, as explained in Chapter Two.

3.2 DVR Modelling and Sensitivity Analysis

The System is modeled and designed in MATLAB 2023a software. The SIMULINK model of DVR has been developed with the necessary boundary conditions, and parameters were according to the reviewed literature. It has been installed into a simple power system to study performance efficiency. Furthermore, in order to have an effective response from DVR, it is desired for the change in the developed model is able to operate in a wide range of load power demand and length of the distribution line (l) from DVR interconnection node to the node whose voltage is to be studied. MATLAB sensitivity analyzer toolbox has been used to perform a sensitivity analysis of the DVR connected system to evaluate how the parameters of a model influenced the output voltage and to determine the certainty of load voltage at the nodes following the DVR interconnection point being more than 90% of the normal threshold value. The complete description of DVR modeling is presented in Chapter Two.

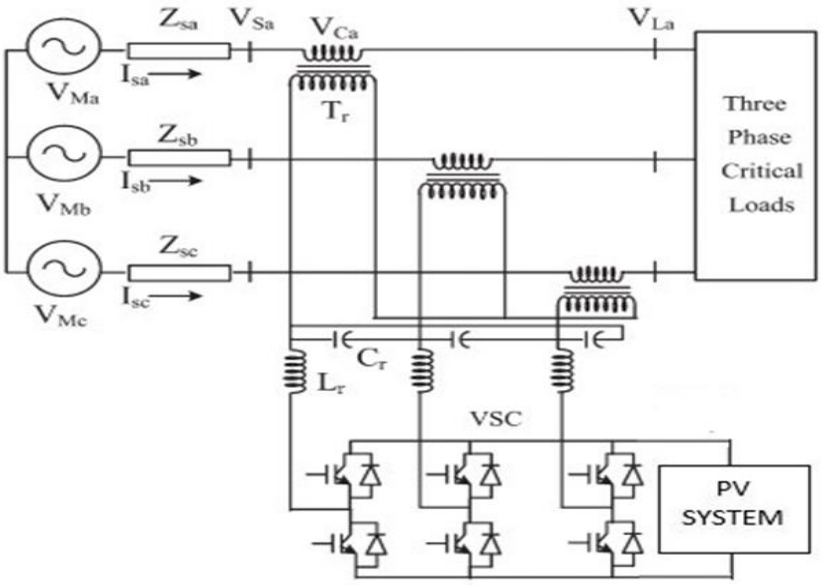

Fig 3.2: Schematic Diagram of the Proposed System

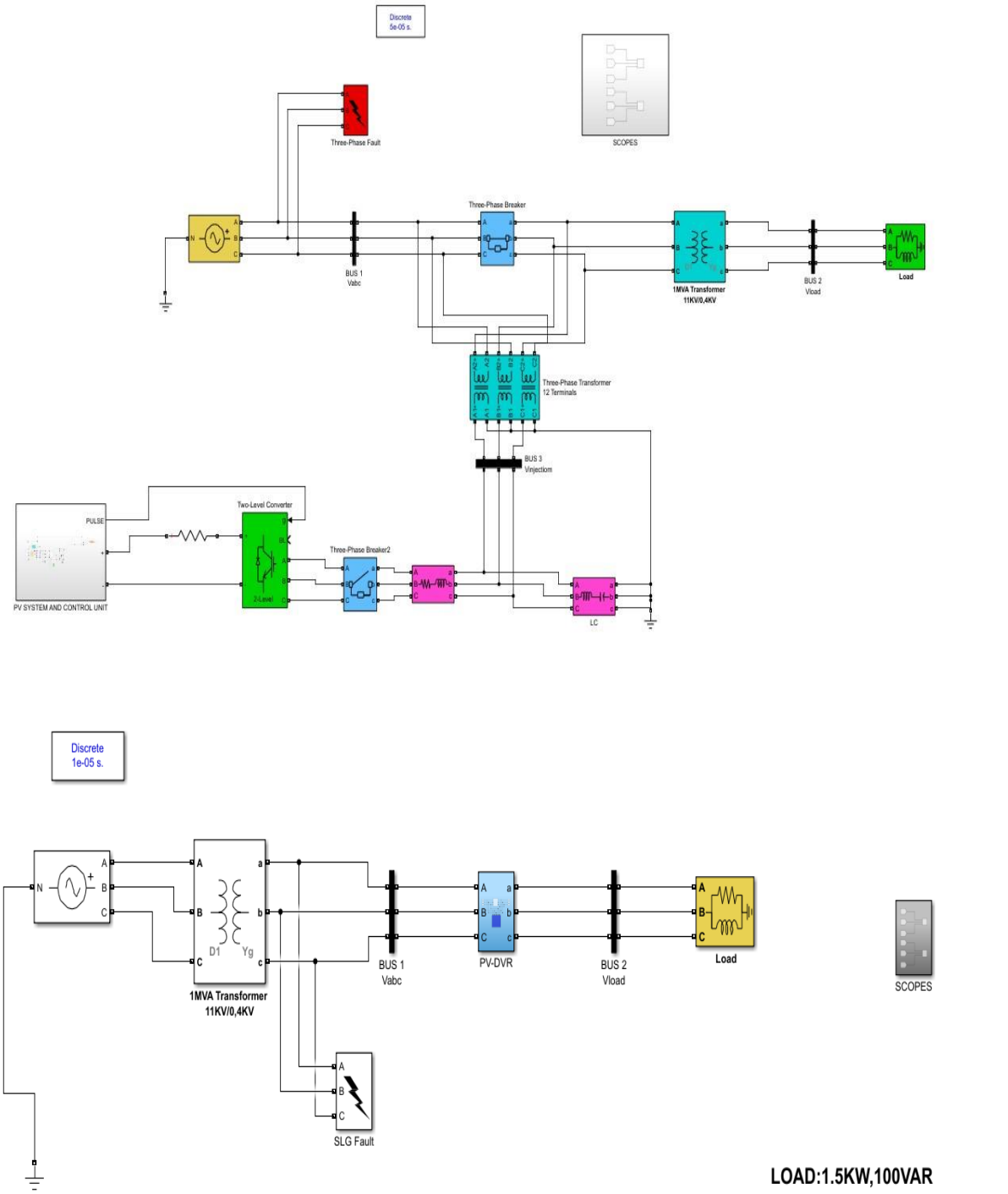

Fig 3.3: Modeling of Proposed System in MATLAB

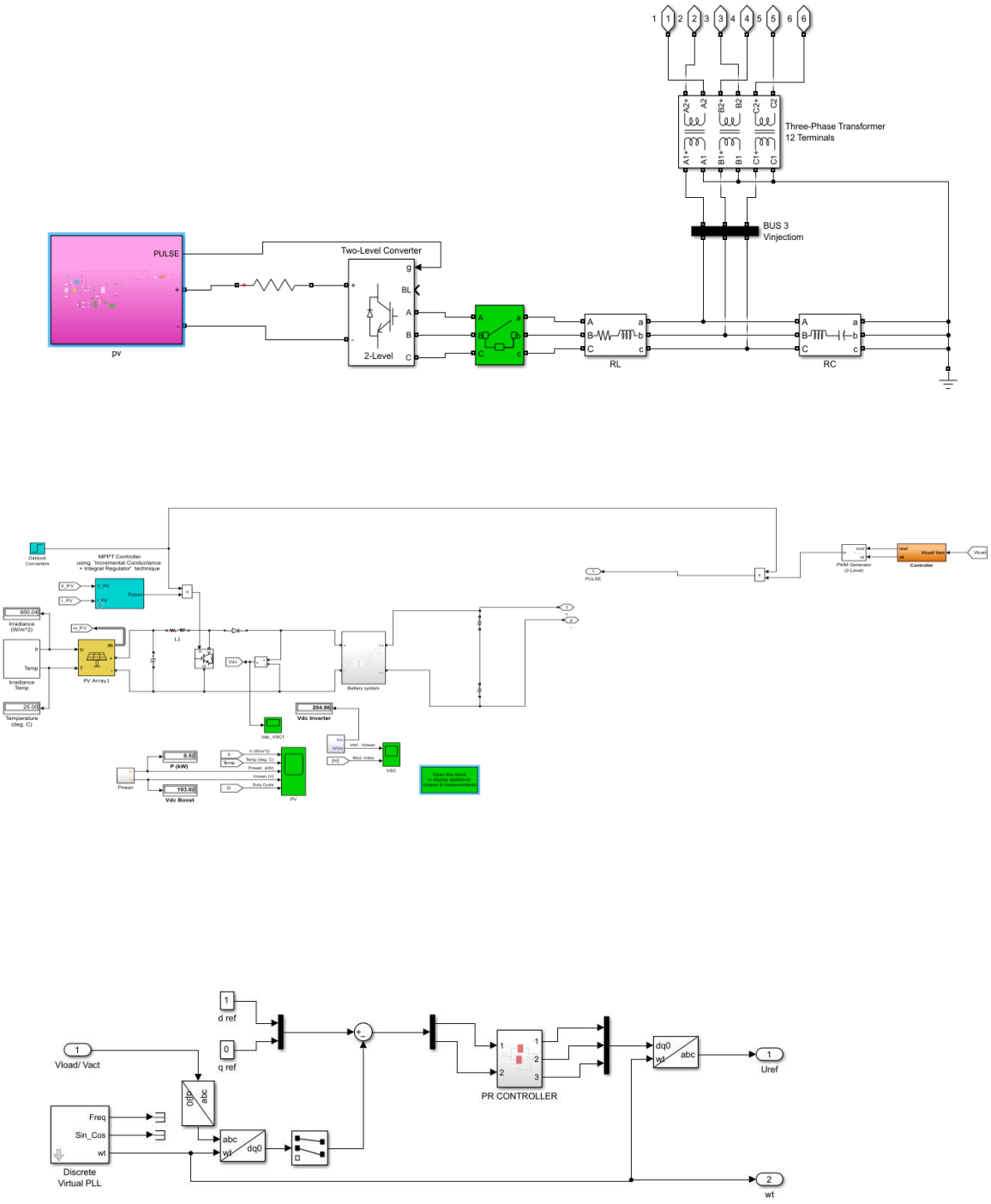

Fig 3.4: Control Blocks with PV System in MATLAB

3.2.1 Parameters Design of DVR

The system described utilizes an 11 kV, 50 Hz three-phase power source that is connected to a transmission line through an 11 kV/0.4 kV transformer configured in a Delta/Star configuration. This transformer steps down the grid voltage to 400 V, enabling the utilization of low-voltage-sensitive loads, and the entire system operates at a frequency of 50 Hz.

To assess the system's performance under various conditions, voltage sags are artificially induced by simulating different faults between the power source and the load. Additionally, voltage swells are externally simulated using a three-phase programmable source within the MATLAB platform. This comprehensive testing helps evaluate how the system responds to voltage fluctuations and ensures its reliability under varying conditions.

PV system with Energy Storage Device

The choice of the energy storage device plays a crucial role in determining the power rating of a Dynamic Voltage Restorer (DVR) and its effectiveness in mitigating voltage sag/swell events. High-voltage energy storage is not well suited for high-voltage systems, which is why DVRs are predominantly employed in medium and low-voltage applications. Given that the energy storage component is one of the costliest parts of a DVR, it must be selected with precision.

To determine the appropriate energy storage device for a Photovoltaic (PV) integrated DVR, several factors need consideration. First, the voltage level at which the PV-integrated DVR is to be connected must be assessed. Then, the desired level of voltage sag mitigation is determined. Based on this, the minimum voltage rating for the energy storage device that meets these requirements is selected.

For the design of a model system with a 1.5 kW load at 400V, a PV system (MATLAB Module –Sunpower SPR-305E-WHT-D) with a rating of 257V and 1.22 kW, along with a 220V, 100AH Lithium Ion Battery for energy storage (resulting in a DC link voltage of 205V), has been chosen. This configuration aims to compensate for almost all conceivable magnitude of voltage sags/swells in the system, in an ideal scenario.

The load voltage requirement dictates the DC voltage requirement for the DVR's energy storage in a radial distribution network. In a radial distribution feeder operating at 11kV, it has been observed that an energy storage system with a voltage rating of 5kV can effectively mitigate voltage sags, restoring voltages at the buses above 0.97 per unit (p.u.) (Gupta, et al., 2010). However, this serves as a preliminary guideline for sizing the DC storage system. The actual load distribution and system parameters must be considered when selecting the voltage level for the DC storage system.

For 11kV systems, a PV system with a rating of 6.12kV and 136.74 kW, along with a 6kV, 1000AH Lithium Ion Battery for energy storage (resulting in a DC link voltage of 6kV), has been chosen. This configuration is designed to mitigate voltage sag effectively.

Further investigation into voltage sag mitigation by DVR involved increasing the voltage level of the DC storage system. For storage levels of 5kV, 5.5kV, and 6kV, the voltages were restored to 0.93 p.u., 0.96 p.u., and 0.99 p.u., respectively. However, when the voltage level was increased to 6.5kV, voltage sag occurred, with voltages reaching up to 1.05 p.u. during the maximum fault conditions simulated in the system. Consequently, the optimal size of 6kV was selected as the voltage level for DC energy storage in both of the 11kV radial distribution networks under investigation.

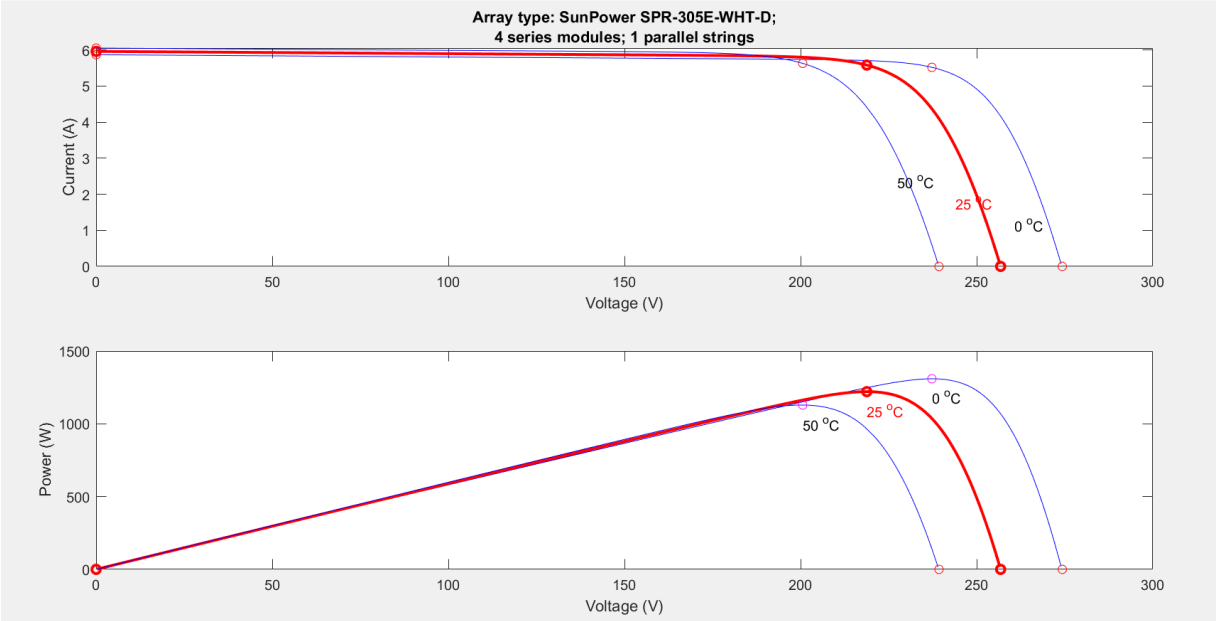

Fig 3.5: PV System I-V and P-V Curves of model test system in MATLAB

Voltage Source Inverter

The choice of the inverter is primarily influenced by several key factors, including the type of connection, power quality standards, cost considerations, gate drive speeds, and overall compatibility with the system. In this context, IGBT switches have been selected as the preferred components for the converters. IGBT switches offer distinct advantages, including ease of control and the ability to operate effectively across a wide power range, which makes them a suitable choice for this application. To implement the inverter circuit, a straightforward design has been adopted for each phase, featuring four IGBTs that are controlled through a relay. This configuration ensures efficient and precise control of the inverter, aligning with the specific requirements and objectives of the system.

Injection Transformer

To determine the appropriate turn ratio (n) for a transformer, it is essential to consider both the desired injection level into the grid and the inverter's capability to provide that injection level. Careful selection of the transformer's voltage ratings is crucial, as underrating can lead to core saturation, while overrating results in unnecessary additional costs. In our design, each phase incorporates a 1.5KVA series injection transformer with a 1:10 turn ratio. The windings are rated at 10kV and 100kV, with a winding resistance of 0.00001 per unit (p.u.) and inductance of 0.0003 p.u. This configuration is designed to operate the load at a rated voltage of 400V.

When operating the DVR in an 11kV system, the transformer's ratings should be carefully chosen to meet the current and voltage requirements of both the grid, DC storage, and inverter. In the study, a MATLAB model was used, featuring three single-phase transformers, each rated at 150KVA with a transformation ratio of 10kV/100kV. This combination of three single-phase transformers effectively interfaces with the three-phase voltage generated by the combination of three single-phase inverters into the 11kV grid. This approach ensures efficient and reliable operation of the DVR within the 11kV system.

Harmonic Filter

In our model, LC filters play a crucial role in eliminating high-frequency harmonic

components from the voltage supplied by the Voltage Source Converter (VSC). As a general guideline, when designing a system where a Dynamic Voltage Restorer (DVR) needs to be operated, the selection of inductance (L) and capacitance (C) values is critical. The inductor (L) should be chosen to provide a high impedance path for high-frequency ripples, effectively blocking these unwanted components, while offering a low impedance path for the fundamental frequency, allowing it to pass through smoothly. The capacitance (C) selection should result in a high-pass filter behavior, with a cutoff frequency approximately half of the inverter switching frequency. This choice ensures that low-frequency components, including the fundamental voltage, can pass through the filter while attenuating the high-frequency harmonics.

For our specific design requirements:

In the 400V system, filters with values of L=0.1H (Henry) and C=5µF (microfarads) were employed. These values effectively filtered out the ripples in the inverter output, resulting in a sinusoidal output voltage suitable for supplying the load.

In the 11kV system, filters with values of L=1e-5H (Henry) and C=4900µF (microfarads) were utilized. These values were found to be effective in eliminating high-frequency components from the inverter output, ensuring that the voltage supplied to the load remained sinusoidal and met the desired quality standards.

By carefully selecting these L and C values, the LC filters contribute significantly to the overall performance and power quality of the DVR system in both the 400V and 11kV environments.

Reference Voltage Generation

The reference voltage generation block plays a pivotal role in the control of the Photovoltaic (PV) integrated Dynamic Voltage Restorer (DVR). It operates by comparing the desired load voltage with the actual voltage at the load terminal. Based on this comparison, it calculates the voltage that needs to be injected or absorbed by the DVR to meet the desired voltage level. The control of the PV integrated DVR relies on this reference voltage. The circuit diagram for generating the reference voltage for controlling the voltage injection in all three phases of the DVR is depicted in Figure 3.4.

Here's a breakdown of the process:

Phase Information Capture: The system first acquires information about the phase of the source voltage using a Phase-Locked Loop (PLL), assuming a frequency of 50 Hz. This phase information is essential for synchronizing the reference voltage generation for each phase.

Desired Voltage Calculation: With the phase information in hand, the system generates the desired voltage ($vpeak$. n (wt)) for each of the three phases (A, B, and C). These desired voltage values are phase-shifted by 120 degrees from each other, as is commonly done in three-phase systems.

Voltage Error Calculation: The actual voltage at the load terminal (Vload) is then subtracted from the desired voltage of each phase at each instant in time. This subtraction process results in the generation of a three-phase reference voltage. This reference voltage reflects the discrepancy between the actual and desired voltages for all three phases.

Control Action: The reference voltage values obtained in the previous step serve as a basis for determining the amount of voltage that the DVR should inject or absorb to correct the voltage to its desired value. This control action is carried out to ensure that the load receives the appropriate voltage.

More comprehensive explanation of the control strategy employed, particularly the utilization of Space Vector Pulse Width Modulation (SVPWM) integrated with a Proportional-Resonant (PR) Controller, is explained in Chapter two, where the control methodology is detailed and discussed in depth. This strategy plays a crucial role in achieving the desired voltage quality and ensuring the effective operation of the PV integrated DVR. Other Details of Control scheme with PR controller are attached in the Appendix.

3.3 Optimal Placement of DVR

Optimal location was determined with the objective of minimization of System Average RMS Frequency Index (SARFI) of the system in the presence of DVR. The objective is given by,

$$SARFI_X = \frac{\sum_{i=1}^{n} n_i x}{n}$$

……..(2.14)

Where,

X=RMS voltage threshold

nix=number of voltage sags lower than the specified threshold

n= total number of connected loads (with all the buses) .The objective function is then given by,

$$y = \min\left(SARFI_X\right) = min\left(\frac{\sum_{i=1}^{n} n_i . x}{n}\right)$$

…… (2.15)

The sag threshold X is considered as 0.9 or 90% and swell threshold is considered 1.1pu or 110%, which indicates that we compute the system average sag frequency based on the number of buses whose voltages go below 90% and go above 110% of the nominal threshold value during a fault.

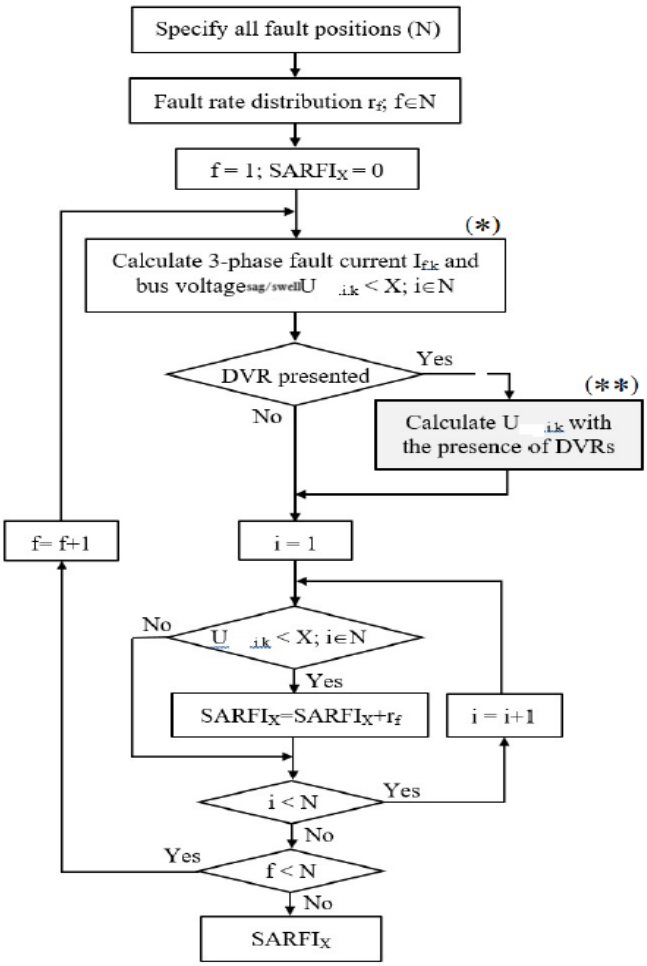

Fig 3.5: Flowchart for Calculation of SARFI

3.4 Selection of Network

In order to achieve the objectives of this thesis, IEEE 13 Node Test Feeder and 11kV Simara Industrial Feeder have been selected. The data for the standard IEEE 13 Node Test Feeder , Section of 11Kv Tanahusur Feeder of Tanahu District (Tanahu DCs) and 11kV Simara Industrial Feeder of Bara District (Simara DCs) has been obtained from the literature review, and the required information is shown in Appendix. The optimal placement of PV-integrated DVR units in all three systems has been achieved through the SARFIX approach. The proposed PV-DVR system has demonstrated remarkable effectiveness in alleviating voltage sag and swell issues across all three systems, even during faulted and overloaded conditions. Furthermore, this advanced PV- DVR technology has exhibited the capability to sustain the

bus voltage at the farthest location at approximately 0.95 per unit, highlighting its robust performance in ensuring consistent and stable power supply.

3.4.1 IEEE 13 Node Test Feeder

The IEEE 13 Node Test System, also known as the IEEE 13 Bus Test System, is a commonly used power distribution system test case in the field of electrical engineering and power systems analysis. It serves as a benchmark system for various studies, simulations, and research related to power distribution and grid analysis. This system represents a simplified but realistic model of a portion of an electrical distribution network. It is a 4.16kV/0.48kV, 60Hz, 3582kW, 1746KVAR system with overhead and underground lines with 1 regulator, one distribution transformer and one circuit breaker. All parameters of the system are attached in Apendix A. Proposed PV integrated DVR was able to maintain the bus voltages nearly around 0.95p.u.to 1 p.u. in all types of faulted conditions

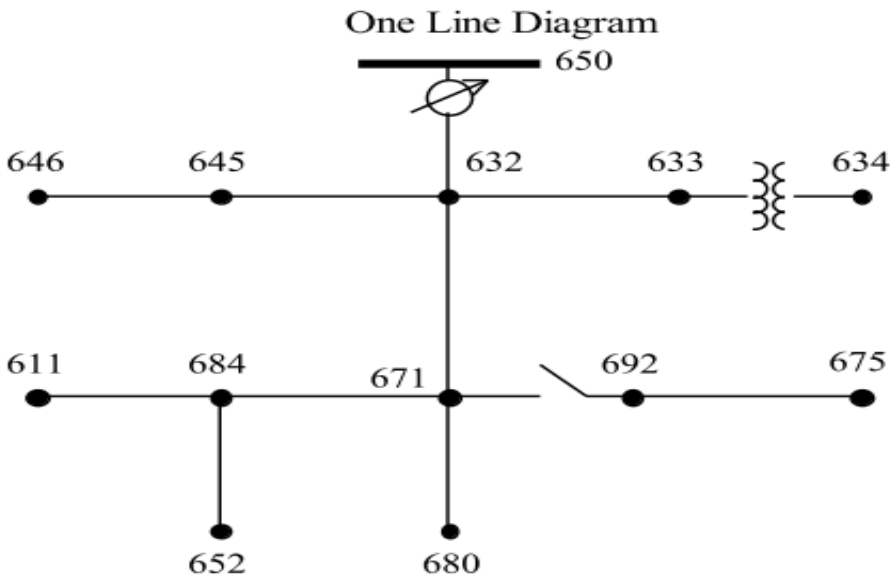

Fig 3.6: IEEE 13 Node Test Feeder

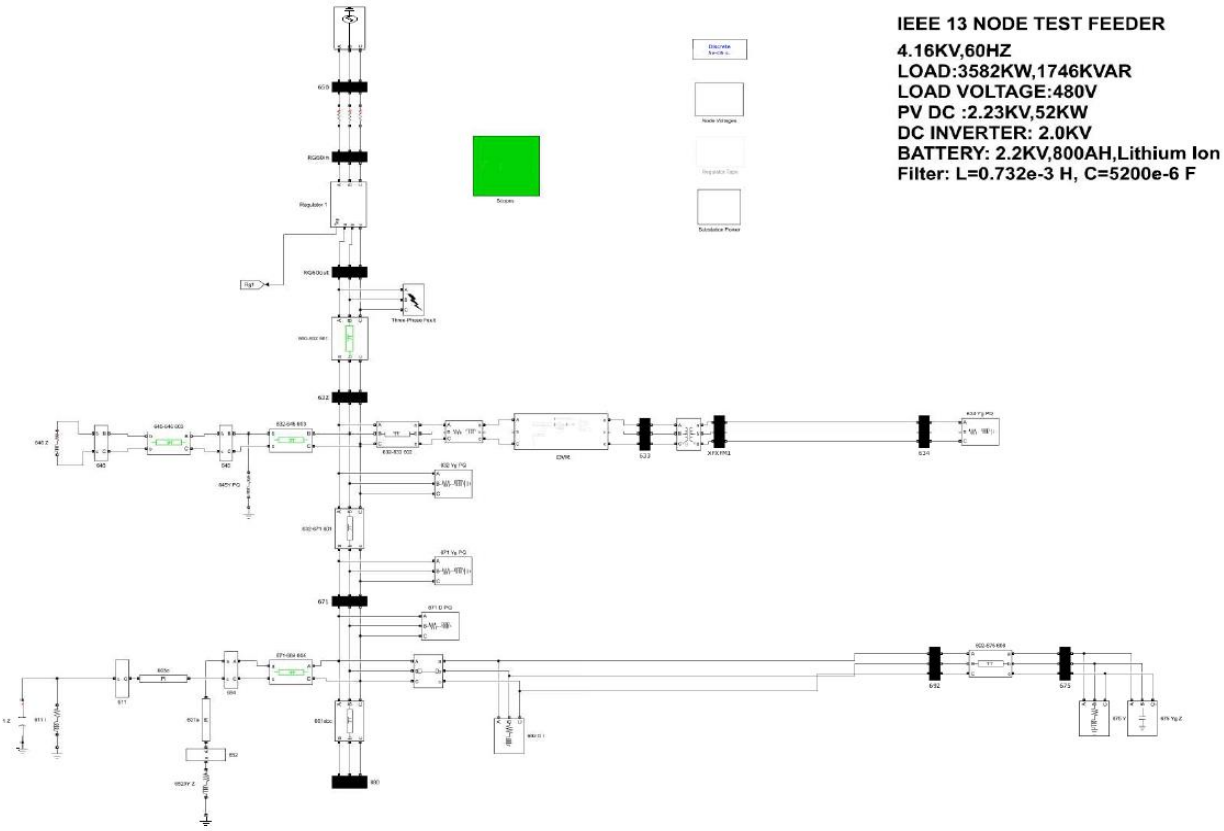

Fig: 3.7: Modeling of IEEE 13 Node Test Feeder with DVR in MATLAB

3.4.2 A Section of 11kV Tanahusur Feeder

The 11kV Tanahusur feeder, situated in Tanahu District within the jurisdiction of Tanahu DCs, Gandaki Province, Nepal, encompasses a 3.2km stretch (with Dog Conductor upto bus 2 and Weasel Conductor thereafter), spanning from Damauli S/S to the line section cut-out in Ghasikuwa. This segment comprises four 11/0.4kV transformers, including one privately owned by Taalghare Wood Industry, with a collective installed capacity of 250Kva.In the feeder the application of PV-DVR is observed in single and well as multiple (Two) locations during various fault conditions i.e. LG, DLG, DL, LLL, LLLG faults. Furthermore, fault locations are discerned through data collection within Tanahu DCs, where the occurrence of faults is most prevalent.

PV-DVR in Single Location of the feeder:

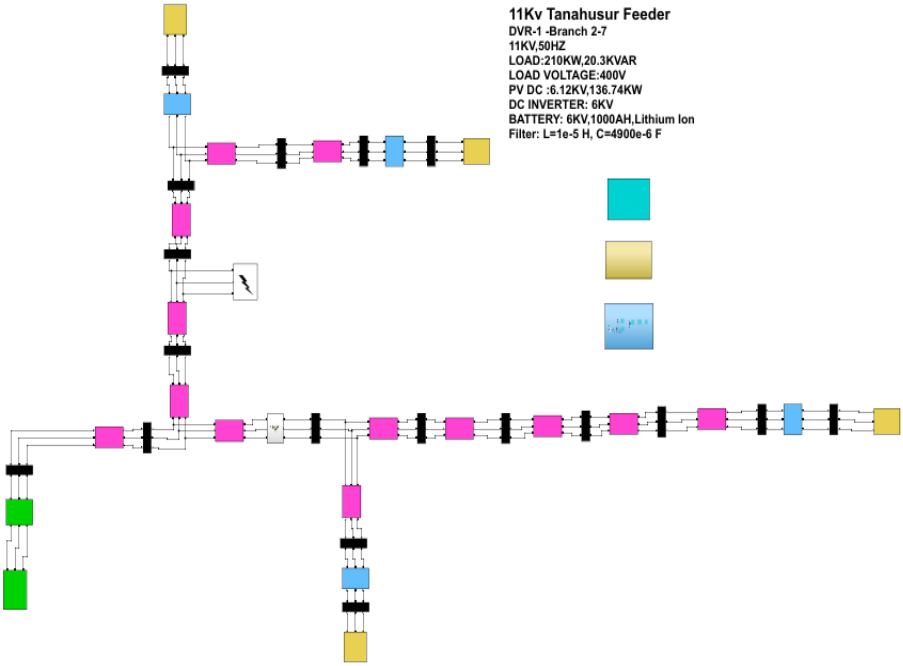

Fig: 3.8: Modeling of 11Kv Tanahusoor Feeder with DVR in MATLAB (single location)

PV-DVR in Multiple (Two) Location of the feeder:

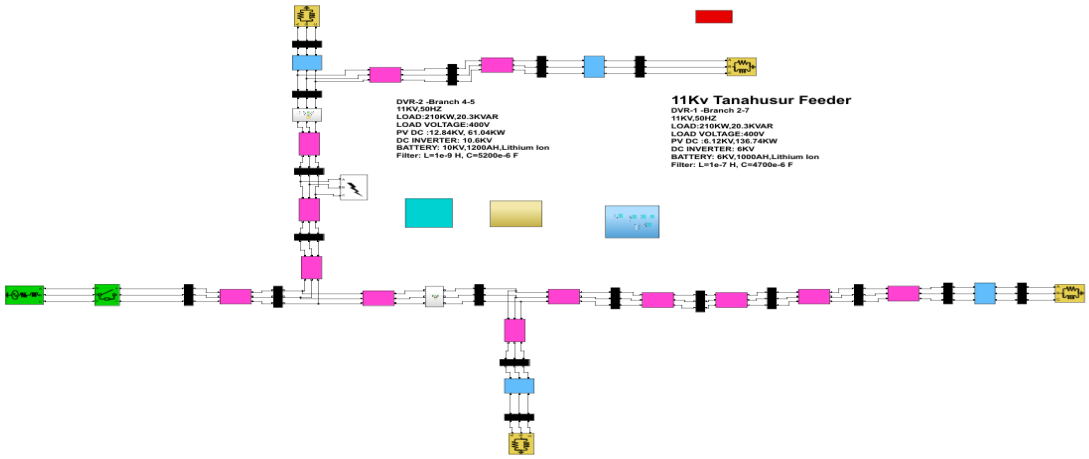

Fig: 3.9: Modeling of 11Kv Tanahusoor Feeder with DVR in MATLAB (Two location)

3.4.3 11kV Simara Industrial Feeder

Normal loading Conditions:

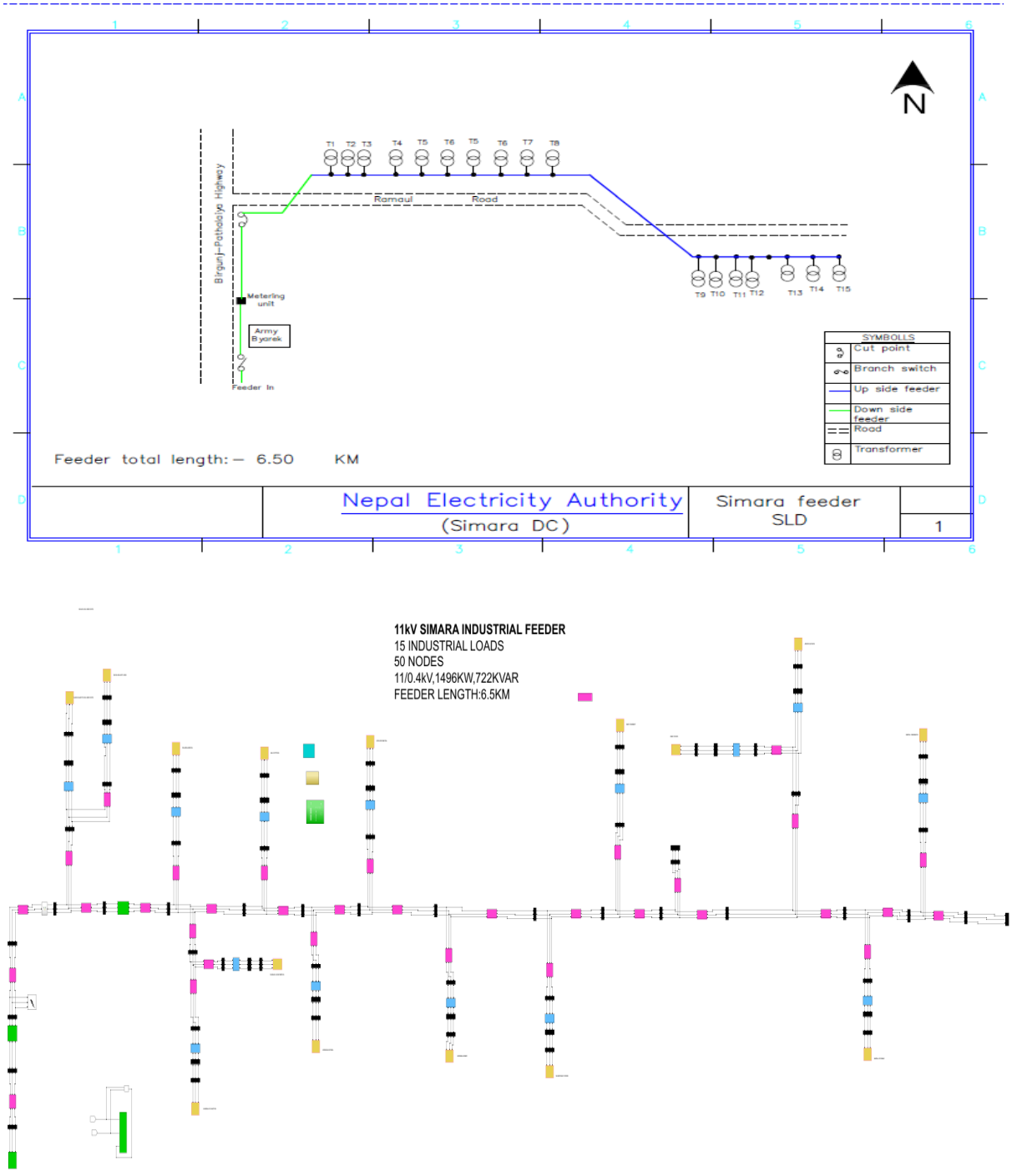

Fig: 3.10: Modeling of 11kV Simara Industrial Feeder with DVR in MATLAB (Normal Loading)

The 11kV Simara Industrial feeder, situated in Bara District within the jurisdiction of Simara DCs, Madesh Province, Nepal, encompasses a 6.5km stretch with all Dog Conductor, spanning from 132/11 Parwanipur S/S to the line section of last Industrial load Nepal Ceramics. This segment comprises of 15 private 11/0.4kV transformers, with a collective installed capacity of 14.07MVA. Notably, it's important to recognize that all connected loads do not operate simultaneously during peak load periods. The feeder's load capacity, with a capacity of approximately 5.71MVA on a Dog Conductor, accommodates a peak loading of 300A. Under normal operating conditions, data gathered from each Time-of-Day (TOD) meter of the connected loads reveals a simulated load demand of 1.66MVA(at one of the instances).

In the feeder the application of PV-DVR is observed in single and well as multiple (Two) locations during various fault conditions i.e. LG, DLG, DL, LLL, LLLG faults. Furthermore, fault locations are discerned through data collection within Simara DCs , where the occurrence of faults is most prevalent. Proposed PV integrated DVR was able to maintain the bus voltages nearly around 1p.u. in all types of faulted conditions. Table Below shows the install capacity of different Industrial load in the samara feeder.

S.N.	Location	Capacity (KVA)
1	Shiv shakti oil and fats	320
2	Shiv shakti agri	700
3	Rajesh metal	4600
4	B.G. Cotton	50
5	Krishna steel 1	850
6	Shubha laxmi metal	600
7	Harsa plastic	110
8	Gorkha feed	800
9	Narayani food product	500
10	RMC cement	1750
11	Win win metal ind .	300
12	Josis Gyavin	196.25
13	Nepal stonex	550
14	Nepal ceramic	1250
15	RMC food	1500
Total		**14076.25**

Table: 3.11: Installed Load of Simara Industrial Feeder

Overloading Conditions:

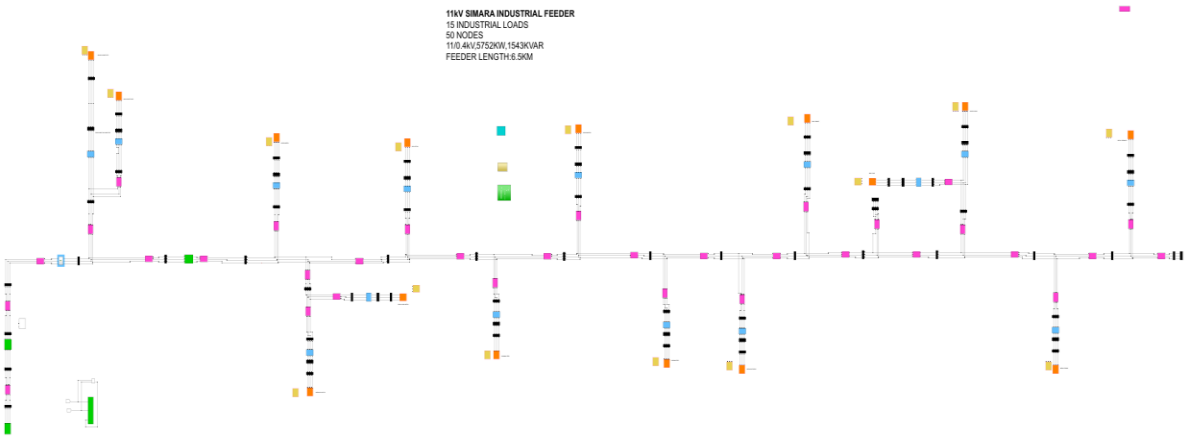

Figure: 3.11: Modeling of 11kV Simara Industrial Feeder with DVR in MATLAB (Overload Loading)

As we know connected loads do not operate simultaneously during peak load periods. The feeder's load capacity, with a capacity of approximately 5.71MVA on a Dog Conductor, accommodates a peak loading of 300A. Under one of the operating conditions, data gathered from each Time-of-Day (TOD) meter of the connected loads reveals a simulated load demand of 5.955MVA(at one of the instances) which is load of 312A on the feeder. The relay for the feeder has an overload setting of 320A. When the current in the feeder reaches 312A, only buses 1, 2, and 3 maintain a voltage of 1 per unit (p.u.), while all buses beyond that experience a voltage drop from 0.83 p.u. to 0.89 p.u., with the farthest bus being the most affected.

After installing a PV Integrated DVR between buses 4 and 5(optimal location), the DVR successfully maintains bus voltage between 0.95 p.u. and 1 p.u. as we move from the farthest bus to the nearest one.

3.5 Modelling and Fault Analysis of Network

All three systems are designed in the MATLAB/ SIMULINK environment where they were simulated and tested for their performance. The developed models were analyzed by conducting fault analysis on it. Different faults LG, LL, LLG, and LLLG faults were created

in each bus, and then the simulations were conducted, and the voltage profiles under the fault conditions were tabulated in Appendix C .

3.6 Discussion on Findings

The effectiveness of the developed DVR model has been validated as the model mitigates voltage sags and swells occurring in the load, even when the fault occurs. Sensitivity analysis has shown that the DVR can respond effectively to change in various parameters and maintain a safe voltage level in the network that demonstrates the feasibility of applying DVR to network. The optimal location has been determined SARFI approach.

3.7 Documentation and Presentation of the Findings

As per the guidelines of IOE, all the results from the research, works have been documented.

CHAPTER 4: SIMULATION AND RESULTS

4.1 Voltage Sag/ Swell and Harmonics Mitigation by PV Integrated DVR in Model Test System.

4.1.1 Compensation of Balanced Voltage Sag and Swell(Model Test System)

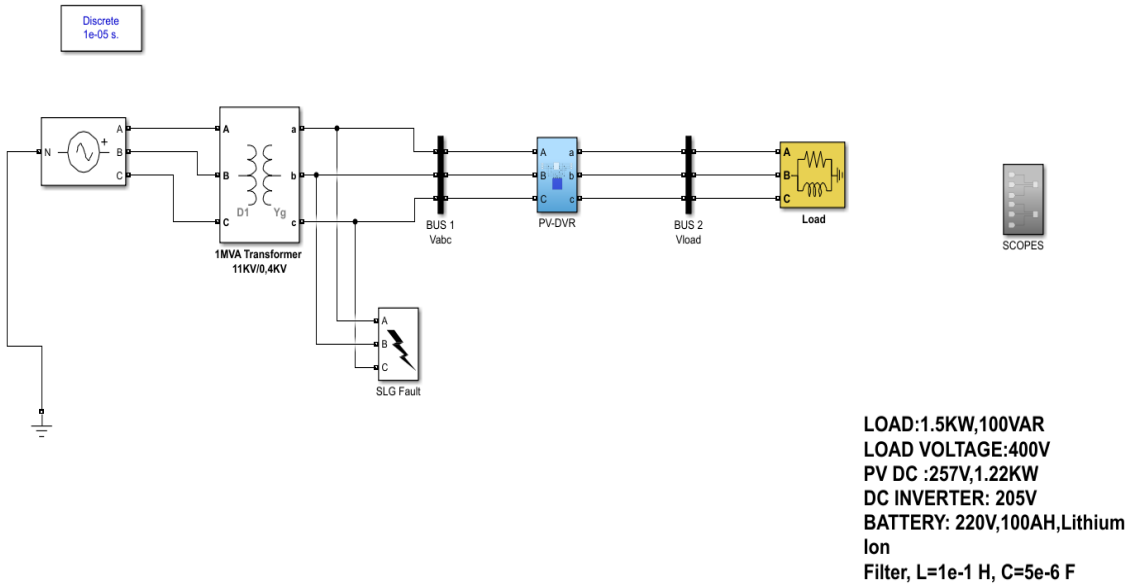

Fig 4.1: Modeling of Proposed System in MATLAB

The investigation of the PV-integrated DVR model's response to various voltage disturbances was conducted through simulation. A three-phase balanced fault scenario was simulated, lasting for a duration of 0.1 seconds, occurring between t=0.2s and t=0.3s. This

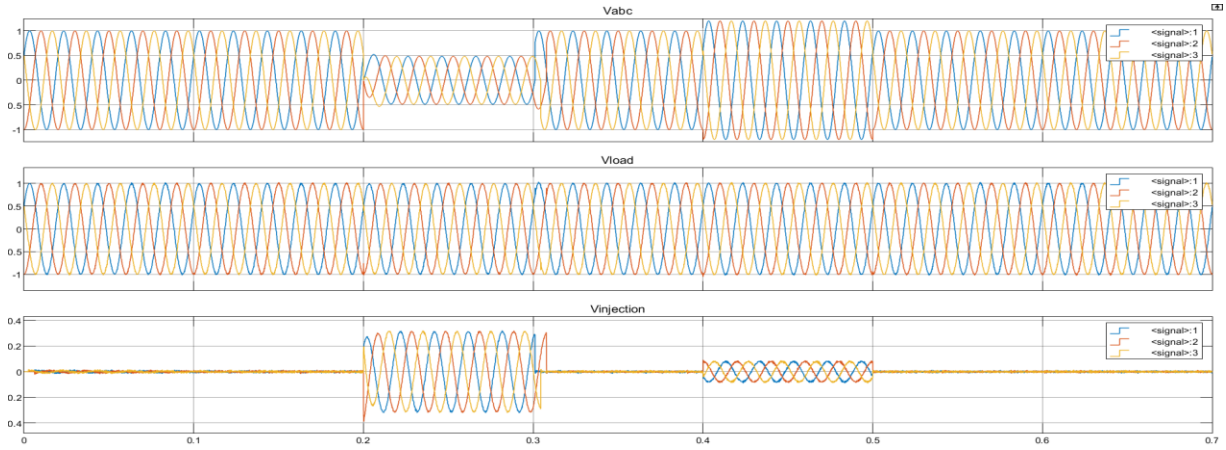

Fig 4.2: Load Voltage (DVR) for a 3-phase fault

simulation aimed to replicate a voltage sag across the load, resulting in the load voltage

decreasing to 80% of its normal value, as illustrated in Figure 4.2 (Vabc). Additionally, a voltage swell was emulated by externally injecting voltage using a programmable voltage source in MATLAB. This injection started at t=0.4s and continued until t=0.5s. During this period, the system's voltage increased to 120% of its nominal value.

The system was then operated in the presence of PV integrated DVR in series with a distribution linefeeding a load. Figure 4.1 (Vload) shows the events after the installation of the DVR. The first figure shows the source voltage during a fault (voltage sag, swell), the second figure shows that the load voltage after DVR has compensated the voltage sag and swell. It can be clearly observed that when the source voltage sags from t=0.2 to 0.3 s and swells from t= 0.4 to 0.5 s, DVR has either injected or absorbed the power for a constant voltage across the load terminal. The third figure (Vinjection) in Figure 4.2 shows the profile of power injection and absorption by the DVR. From the third figure, it can be seen that the DVR has injected voltage (power) into the load from t=0.2s to t=0.3s for voltage sag whereas, DVR has absorbed the excess voltage from t=0.4s to 0.5s for voltage swell. It is seen that the injected voltage by DVR, during sag/swell varies to bring back the load voltage.

It has been shown that the developed DVR model mitigates balanced voltage sags and swells occurring in the load, even when the source side voltage has sagged.

4.1.2 Compensation of Unbalanced Voltage Sag and Swell

Balanced faults are the least occurring events in power systems, with unbalanced fault unbalanced faults occurring for more than 95% of the time. Among different faults, Single Line to Ground (SLG) faults are the most frequent– responsible for almost 80%of the total number of faults. It is important that the modeled DVR is able to compensatefor the unbalanced voltage sags during SLG faults occurring in the systems.

For this, an unbalanced fault (SLG) fault has been simulated for the time duration of

0.2 s to 0.3 s, Waveforms of load voltage under this unbalanced fault show that Phase A has decreased to 10% of its normal operating voltage while the phases B and C and still healthy.

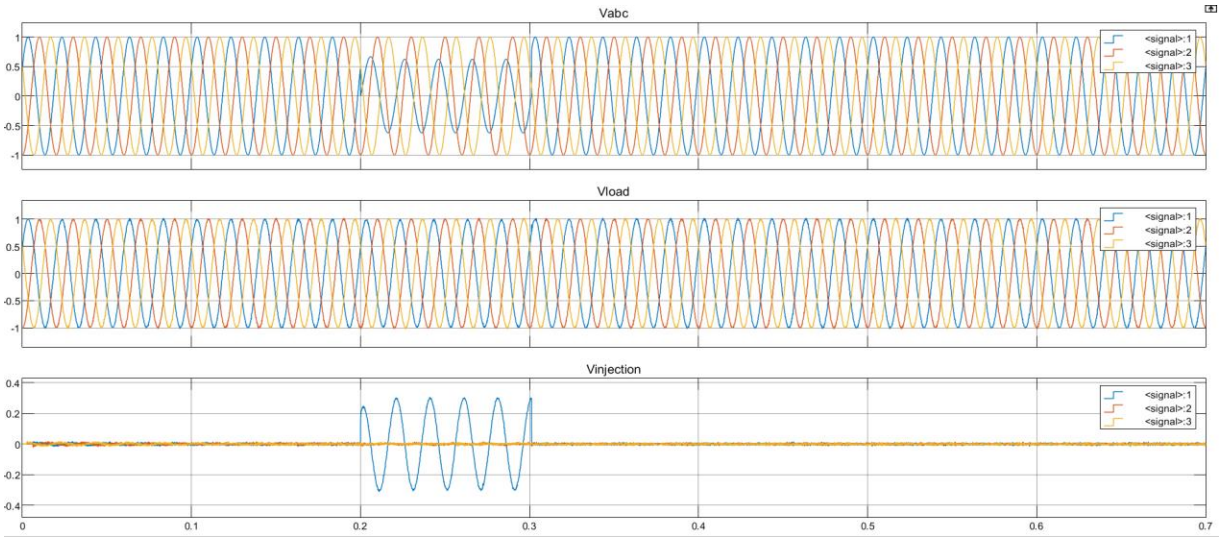

Fig 4.3: Load Voltage (DVR) for a SLG fault

It can be clearly observed that when the source voltage sags from t=0.2 to 0.3 in Phase A. DVR has injected voltage for phase A.

4.1.3 Harmonics of the Modal Test system

PV integrated DVR with space Vector Pulse width Modulation with PR Controller was also able to decrease the THD during balanced three phase fault from 12.97% to 1.52% when fed with 3rd and 5th Harmonics in the system by programmable Voltage Source in MATLAB .

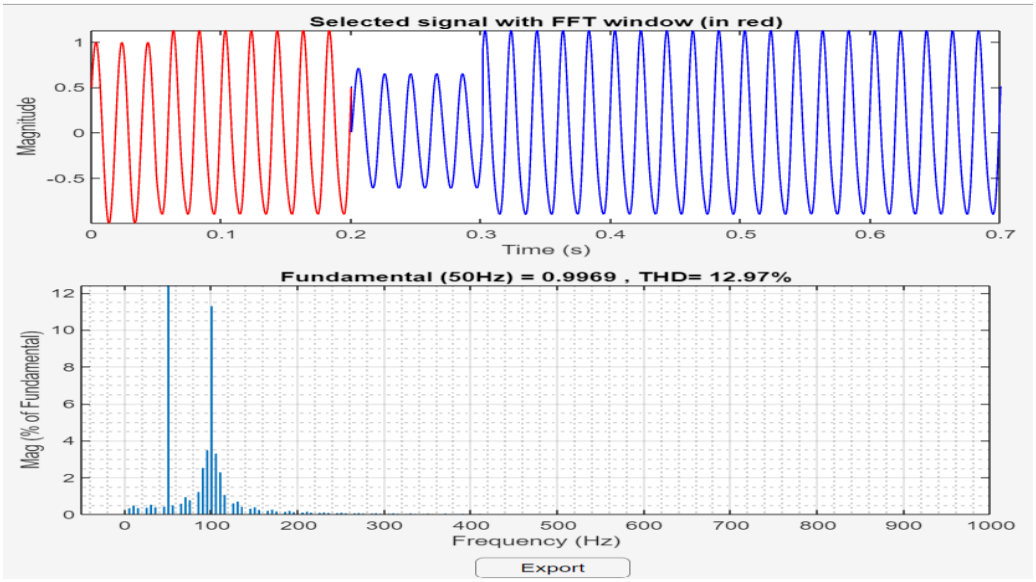

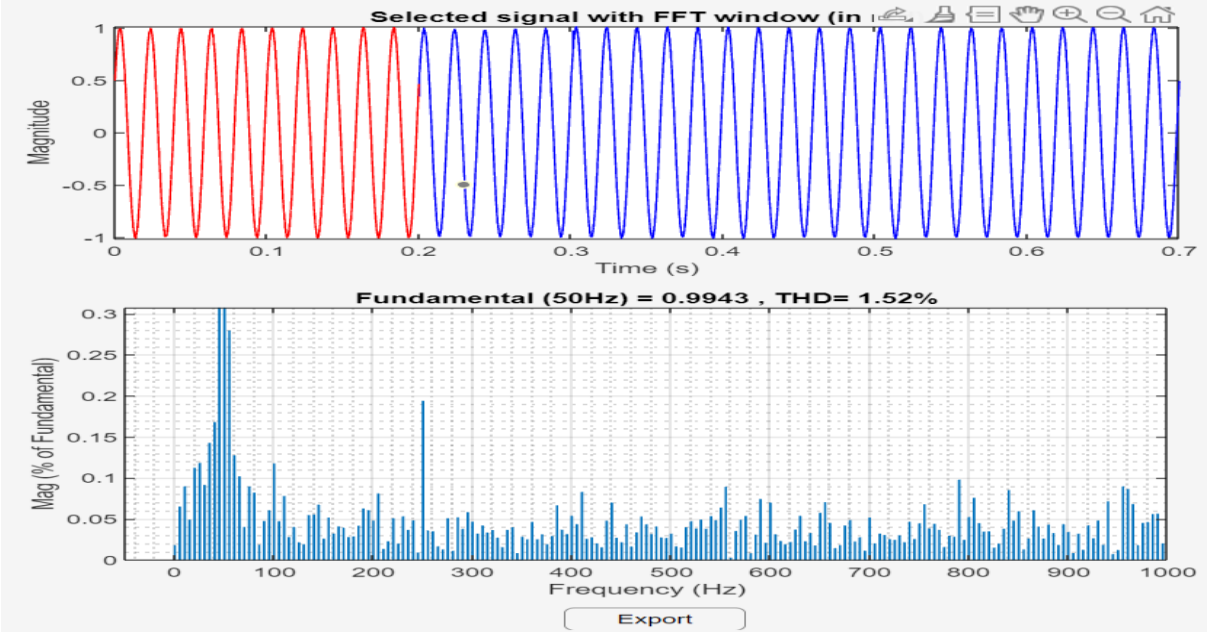

Fig 4.4: Harmonics of the System before and after Installation of DVR in model test system during fault

4.2 Sensitivity Analysis

One of the main ideas behind carrying out sensitivity analysis is to find various system parameters that have the highest impact on the output voltage of the system, this relation between parameters and output is best defined by the correlation coefficient from whichwe can infer the magnitude and direction of the input-output relationship. This correlation between the parameters and output voltage can be studied by generating some statistical data from sensitivity analysis. Correlation of input parameters– load power demand (S) and distribution line length (l) was carried out using data from sensitivity analysis. The result of input-output correlation is shown in Figure 6.5, which clearly indicates a negative correlation between the output and both the input parameters, suggesting an obvious fact that the output voltage reduces with increasing load power demand and line length. Power Demand of the load (S) has a very high correlation coefficient to the output forall three different correlations studied, which is an indication that output voltage (V2) is most influenced by the load power demand by the load when compared to the line length. The correlation of load power with the output voltage (V2) is around -0.9, whilethat of line length is around -0.4 to be exact, suggesting that we must be more cautiouswhile altering

the load so that the load voltage does not fall below the safe operating range.

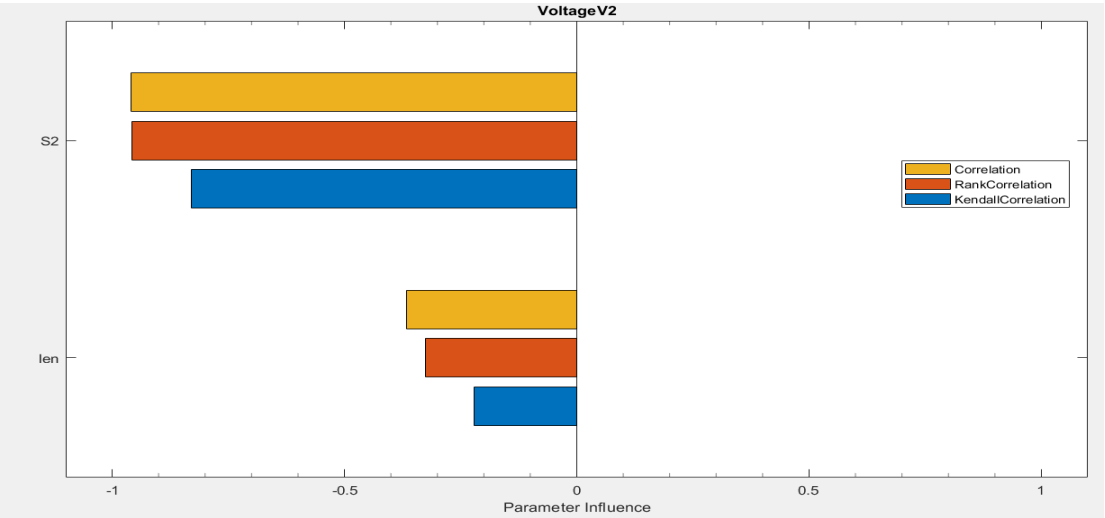

Fig 4.5: Correlation between output voltage and input parameter

4.3 Voltage Sag/ Swell and Harmonics Mitigation by PV Integrated DVR in IEEE 13 Node Test Distribution System.

4.3.1 Optimal Location of DVR

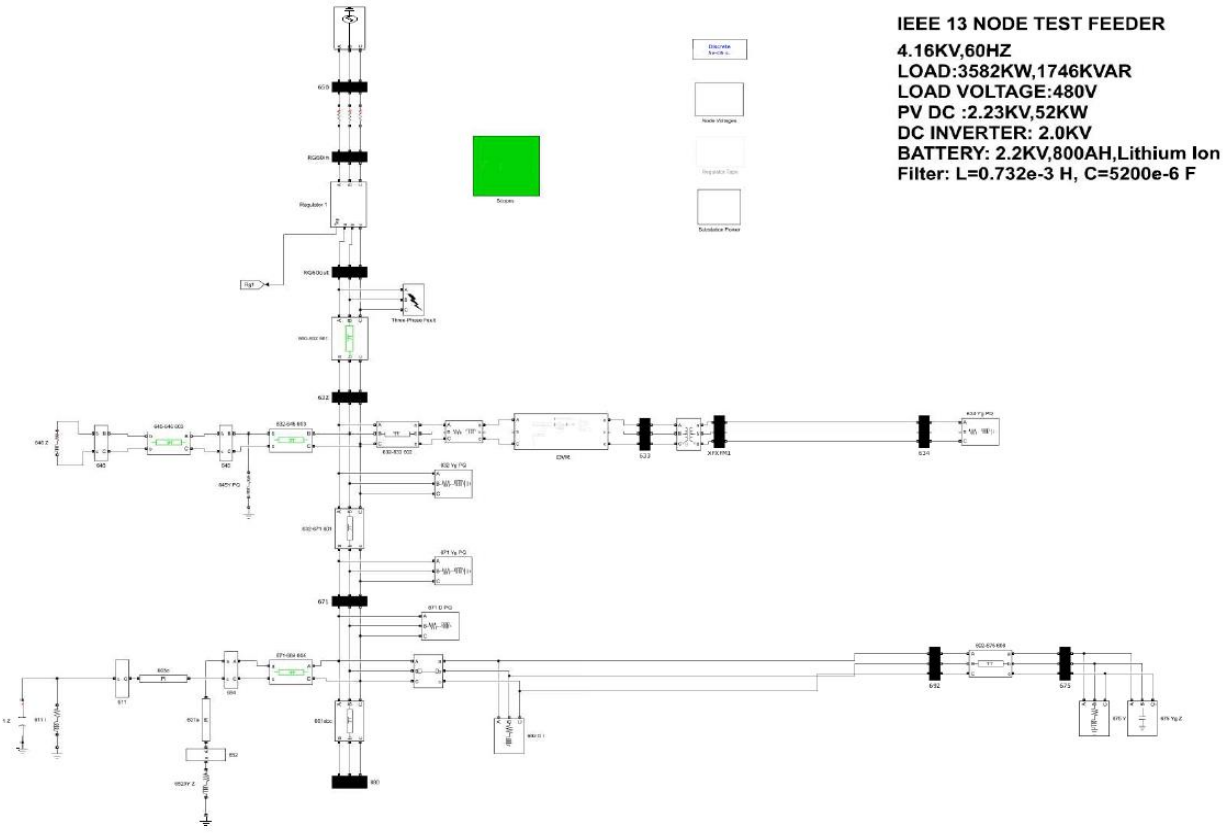

Fig: 4.6: Modeling of IEEE 13 Node Test Feeder with DVR in MATLAB

IEEE 13 Node Test Distribution Feeder have been modeled in MATLAB/SIMULINK environment, and the same model has been simulated for different faults scenario and the values of the post fault voltages were measured and were used for SARFI Calculation for Optimal Location of PV-Integrated DVR.

Following the procedure of optimization, it was observed that at node 633(i.e. between branch 632-633) lowest value of SARFI 6.66% among the three-phase bus was observed.

Then DVR was placed in the node to observe the performance. As was the most vulnerable node. Figure 4.7 shows the SARFI values of all the three phase buses of the system.

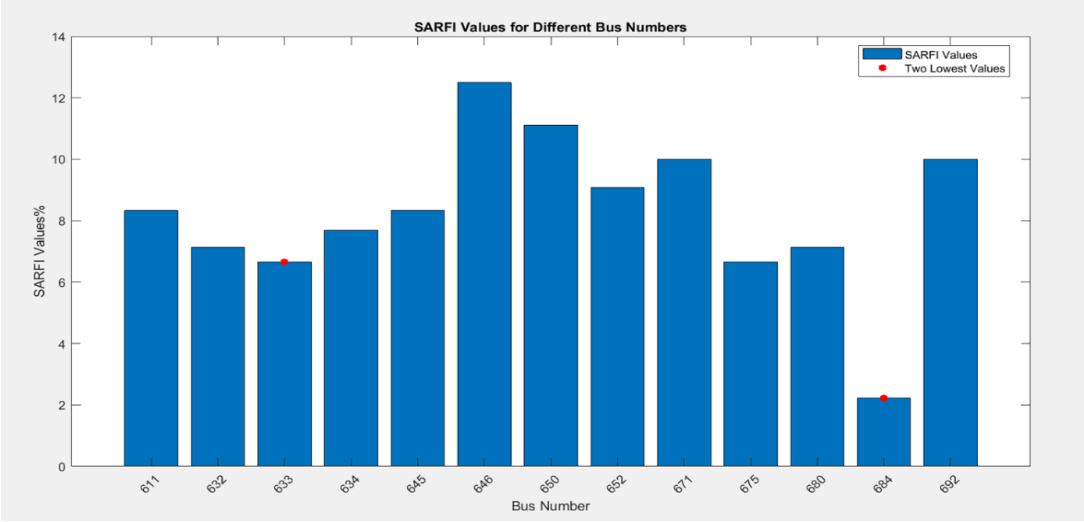

Fig 4.7: SARFI values at different buses of IEEE 13 node Test System

As a result, branch 632-633 , in IEEE 13 node system was chosen as the optimal location.

The maximum vulnerability of a node in the system can be attributed to its location in the system along with the load distribution such that for most of the faults in the system,the vulnerable bus lies in the fault current-carrying path as a result has maximum valuefor its voltage deviation from the rated voltage.

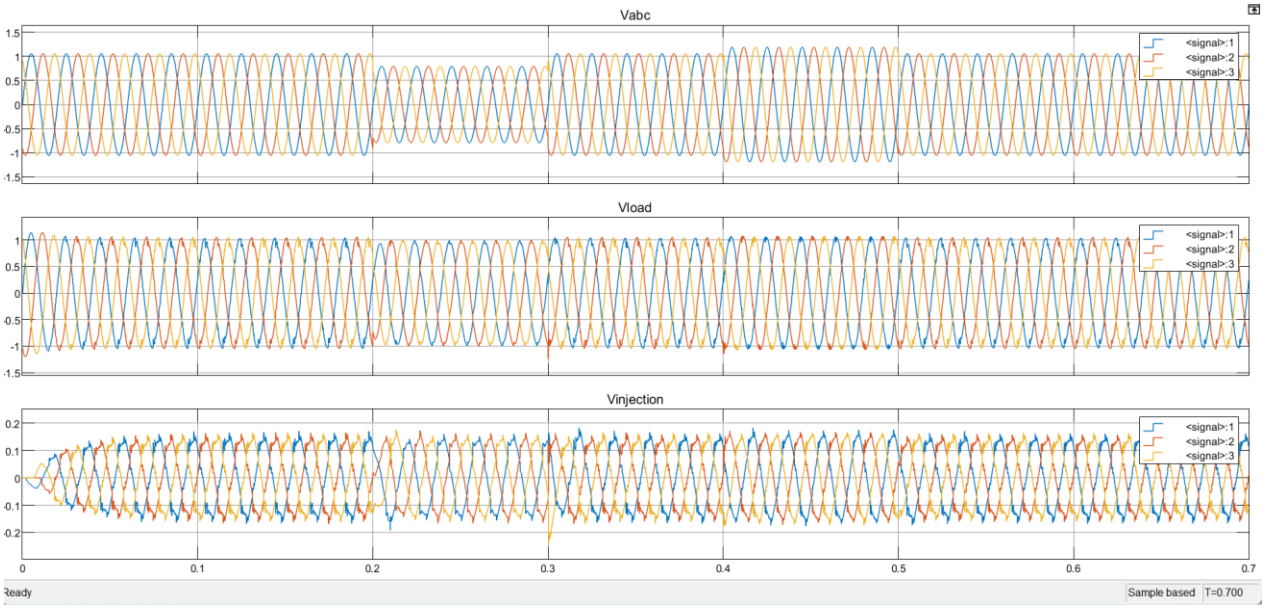

Figure 4.8: Voltage profile before and after placement of DVR in branch 632- 633 during 3 phase balanced fault.

It has been shown that the developed DVR model is able to mitigate balanced voltagesags between t=0.2s to 0.3s and swells between t=0.4s to 0.5s occurring in the load, even when the source side voltage has sagged to 80% and swelled to 110% of Nominal Voltage value using Programmable Voltage source in MATLAB. This model is tested in different radial distribution systems in different Fault conditions and Fault location, to effectively restore the voltages in the system buses under certain undesired events.

4.3.2 Harmonics of the IEEE 13 node Test system

PV integrated DVR with space Vector Pulse width Modulation with PR Controller in IEEE 13 node Test System was also able to decrease the THD during balanced three phase fault from 106.58% to 6.35% in 60Hz System.

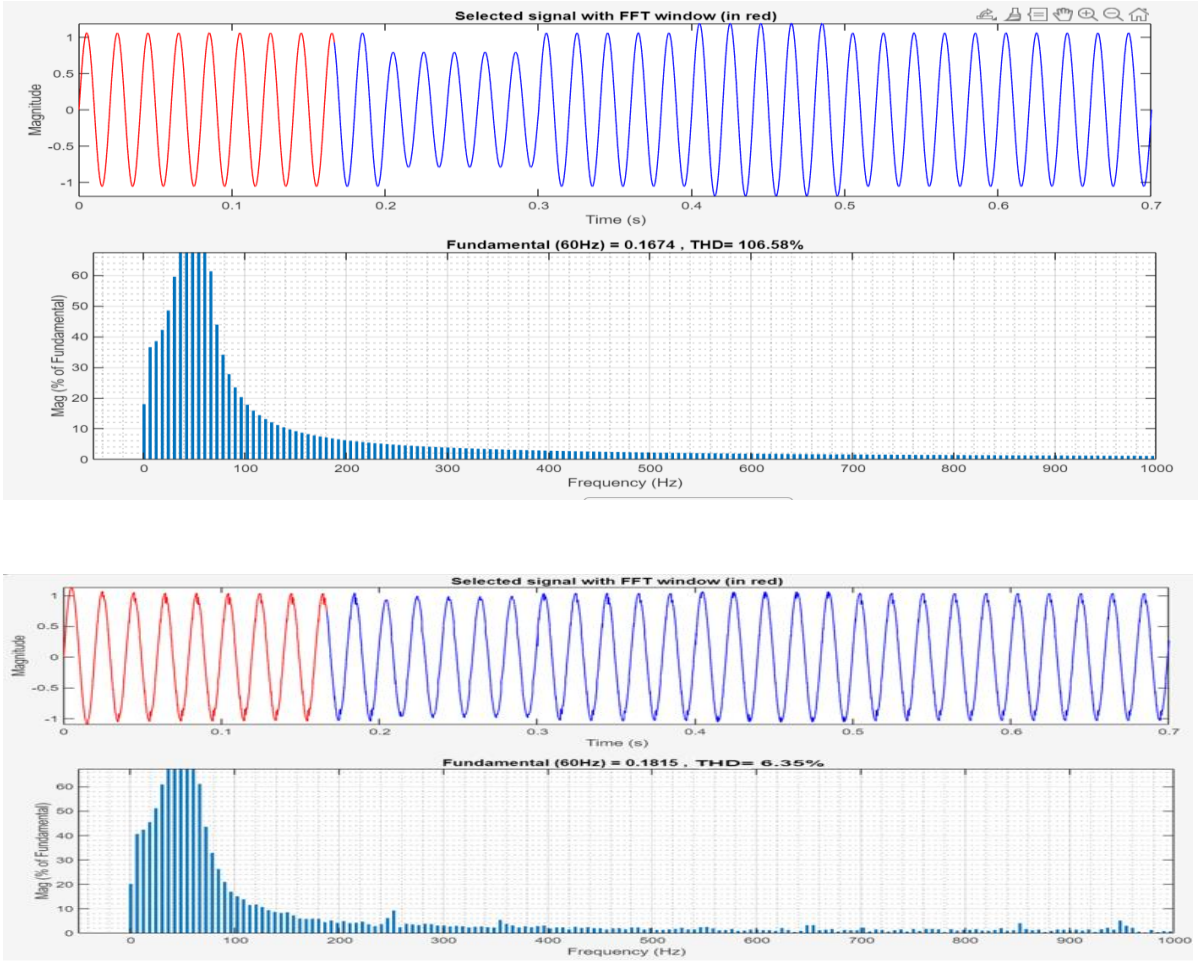

Fig 4.9: Harmonics of the System before and after Installation of DVR in IEEE Test system during fault conditions

4.4 Voltage Sag/ Swell and Harmonics Mitigation by PV Integrated DVR in Section of 11Kv Tanahusur Feeder.

4.4.1 Optimal Location of DVR

11kV Tanahusur Distribution Feeder have been modeled in MATLAB/SIMULINK environment, and the same model has been simulated for different faults scenario and the values of the post fault voltages were measured and were used for SARFI Calculation for Optimal Location of PV-Integrated DVR.

Following the procedure of optimization, it was observed that at bus 7(i.e. between branch 2-7) lowest value of SARFI was 6.09% and second lowest value of SARFI was 7.2% at bus 5(i.e. between branch 4-5) . Then DVR was placed in the node to observe the performance. As was the most vulnerable node. Figure 4.10 shows the SARFI values of all the 11kV buses of the system.

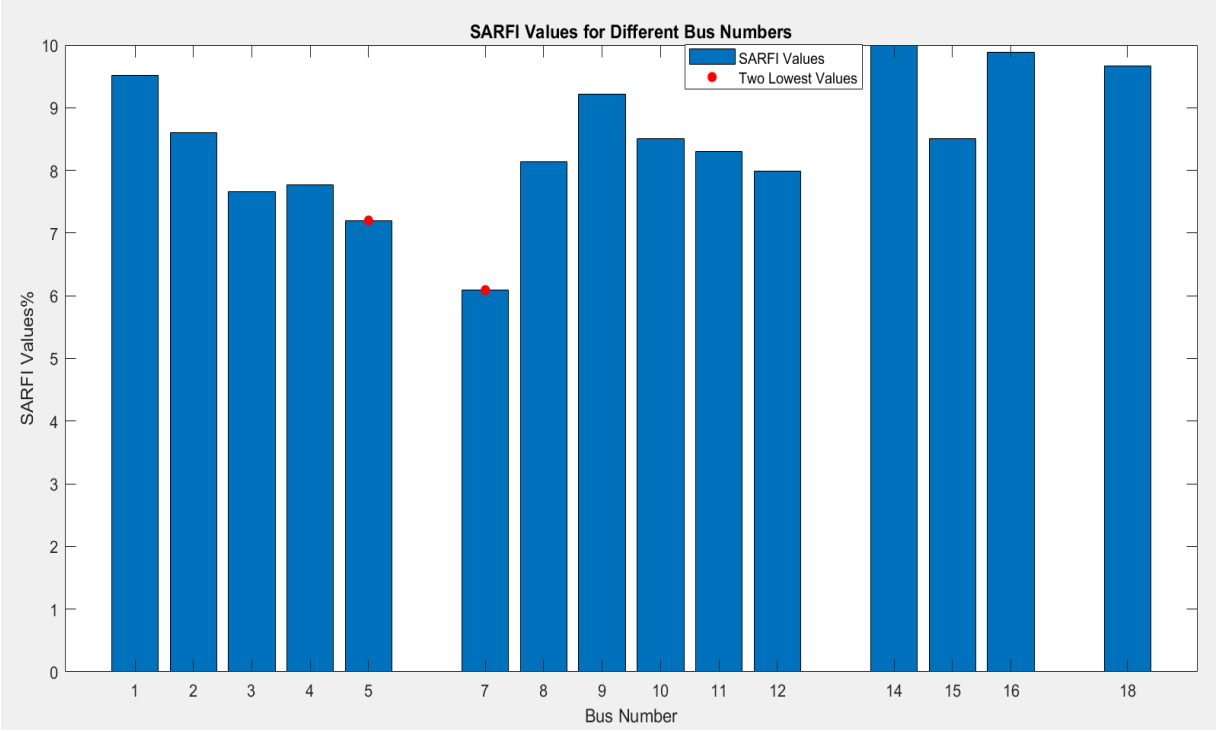

Fig 4.10: SARFI values at different buses of section of 11kV Tanahusur feeder

4.4.2 PV Integrated DVR at Single Location-Tanahusur Feeder

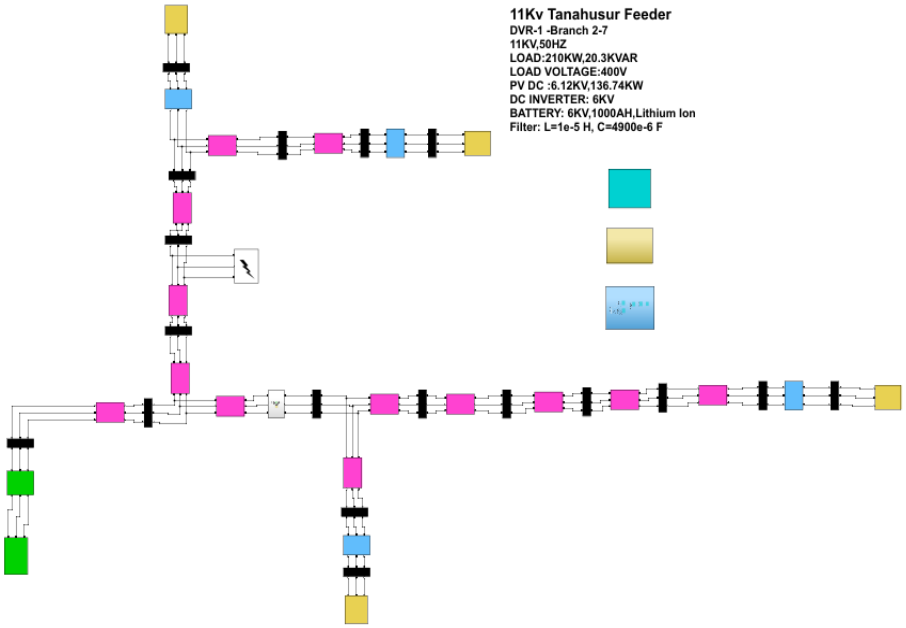

Fig: 4.11: Modeling of 11kV Tanahunsur Feeder with PV integrated DVR in MATLAB

As a result, branch 2-7 , in the section of 11 kV Tanahusur feeder was chosen as the optimal location.

The maximum vulnerability of a node in the system can be attributed to its location in the system along with the load distribution such that for most of the faults in the system, the vulnerable bus lies in the fault current-carrying path as a result has maximum value for its voltage deviation from the rated voltage.

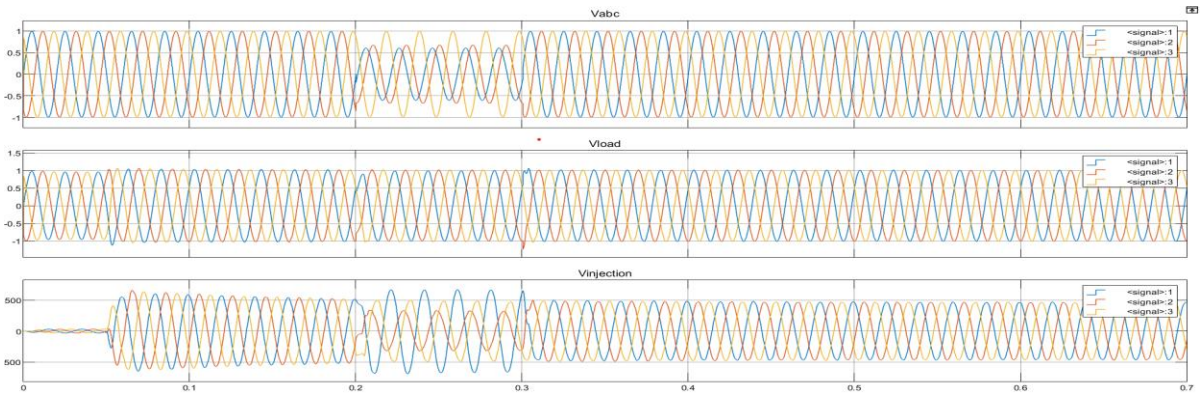

Fig: 4.12: Input and Output voltages of Branch 2-7

Figure 4.12 illustrates the input and output characteristics of the branch housing the PV-DVR.

A DLG fault is deliberately induced at the system's most critical location, and the resulting perturbations are effectively mitigated. The PV-DVR demonstrates success in rectifying voltage sags and swells, bringing them in close proximity to the 1 per unit (p.u.) reference value. Additionally, it efficiently addresses harmonics present in the system, even when subjected to various fault conditions.

Detailed results for different fault scenarios, including Single Line-to-Ground (SLG), Line-to-Line-to-Line-to-Ground (LLLG), Line-to-Line-to-Line (LLL), and Line-to-Line (LL) faults, are tabulated in the Appendix B for comprehensive analysis.

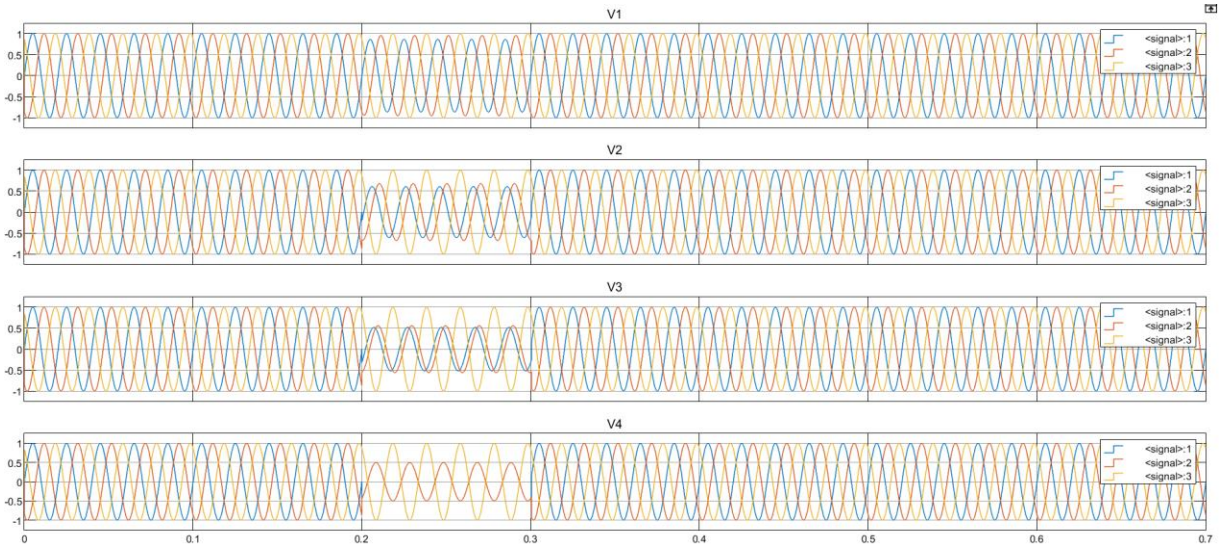

Fig: 4.13: 11kV bus output voltages that precede of DVR optimal position

The most suitable location for the installation of a Dynamic Voltage Restorer (DVR) is in branch 2-7. Figure 4.13 provides a visual representation of the voltage outputs at various buses that precede the DVR installation point. Notably, the voltages at buses V1, V2, V3, and V4 are not effectively compensated by the DVR during fault periods due to their relative positions.

Similarly, buses V5, V15, and V16, which operate at 11kV, are situated in a distinct section of the power line, separate from the DVR installation site. Consequently, these buses also remain susceptible to faults without the benefit of DVR intervention.

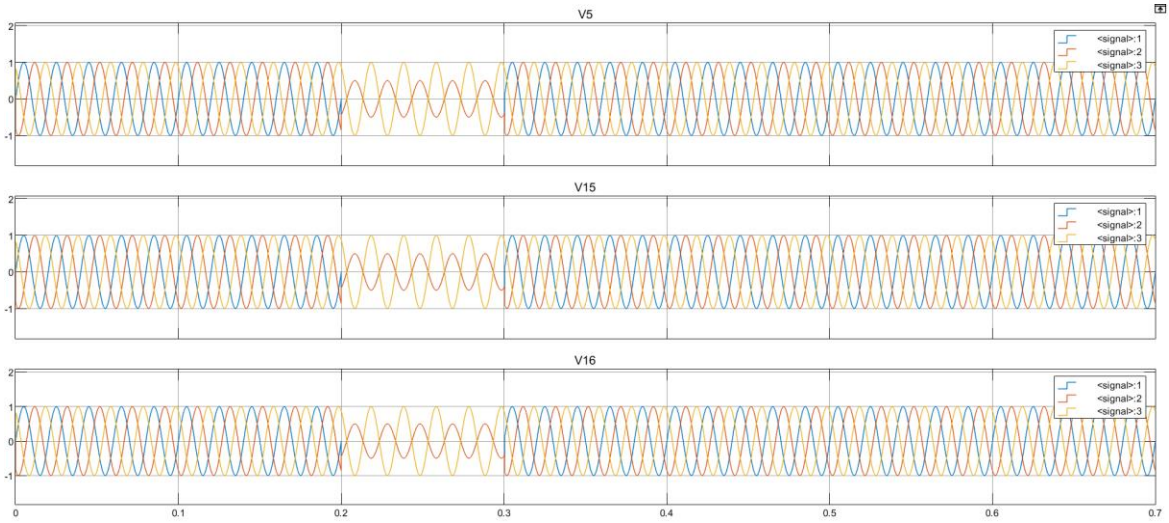

Fig: 4.14: 11kV bus output voltages on the buses that lies in other section of DVR optimal position

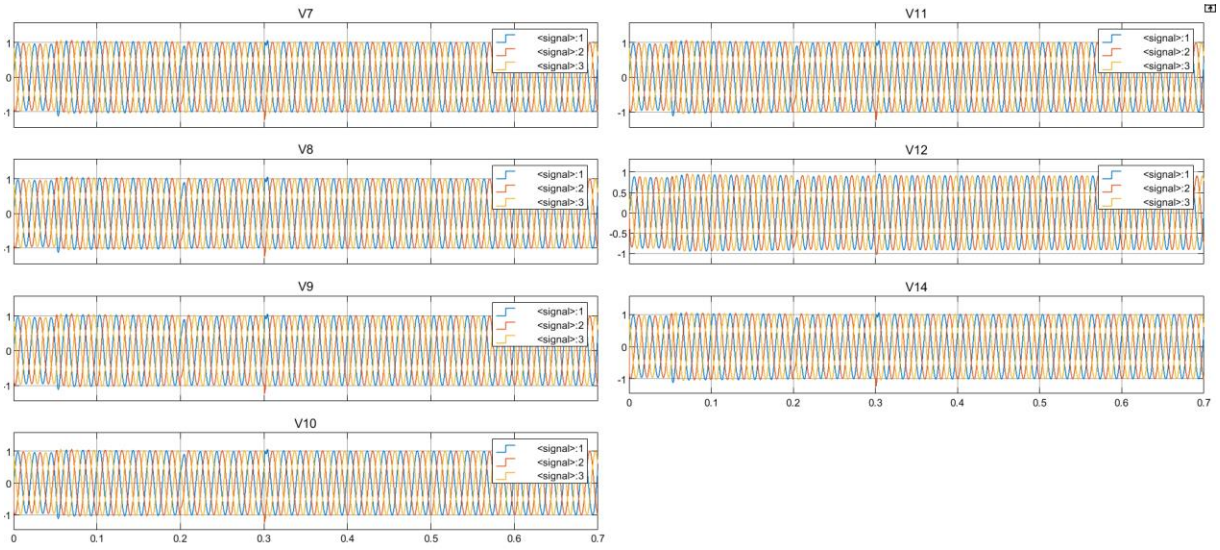

Fig: 4.15: 11kV bus output voltages on the 11kV buses after DVR optimal position

Figure 4.15 provides a representation of the bus output voltages occurring downstream of the strategically placed DVR. The integration of a Photovoltaic (PV) system with the DVR proves to be highly effective in maintaining the voltage levels within a desirable range for all connected buses, including V7, V8, V9, V10, V11, V12, and V14.Also, this section happens to be the longer section with critical loads.Even under fault conditions, this integrated system excels in preserving the bus voltages. The farthest bus from the DVR, V12, maintains a voltage output of 0.98 per unit (p.u.), demonstrating the system's robust performance in challenging scenarios. Additionally, the voltage at the small industrial bus, V14, is

consistently held at 1 p.u., underscoring the system's reliability in ensuring stable Voltage supply,even for critical loads.

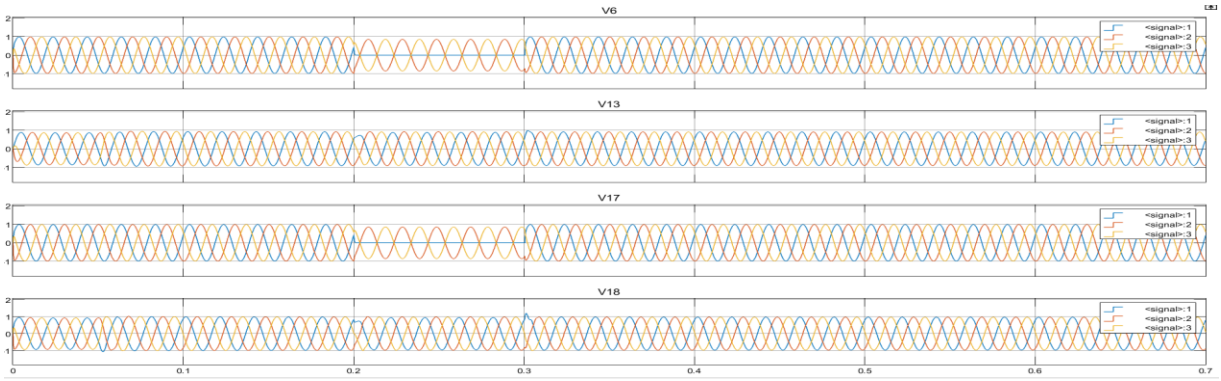

Fig: 4.16: 0.4kV bus output voltages after DVR optimal placement

The optimal placement of the PV-DVR system plays a pivotal role in determining the overall health of load bus voltages. As depicted in Figure 4.16, it becomes evident that the load voltages of V13 and V18, situated within the section of the power line where the DVR is strategically positioned, experience significant compensation, nearly reaching 1 per unit (p.u.) voltage levels.

However, it is worth noting that load buses in other sections of the power distribution network remain vulnerable to voltage faults during periods of electrical disturbances.

4.4.3 Harmonics of PV Integrated DVR at Single Location

PV integrated DVR with space Vector Pulse width Modulation with PR Controller in 11kV Tanahunsur feeder was also able to decrease the THD during DLG fault from 15.46% to 2.78% for 30 cycles starting from t=0.2s to t=0.6s in 50Hz System. The DVR integrated system decreases the overall harmonics in the system.

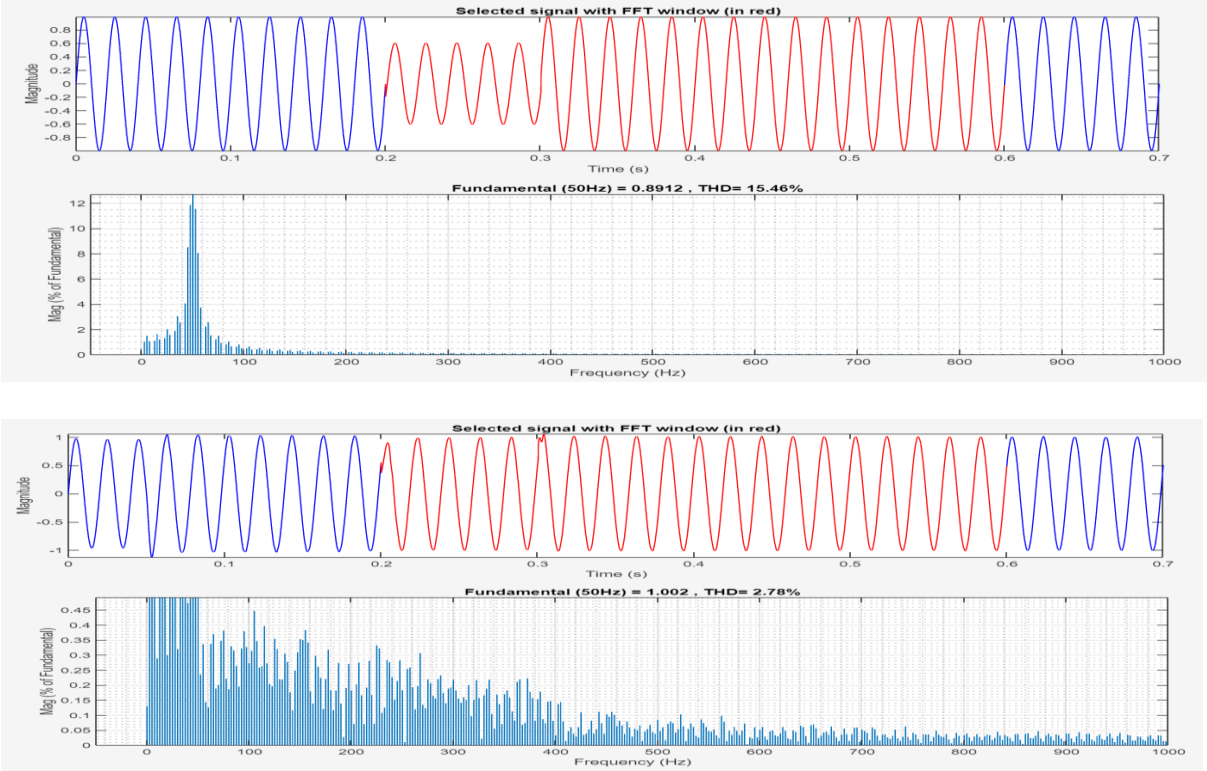

Fig 4.17: Harmonics of the System before and after Installation of DVR in 11kV Tanahunsur Feeder during fault conditions

4.4.4 PV Integrated DVR at Multiple Location (Two Locations)-Tanahusur Feeder

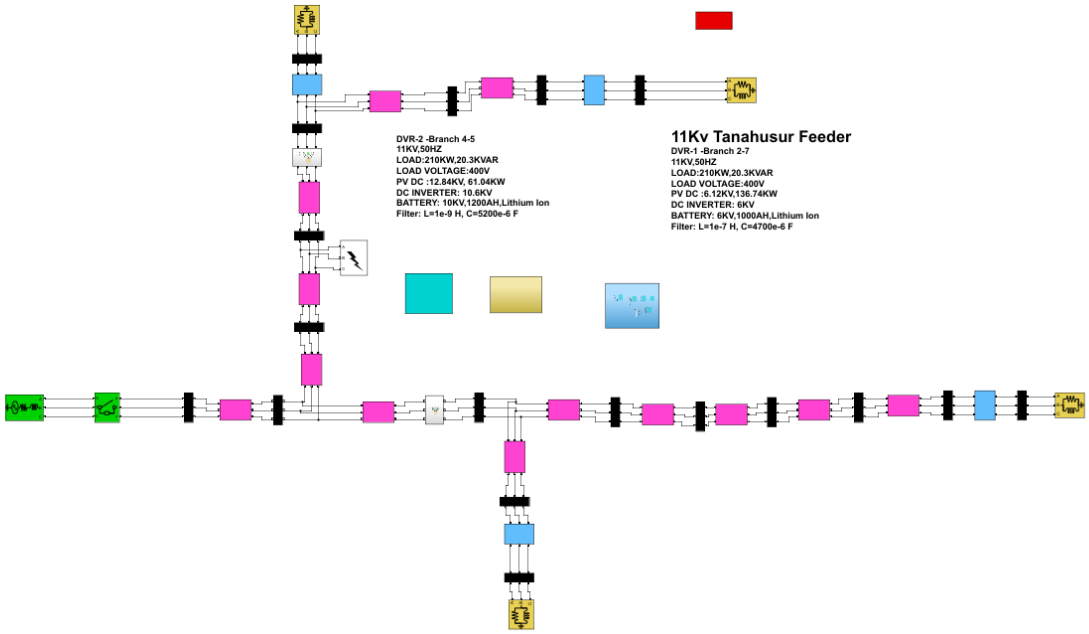

Fig: 4.18: Modeling of 11Kv Tanahusoor Feeder with DVR in MATLAB (Two location)

The primary selection for DVR installation was at branch 2-7, which was deemed the optimal location based on the SARFI calculation. This choice is underpinned by a SARFI value signifying effective voltage stability enhancement.

However, it's noteworthy that the SARFI assessment also identified an alternative, the second-best optimal position for DVR installation, which is at bus 5, located between branches 4 and 5. This site demonstrated a SARFI value of 7.2%, indicating its considerable potential in mitigating voltage disturbances. Nonetheless, the introduction of a second DVR, DVR2, demands careful consideration. DVR2 should be configured with distinct parameters compared to DVR1, as the latter already exerts a specific impact on the power system. This differentiation is essential to ensure the coexistence of both DVR systems without causing operational conflicts. In DVR1, the integrated PV system boasts a 7.1 kV capacity, generating 136.74 kW, and is coupled with an inverter input rated at 6 kV. In contrast, DVR2 features a unique configuration, comprising a 12.8 kV system with a capacity of 61.04 kW and an inverter input rated at 10.6 kV. These disparate specifications are thoughtfully designed to effectively address voltage sag and swell issues while allowing both DVR systems to function harmoniously, safeguarding the overall stability of the power network.

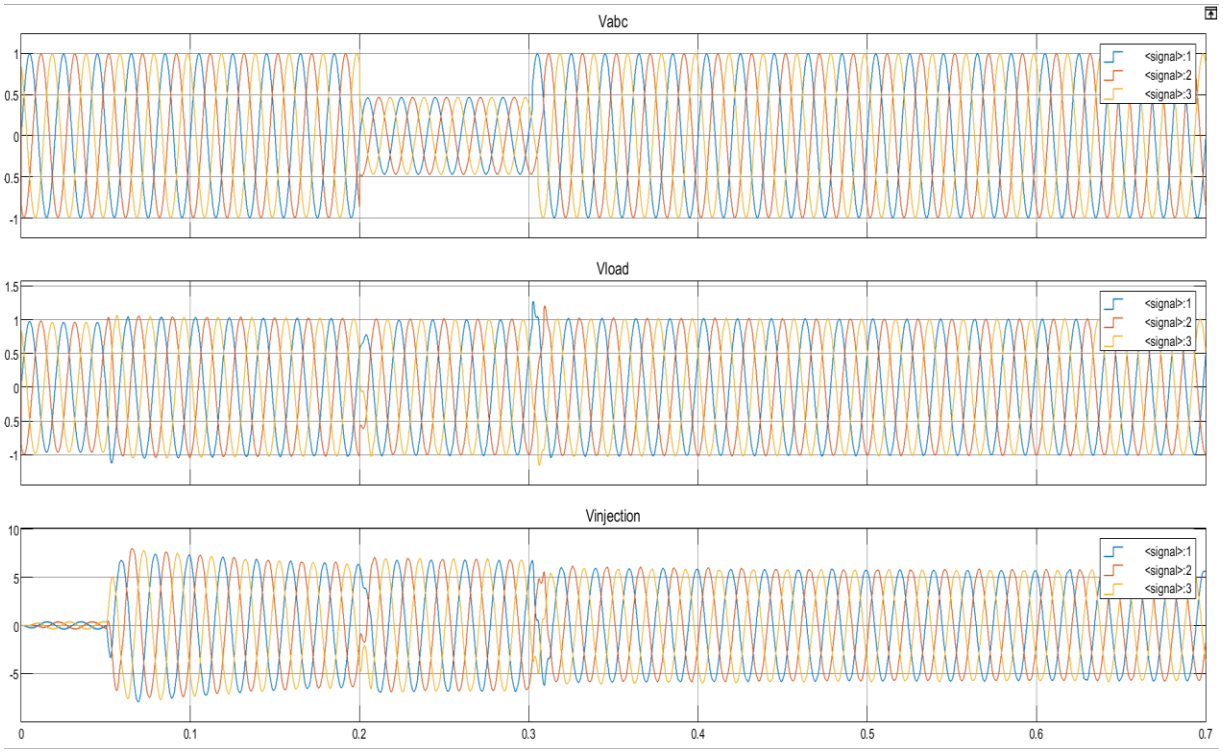

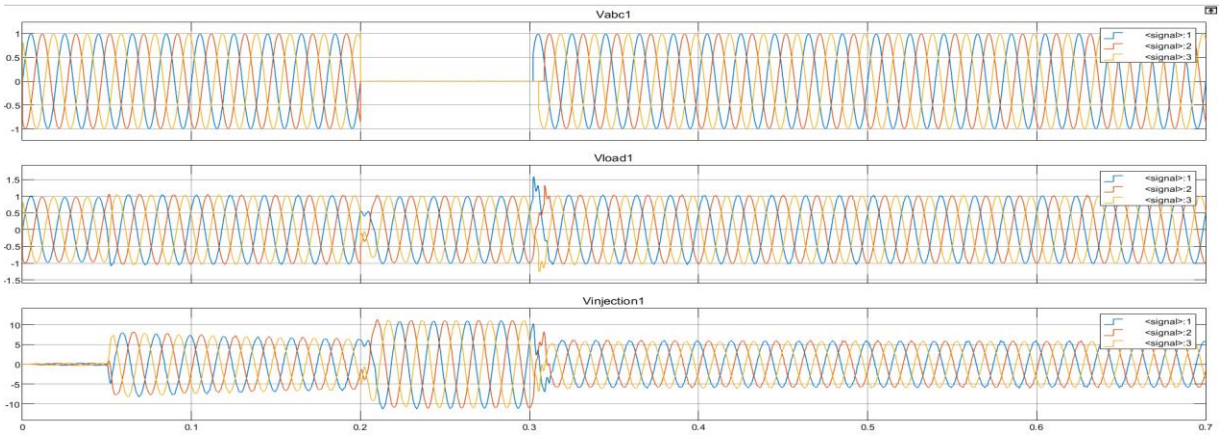

Fig: 4.19: DVR1 AND DVR2 Voltage outputs (Two location)

Figure 4.19 illustrates the input and output characteristics of the branch housing the PV-DVR1 and DVR2. A three phase fault is deliberately induced at the system's most critical location, and the resulting perturbations are effectively mitigated. The PV-DVR demonstrates success in rectifying voltage sags and swells, bringing them in close proximity to the 1 per unit (p.u.) reference value. Additionally, it efficiently addresses harmonics present in the system, even when subjected to various fault conditions.

Detailed results for different fault scenarios, including Single Line-to-Ground (SLG), Line-to-Line-to-Line-to-Ground (LLLG), Line-to-Line-to-Line (LLL), and Line-to-Line (LL) faults, are tabulated in the Appendix B for comprehensive analysis.

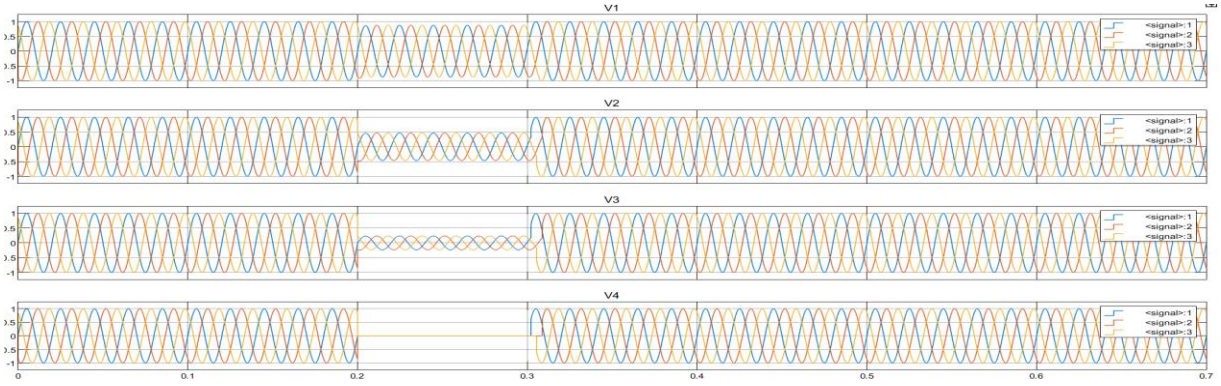

Fig: 4.20: Voltage outputs of the buses that precede of DVR1 and DVR2

The two suitable location for the installation of a Dynamic Voltage Restorer (DVR) is in branch 2-7 and 4-5. Figure 4.20 provides a visual representation of the voltage outputs at

various buses that precede the DVR installation point. Notably, the voltages at buses V1, V2, V3, and V4 are not effectively compensated by the DVR during fault periods due to their relative positions.

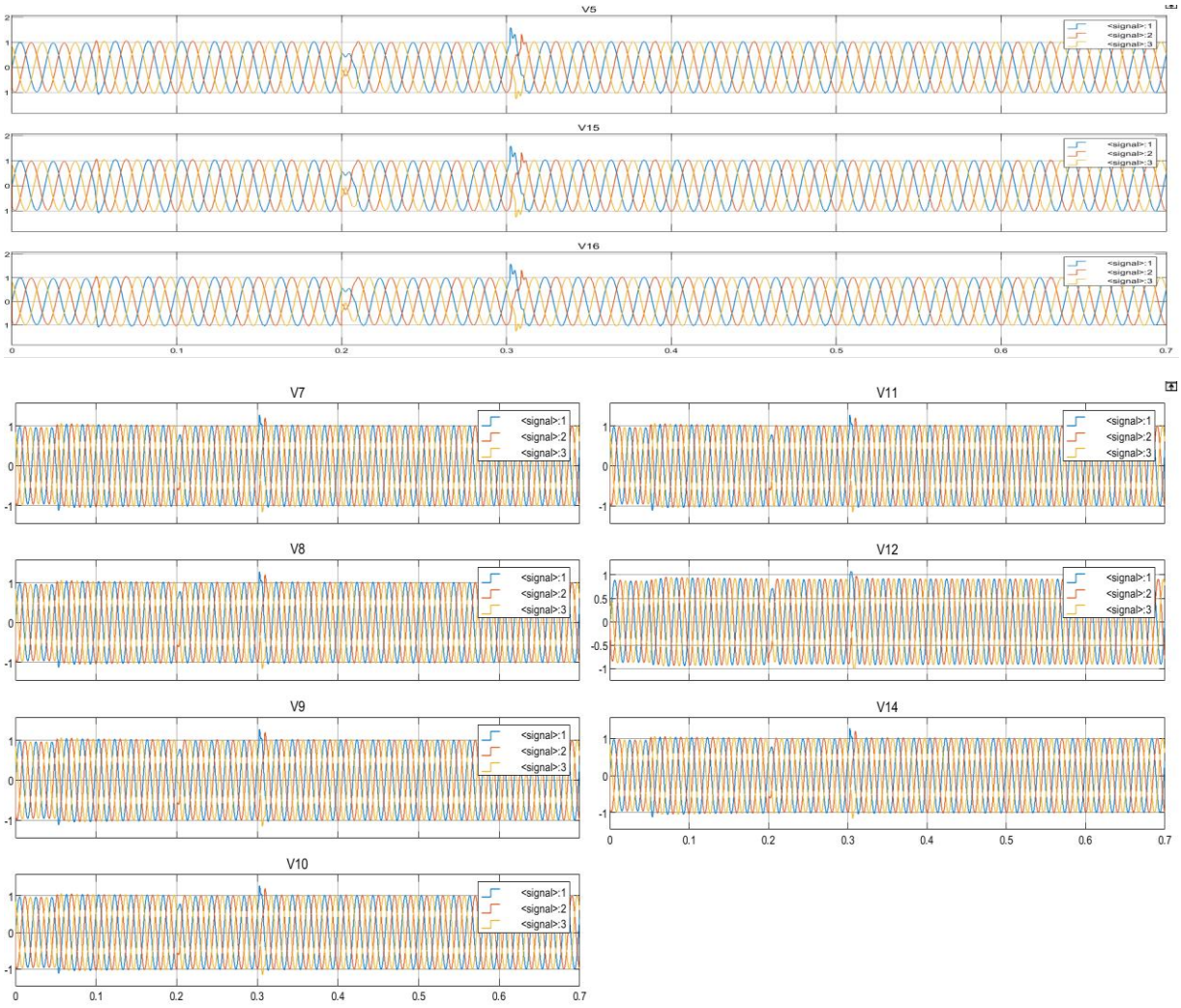

Fig: 4.21: Voltage outputs of the 11kV buses that are on downstream of DVR1 and DVR2

Figure 4.21 provides a representation of the bus output voltages occurring downstream of the strategically placed DVR1 at bus 2-7 and DVR 2 at bus 4-5. The integration of a Photovoltaic (PV) system with the DVR1 proves to be highly effective in maintaining the voltage levels within a desirable range for all connected buses, including V7, V8, V9, V10, V11, V12, and V14.Also, this section happens to be the longer section with critical loads.

Even under fault conditions, this integrated system excels in preserving the bus voltages. The farthest bus from the DVR, V12, maintains a voltage output of 0.98 per unit (p.u.),

demonstrating the system's robust performance in challenging scenarios. Additionally, the voltage at the small industrial bus, V14, is consistently held at 1 p.u., underscoring the system's reliability in ensuring stable voltage supply, even for critical loads. Similary DVR2 proves effective in maintaining the voltage levels within a desirable range for buses, including V7, V8, V5, V15, V16.

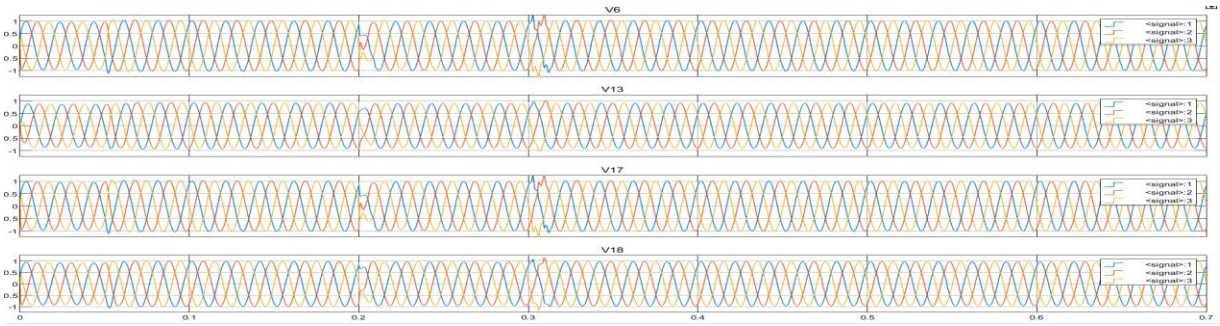

Fig: 4.22: 0.4kV load bus output voltages after DVR1 and DVR2 optimal placement

The optimal placement of the PV-DVR1 and DVR2 system plays a pivotal role in determining the overall health of load bus voltages. As depicted in Figure 4.22, it becomes evident that the load voltages of V13 and V18, situated within the section of the power line where the DVR1 and load voltage of V6 and V17 is strategically positioned, experience significant compensation, nearly reaching 1 per unit (p.u.) voltage levels.

It's important to highlight that during periods of electrical disturbances, specifically when only one DVR was incorporated into the system, load buses V6 and V17 continued to remain susceptible to voltage faults. However, with the strategic placement of DVR2 alongside DVR1, a remarkable transformation occurred.With both DVR1 and DVR2 optimally positioned, the voltage levels at all four load buses (V6, V13, V17, and V18) were consistently maintained at nearly 1 per unit (p.u.), demonstrating a significant improvement in voltage stability. Even the farthest load bus, V13, managed to uphold its voltage above 0.95 p.u. post-installation of DVR2.

4.4.5 Harmonics of PV Integrated DVR at Multiple (TWO) Location

The integration of PV with DVR1, utilizing Space Vector Pulse Width Modulation (SVPWM) in conjunction with Proportional-Resonant (PR) controllers, within the 11kV Tanahunsur feeder yielded satisfactory results. Specifically, during a three-phase balanced fault scenario,

the Total Harmonic Distortion (THD) was reduced substantially, decreasing from an initial 18.22% to a remarkable 2.78%. This outcome highlights the exceptional capability of DVR1 in harmonics mitigation. On the other hand, DVR2, while also proving effective, exhibited a slightly higher THD reduction during the same three-phase balanced fault scenario. The THD decreased from 39.32% to 6.31%. Although this figure is slightly above the generally acceptable limit of 5%, it underscores the significance of incorporating both DVRs into the system.

In summary, the synergistic combination of PV-integrated DVR1 and DVR2 successfully decreased THD levels, addressing harmonic issues during electrical faults. While DVR2 may slightly surpass the acceptable limit, the tandem deployment of both DVRs ensures a comprehensive solution for harmonic management within the power network.

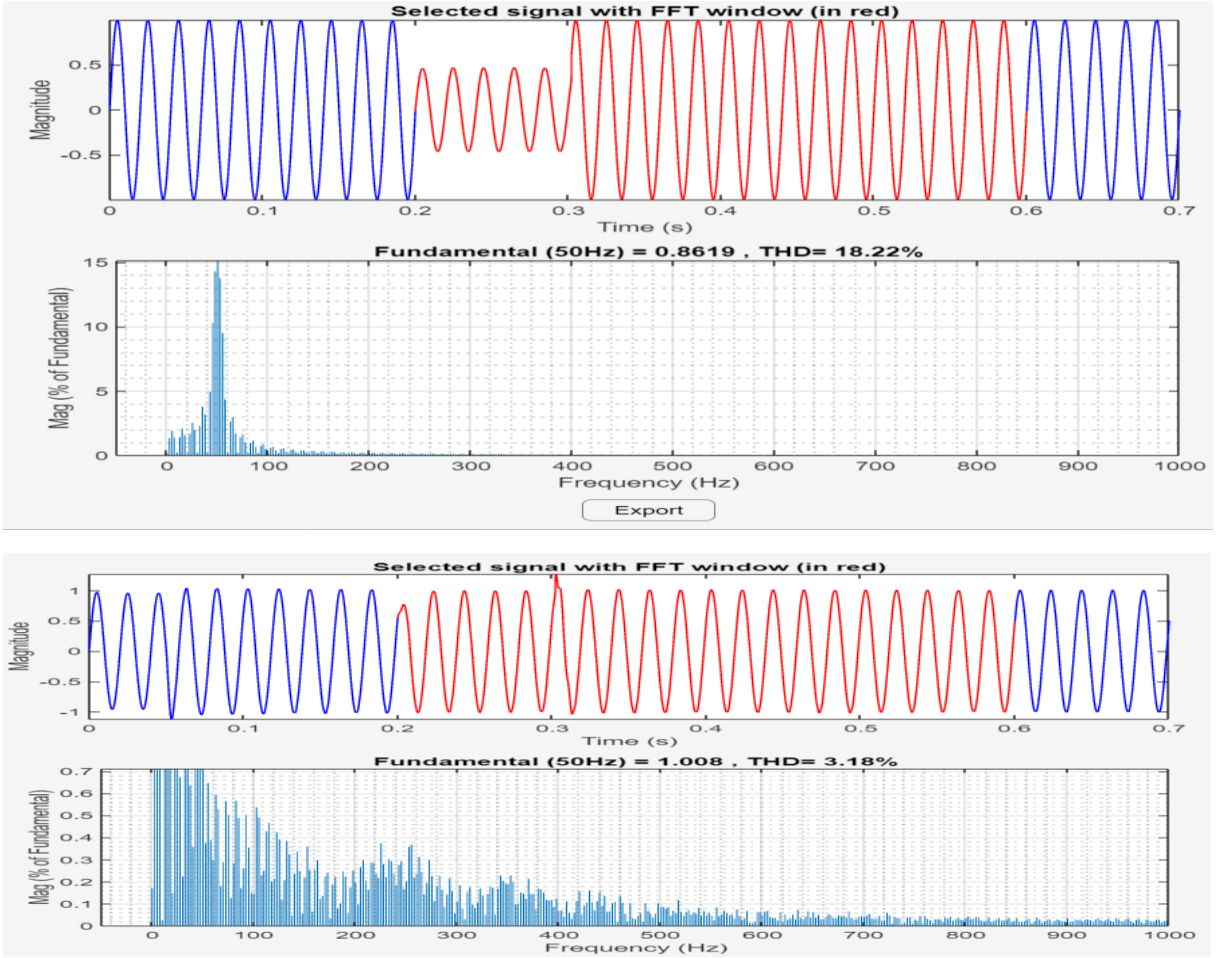

Fig 4.23: Harmonics of the System before and after Installation of DVR1 in 11kV Tanahunsur Feeder during fault conditions

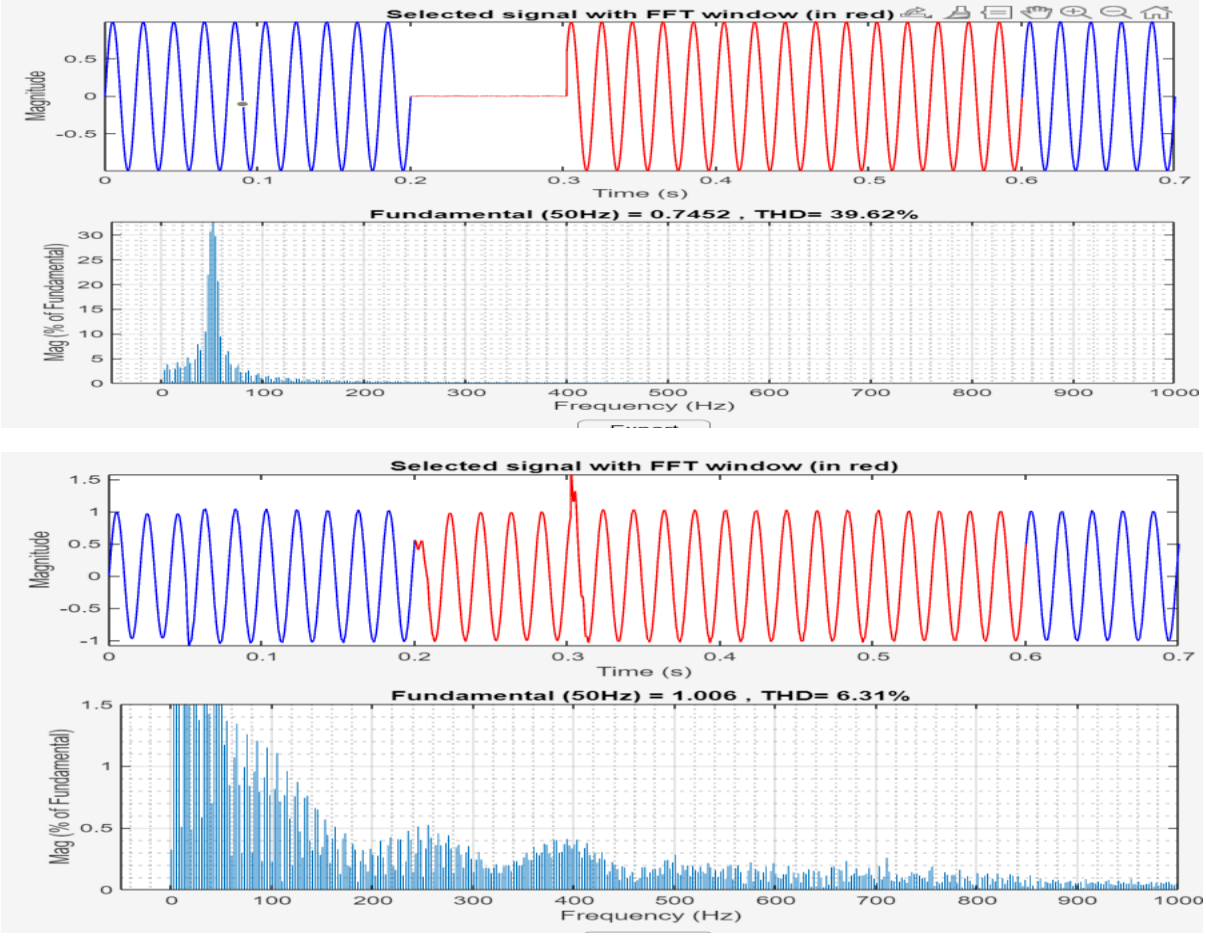

Fig 4.24: Harmonics of the System before and after Installation of DVR2 in 11kV Tanahunsur Feeder during fault conditions

4.5 Voltage Sag/ Swell and Harmonics Mitigation by PV Integrated DVR in 11kV Simara Industrial Feeder.

4.5.1 Optimal Location of DVR

The 11kV Simara Industrial Distribution Feeder has been modeled within the MATLAB/SIMULINK environment. This comprehensive model incorporates load data obtained from Time-of-Day (TOD) meters installed at all 15 consumer sites. It undergoes simulation for various fault scenarios, with post-fault voltage values meticulously recorded. These voltage measurements form a critical component for the subsequent calculation of the SARFI, aiding in the identification of the optimal location for the PV-Integrated Dynamic Voltage Restorer (DVR).

Following the prescribed optimization procedure, the analysis revealed that the lowest SARFI value, denoting superior voltage stability, was recorded at bus 5, situated between branches 4 and 5, with a SARFI value of 8.2%. Notably, the second lowest SARFI value, at 9.11%, was observed at bus 12, found between branches 11 and 12. Bus 12 also emerges as a significant consideration due to its vulnerability and high load capacity, hosting Rajesh Metal with an installed transformer capacity of 4600KVA.Ultimately, the decision was made to place the DVR at bus 5, recognized as the most optimal position, to closely monitor its performance. It was a prudent choice, particularly given bus 12's vulnerability. Figure 4.25 provides a visual representation of SARFI values across all 11kVbuses within the system.

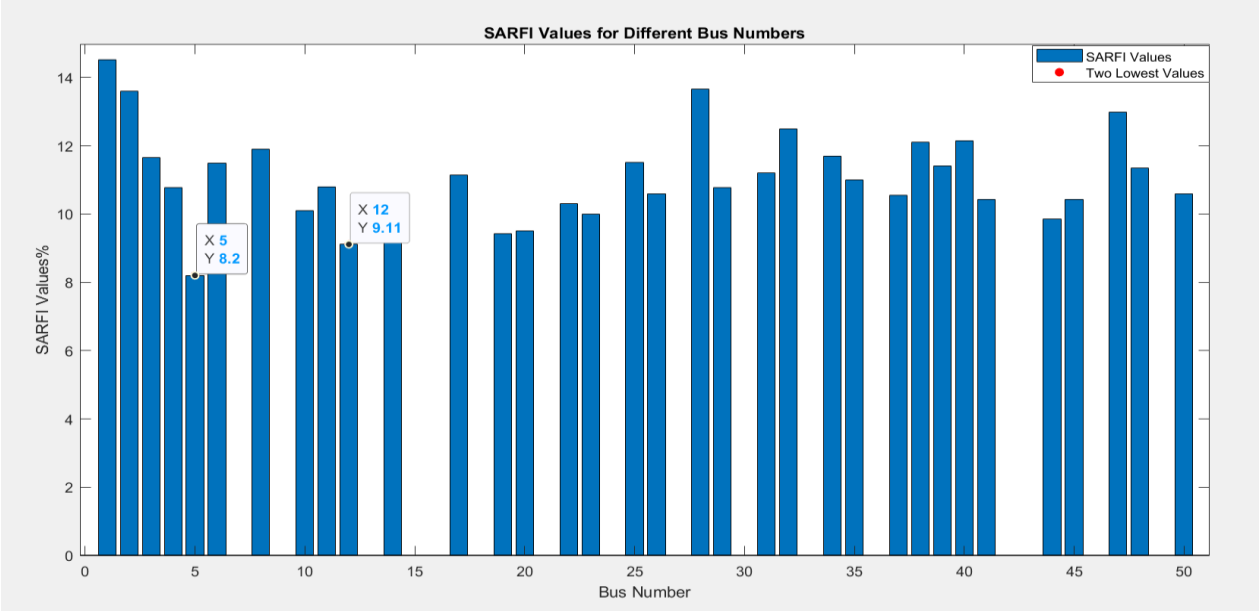

Fig 4.25: SARFI values at different buses samara industrial feeder

4.5.2 PV Integrated DVR at Normal Loading Condition-Simara Industrial Feeder

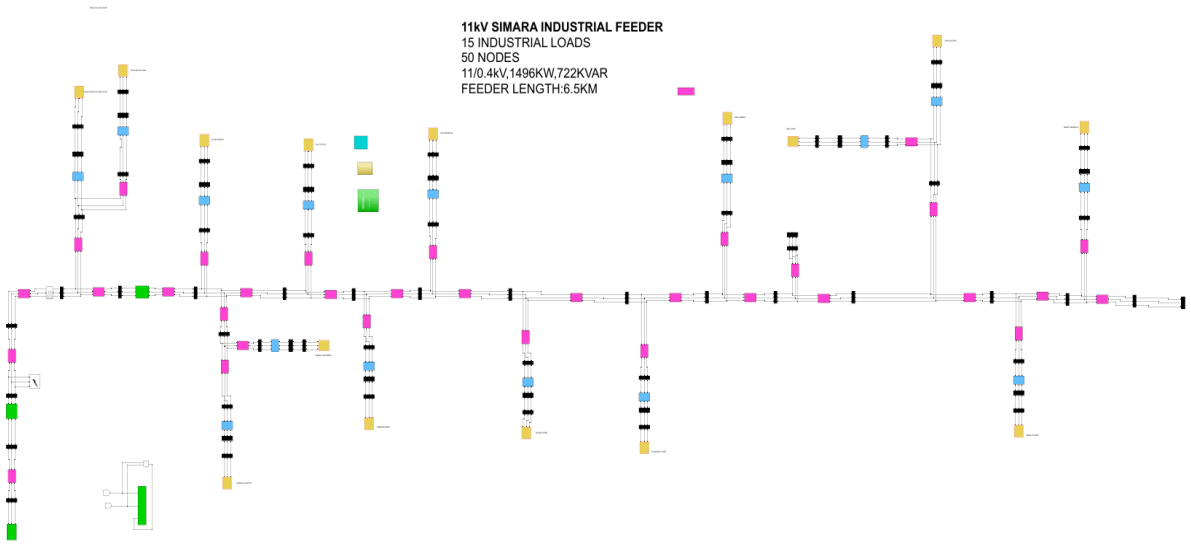

Fig 4.26: 11kV Simara Industrial Feeder in MATLAB

As a result, branch 4-5 ,in the section of 11 kV Simara Industrial feeder was chosen as the optimal location. A 7.2kV, 512kW PV system has been effectively deployed in a DVR (Dynamic Voltage Restorer) to successfully mitigate voltage sags and swells. However, it is worth noting that a smaller 34.18kW PV system (SPR-305E-WHY-D) is capable of mitigating these voltage fluctuations as well. Implementing a 13.2kV, 1MW PV system. This robust infrastructure could serve as an exceptional solution for ensuring uninterrupted power supply to critical loads even when the grid supply is unavailable under normal operating conditions. With this enhanced setup, we will only have the capacity to mitigate voltage sags and swells but also the capability to act as a backup power source when the grid encounters disruptions. This provides a more comprehensive and reliable power supply solution, ensuring that essential operations remain unaffected even during grid outages or fluctuations. In essence, this larger PV system represents a significant step towards ensuring uninterrupted power for critical applications, enhancing resilience, and minimizing downtime.

Figure 4.27 illustrates the input and output characteristics of the branch housing the PV-DVR. A LL fault is deliberately induced at the system's most critical location, and the resulting perturbations are effectively mitigated. The PV-DVR demonstrates success in rectifying

voltage sags and swells, bringing them in close proximity to the 1 per unit (p.u.) reference value. Additionally, it efficiently addresses harmonics present in the system, even when subjected to various fault conditions.

Detailed results for different fault scenarios, including Single Line-to-Ground (SLG), Line-to-Line-to-Line-to-Ground (LLLG), Line-to-Line-to-Line (LLL), and Line-to-Line (LL) faults, are tabulated in the Appendix C for comprehensive analysis

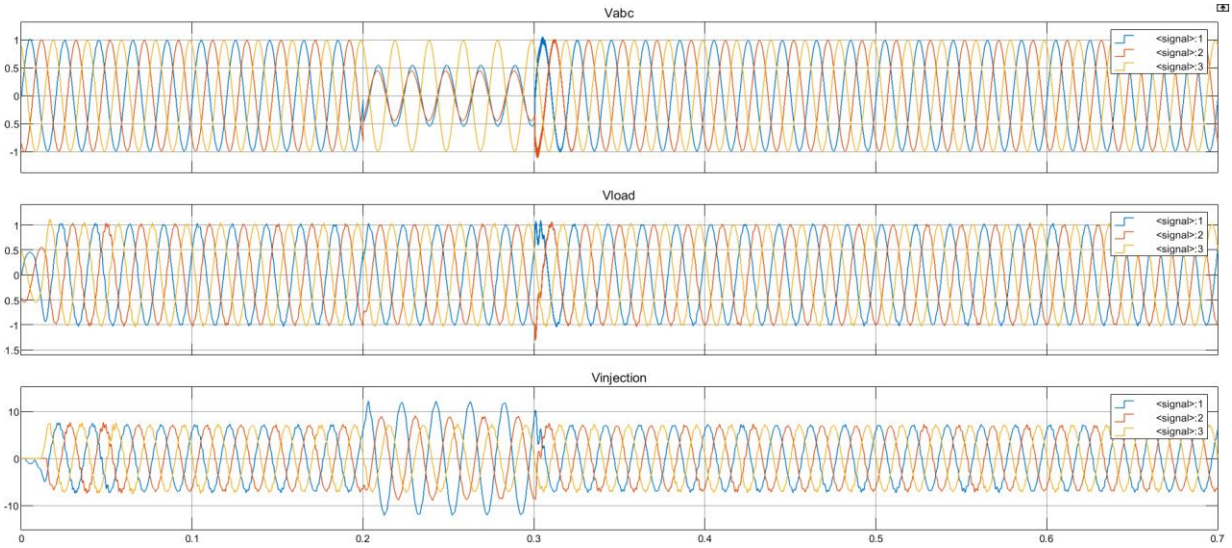

Fig 4.27: Input and output Voltages of installed PV-DVR in simara feeder in MATLAB

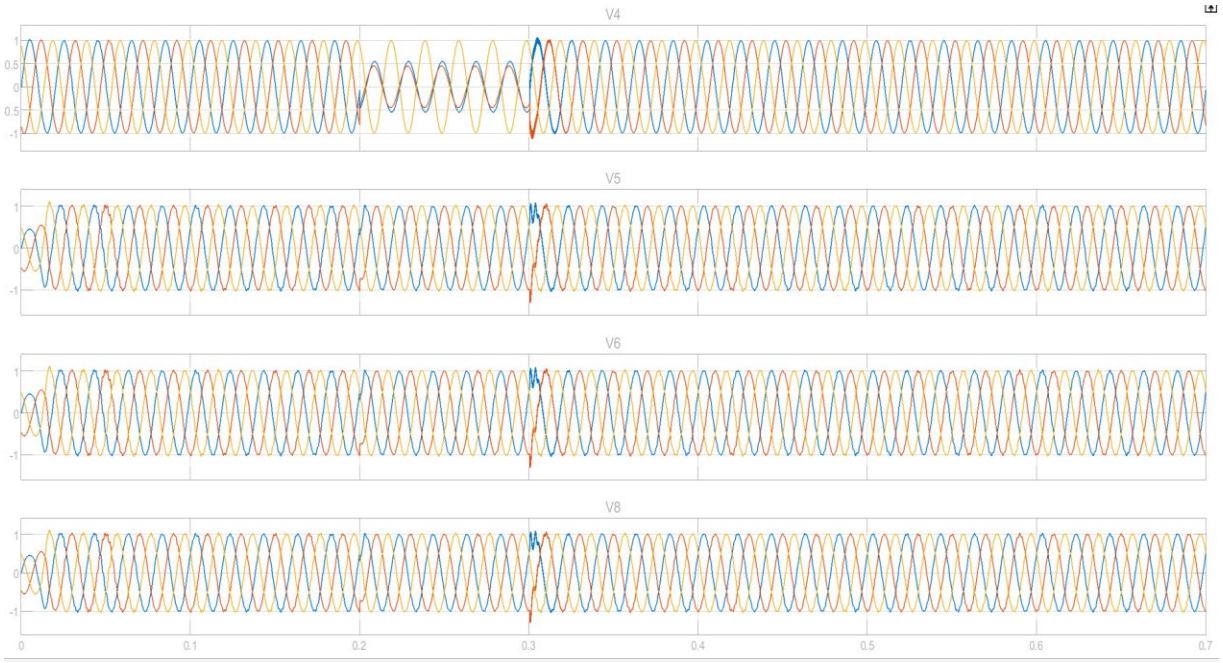

Fig 4.29: Input and output Voltages different 11kV buses after implementation of PV-DVR in simara feeder

The most suitable location for the installation of a Dynamic Voltage Restorer (DVR) is in branch 4-5. Figure 4.28 provides a visual representation of the voltage outputs at various buses that precede and buses in the downstream of the DVR installation point. Notably, the voltages at buses V2, V3, and V4 are not effectively compensated by the DVR during fault periods due to their relative positions.

However, It effectively compensates for the voltage fluctuations not only at bus V5 but extends its support seamlessly to cover all buses up to the final bus, V50 (i.e nearly 0.98p.u.), during fault occurrences. Furthermore, this compensation encompasses all the load buses within this network.

This means that regardless of where the voltage fault occurs within this range, the DVR system steps in with its voltage correction capabilities. It ensures that all connected load buses continue to receive stable and reliable power, maintaining the integrity of the entire electrical

distribution system. This comprehensive voltage compensation capability highlights the DVR system's exceptional ability to safeguard critical operations and equipment against the adverse effects of voltage fluctuations.

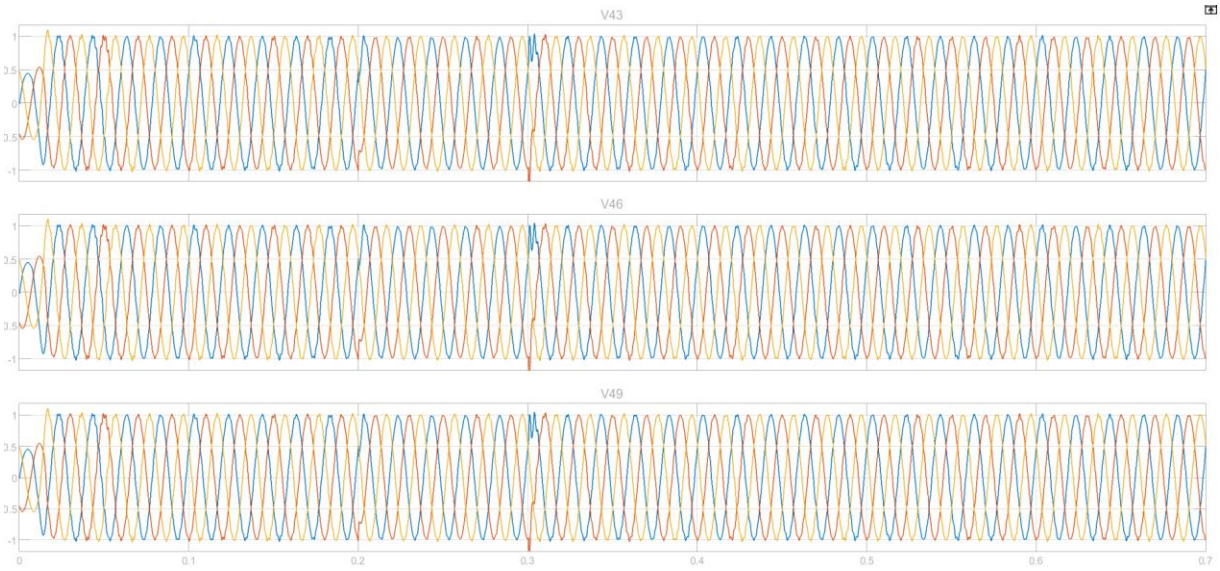

Fig 4.30: Input and output Voltages different load (0.4kV) buses after implementation of PV-DVR in simara feeder

The optimal placement of the PV-DVR system plays a pivotal role in determining the overall health of load bus voltages. As depicted in Figure 4.30, it becomes evident that even farthest load bus voltages of V49, experienced significant compensation, nearly reaching 1 per unit (p.u.) voltage levels. Indeed, a noteworthy observation emerges when examining voltage waveforms in the context of the DVR system's operation. Specifically, it becomes apparent that for a brief period ($t < 0.1$ sec), the DVR exhibits a discernible delay in its voltage compensation response. This delay is primarily attributed to the inherent characteristic of the DC voltage generated by the PV system, which necessitates a finite amount of time to reach its saturation level, as vividly illustrated in Fig 4.31. This intriguing phenomenon is predominantly noticeable in larger electrical systems, particularly those hosting substantial loads. It underscores the complexity of managing voltage fluctuations in more extensive networks, where the interplay between various elements introduces unique challenges. Conversely, in smaller feeder systems with relatively modest loads, such as the 11 Tanahusur Feeder, we do not observe a similar waveform behavior.Additionally, it's essential to acknowledge that, in the larger system, transient fluctuations or "jerk" in the voltage waveforms can occur precisely during the period of fault clearing and breaker operation. It's

important to emphasize that this occurrence is entirely normal under such circumstances. These transient voltage variations are a consequence of the swift and controlled actions taken to rectify faults, ensuring the system's stability and safety. In essence, they are a testament to the precision and effectiveness of fault-clearing mechanisms within the larger power distribution framework.

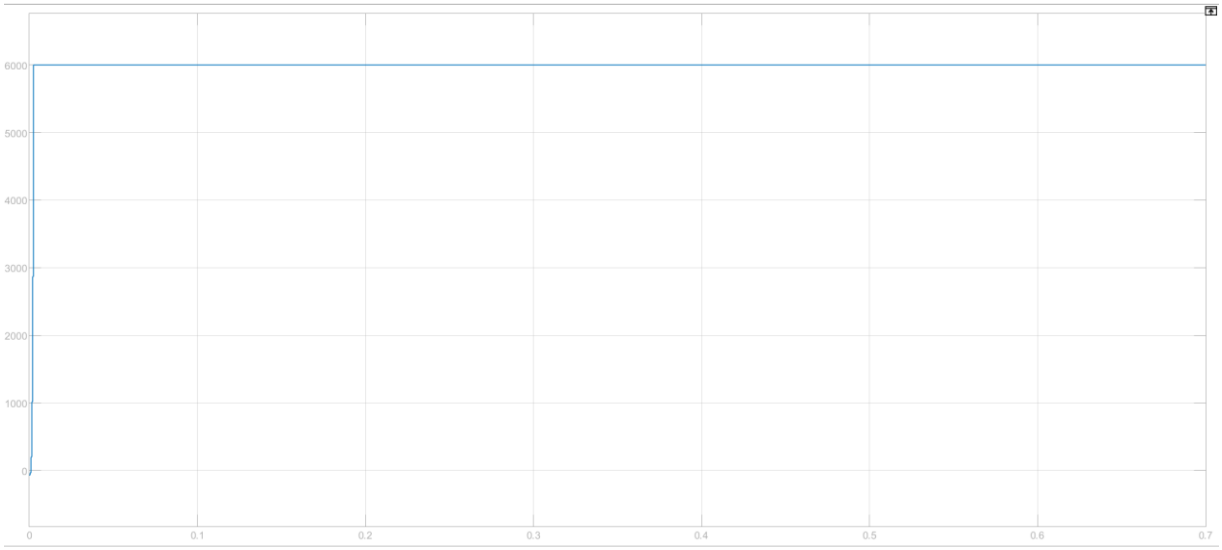

Fig 4.31: Inverter input Voltage (DC-link) PV-DVR in simara feeder

4.5.3 Harmonics of PV Integrated DVR Simara Industrial feeder under normal loading conditions

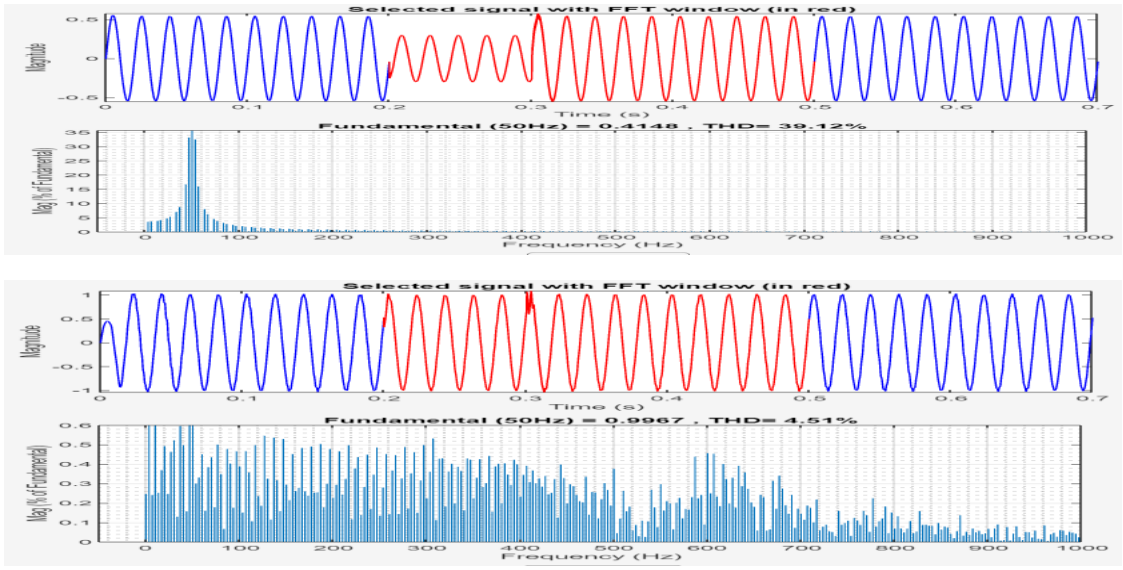

Fig 4.32: Harmonics of the System before and after Installation of DVR in 11kV Simara Feeder during Fault conditions

The integration of a Photovoltaic (PV) system into the Dynamic Voltage Restorer (DVR) system, utilizing Space Vector Pulse Width Modulation (SVPWM) with a Proportional-Resonant (PR) controller, represents a significant advancement in the management of power quality within the 11kV Simara Industrial feeder. This innovative approach has yielded impressive results, particularly in mitigating Total Harmonic Distortion (THD) during line-to-line (LL) faults.During a fault condition spanning 25 cycles, commencing at t=0.2s and concluding at t=0.5s, within the 50Hz system, the DVR integrated system succeeded in reducing THD from an initially high 39.12% to an astonishingly low 4.51%. This remarkable achievement highlights the system's remarkable ability to substantially diminish harmonic distortions and stabilize voltage profiles during fault scenarios. However, it's worth noting that while the overall performance is commendable, the harmonics results are categorized as satisfactory, falling just below the 5% threshold. The reason for this lies in the complexity introduced by the integration of numerous switching devices within the PV control and converters utilized for battery management. These components, although crucial for system functionality and grid backup capabilities, inherently introduce slightly higher harmonics into the system. Interestingly, an alternative approach using a PV system without a battery, relying solely on a capacitor for sag and swell compensation (without grid backup), has yielded even more remarkable outcomes. In this scenario, the THD in the system was reduced to less than 1%, showcasing an exceptional level of harmonic mitigation.

In summary, the integration of PV technology into the DVR system has undoubtedly improved power quality in the 11kV Simara Industrial feeder. While the harmonics results are satisfactory (<5%) when employing a battery-backed PV system, opting for a PV system with a capacitor for compensation (without grid backup) can yield even more outstanding results, reducing THD to less than 1%. This demonstrates the importance of considering specific system requirements and priorities when designing power quality solutions for industrial feeders.

4.5.4 PV Integrated DVR at OverLoading Condition- Simara Industrial Feeder

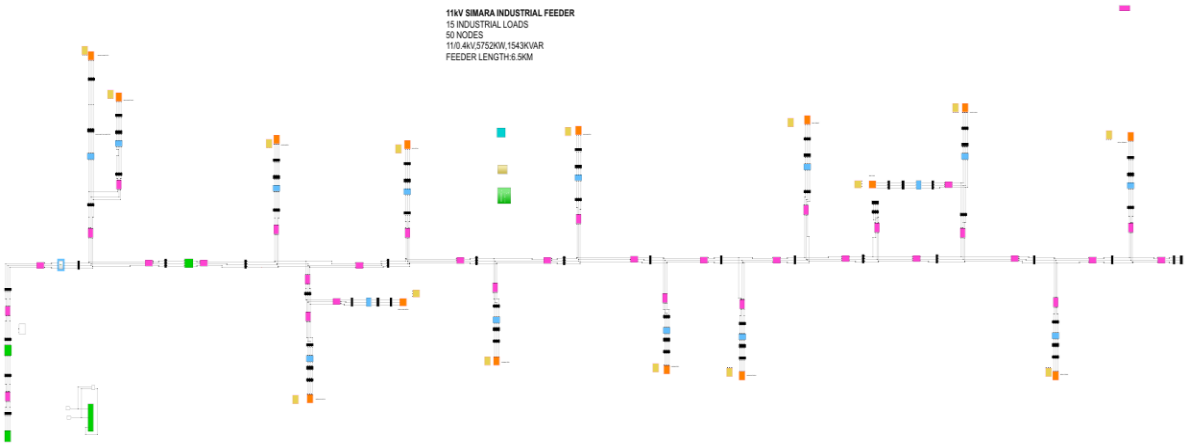

Fig 4.33: Simara Feeder Overloaded condition Matlab Simulations

During peak load periods, it's clear that not all connected loads are in operation simultaneously. The feeder, with a capacity of approximately 5.71MVA on a Dog Conductor, can handle a peak load of 300A. However, under specific operating conditions, data from Time-of-Day (TOD) meters on connected loads indicate a simulated load demand of 5.955MVA (at one instance), equivalent to a 312A load on the feeder. The feeder's relay is set to trip at 320A. When the current reaches 312A, only buses 1, 2, and 3 maintain a voltage of 1 per unit (p.u.), while all buses beyond experience a voltage drop from 0.84 p.u. to 0.89 p.u., with the farthest bus being the most affected.

To address this voltage issue, a Dynamic Voltage Restorer (DVR) was optimally placed at the branch 4-5 section of the 11kV Simara Industrial feeder. A 7.2kV, 1710 kW PV system was effectively integrated into the DVR, successfully mitigating voltage fluctuations. Remarkably, a smaller 34.18kW PV system (SPR-305E-WHY-D) also proves capable of mitigating these voltage fluctuations. Furthermore, a robust 13.2kV, 3MW PV system was implemented. This setup not only addresses voltage sags and swells but also serves as a backup power source during grid disruptions. This comprehensive solution ensures uninterrupted power for critical loads, enhancing resilience and minimizing downtime. In essence, the larger PV system marks a significant step toward ensuring reliable power for essential applications, even in the face of grid outages or fluctuations.

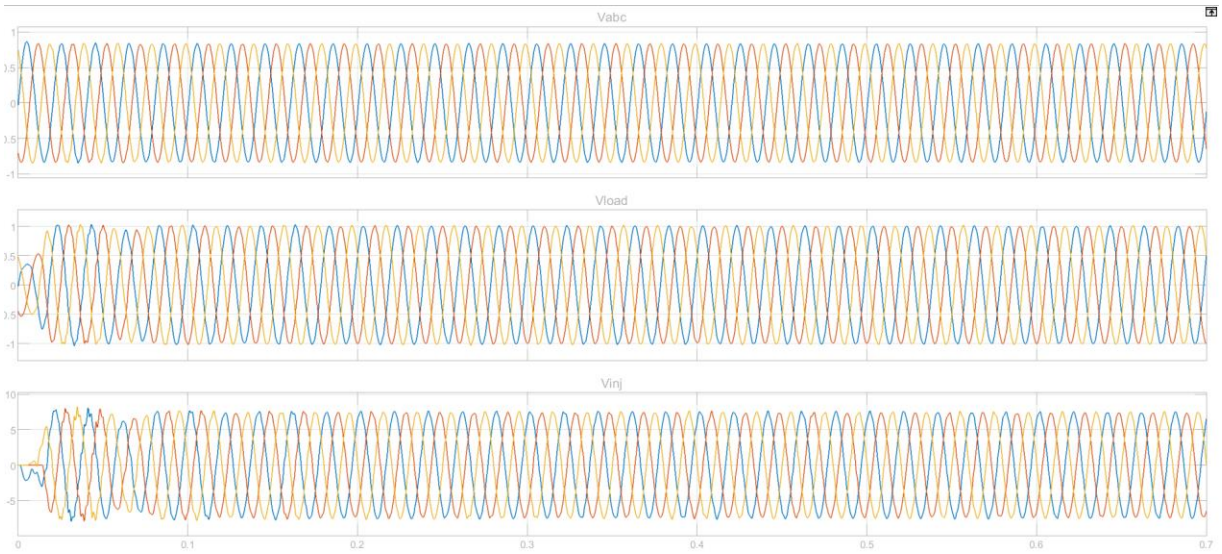

Fig 4.34: Input and output Voltages of installed PV-DVR in simara feeder in MATLAB in feeder overload conditions

Figure 4.34 depicts the input and output characteristics of the branch housing the PV-DVR. During the feeder's overload condition, only buses V1, V2, and V3 manage to maintain their voltage close to 1 per unit (p.u.).However, following the strategic placement of the DVR, The DVR consistently maintains the voltage levels within the range of 0.95 p.u. to 0.99 p.u. across all 11kV buses and load buses, including the farthest 11kV bus, V50, and the farthest load bus, V49. This performance is illustrated in Figures 4.35 and 4.36.

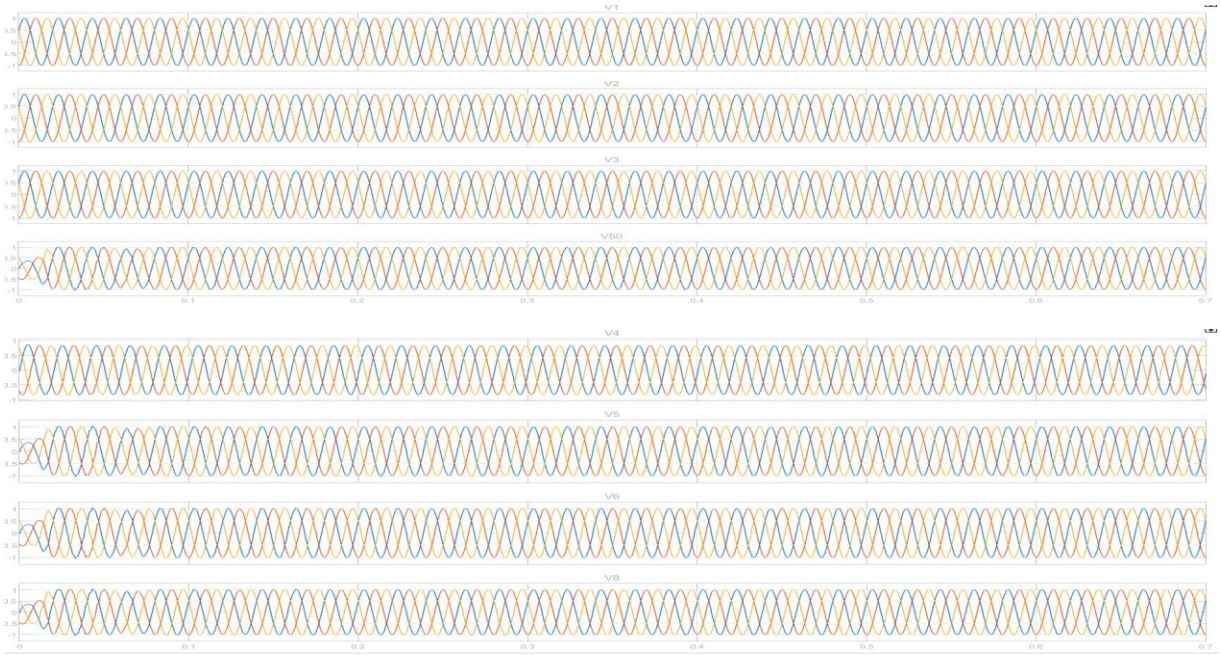

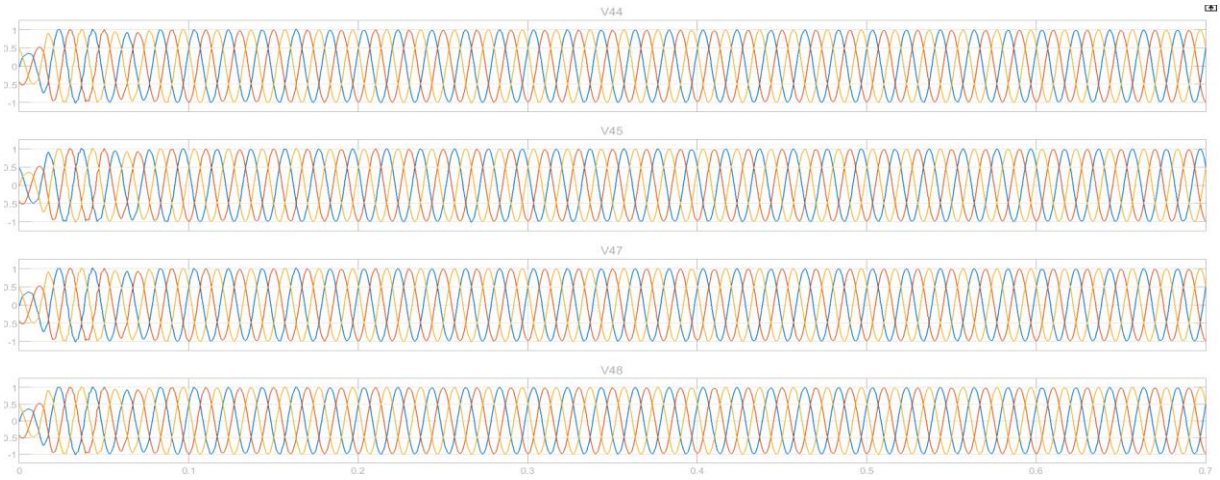

Fig 4.35: Output Voltages different 11kV buses after implementation of PV-DVR in simara feeder in feeder over-load conditions.

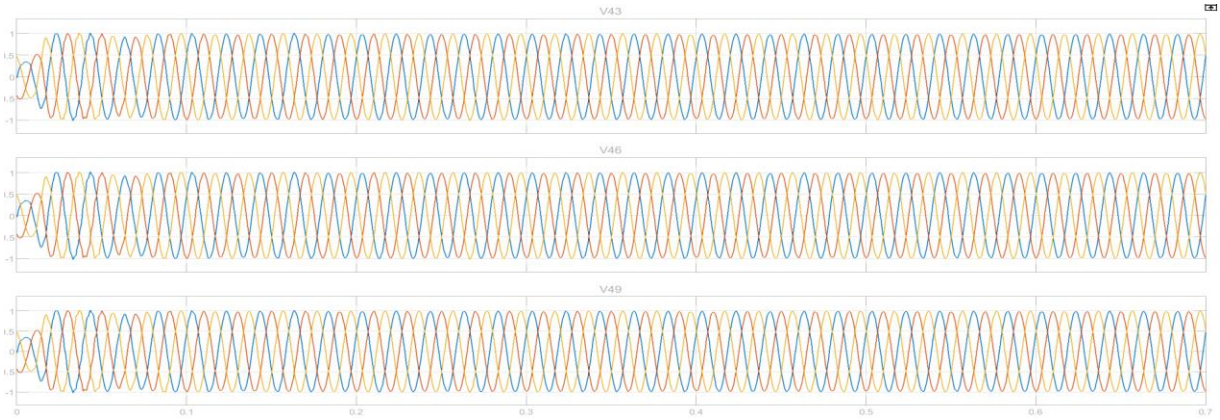

Fig 4.36: Output Voltages different load (0.4kV) buses after implementation of PV-DVR in simara feeder in feeder over-load conditions.

4.5.5 Harmonics of PV Integrated DVR Simara Industrial feeder under Over-loading conditions

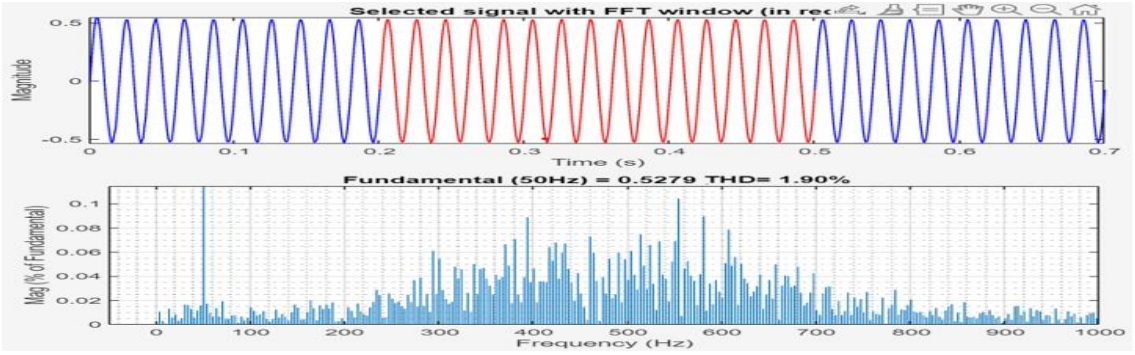

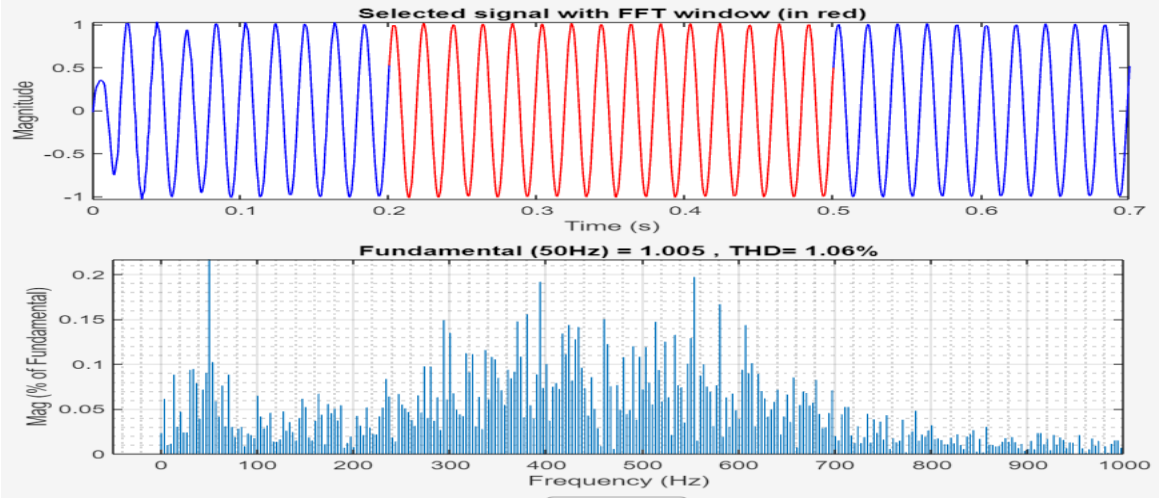

Fig 4.32: Harmonics of the System before and after Installation of DVR in 11kV Simara Feeder during overload conditions.

The integration of a Photovoltaic (PV) system into the Dynamic Voltage Restorer (DVR) system, utilizing Space Vector Pulse Width Modulation (SVPWM) with a Proportional-Resonant (PR) controller, represents a significant advancement in the management of power quality within the 11kV Simara Industrial feeder. This innovative approach has yielded impressive results, particularly in mitigating Total Harmonic Distortion (THD) during feeder-overloaded conditions. Spanning 25 cycles, commencing at t=0.2s and concluding at t=0.5s, within the 50Hz system, the DVR integrated system succeeded in reducing THD from an initiaL 1.90% to lower 1.06%.

CHAPTER 5: CONCLUSION LIMITATIONS AND RECOMMENDATIONS

5.1 Conclusions

The following conclusions can be deduced from the findings:

- Simulink model of PV integrated DVR has been modelled with essential controls in MATLAB/SIMULINK environment and tested with a modelled system comprising of a single source modelled as a negative PQ load that feeds a loadof rating P=1.5kW and Q=100VAR through a distribution line and transformers.During voltage sag, load voltage dropped down to 0.8 p.u. that is by 80% of itsnormal voltage, and during the event of voltage swell, voltage rose to 120% of the nominal rated voltage. The integration of the DVR model resulted in the restoration of bus voltage from 0.8p.u. to 0.97p.u. during voltage sag and swell and restoration of voltage from 1.2p.u. to 0.98p.u. during voltage swell. During sag/swell, DVR injected/absorbed the power into/from the load. Thus, a working model of DVR capable of operating during both sag and swell has been designed and modelled.
- Sensitivity analysis was performed for the developed model of DVR with a simple test system with two nodes where DVR was connected to the first node,and the voltage at the other node was observed during fault for a different combination of load demand and line length. From the study of the correlation between the input variables and (load demand and line length) and the voltage during a fault,it was found that load power demand has a substantial contribution to the voltage drop than the line length. distribution system.
- In optimization results to locate the optimal place for DVR in all three systems which were based on finding the minimum value of SARFI (System Average RMS Frequency Index) of the system in the presence of DVR during the event of voltage sag and swell. With this optimization process, the optimal location for DVR in IEEE 13 Node system was found out to be branch 632- 633. This location had minimum SARFI of 6.66% among all other possible locations. And optimal location for placement of PV integrated DVR in the 11kV Tanahunsur section was found to be branch 2-7 with minimum SARFI value of 6.09% and second best option for multiple

DVR application was found to be branch 4-5 with the SARFI values of 7.2%. Similarly, the optimal location corresponding to the location for which SARFI was minimumin the 11Kv simara was found out to be in branch 4-5 With DVR located in the line SARFI had a minimum value of 8.2% when compared to all other location. Using this Optimization technique based on SARFI, the optimal location for DVR, for three test systems.

- In, DVR interconnection point, In both cases, PV integrated DVR at the optimal location was able to restore the voltage above 0.95 p.u during fault condition and overloaded condition.
- Proposed DVR system is able to reduce the THD below 5% in all three Test systems.

5.2 Assumptions and Limitations

- The study is limited to 11kV radial distribution system.
- Voltage disturbances due to faults and overload have only been considered.
- The number of DVR integrated into a distribution system is limited to two.
- The magnitude of voltage has only been considered.
- Unequal voltage profile has not been taken into consideration.
- Capacitor compensation in the S/S and load side in the real world scenario of the feeder has not been considered.
- Harmonics result of the thesis is satisfactory (<5%) but can be improved.
- Data's that could be found has been either taken as default value of Matlab or has be assumed on the basis of Verbal communication with the staff of the DCs involved.

5.3 Future Aspects and Recommendations

Moreover, an essential continuation of this thesis could involve the comprehensive techno-economic analysis of PV integrated Dynamic Voltage Restorer (DVR). Additionally, the design of a PV system as a supplementary power source for the grid, capable of operating within an isolated system or being synchronized within intricate grid networks, holds promise for future exploration.

Further recommendations pertinent to this thesis include:

- Conducting in-depth field studies to validate the proposed methodology under diverse operating conditions.
- Exploring the integration of advanced control algorithms for improved performance and adaptability in varying grid scenarios.
- Evaluating the impact of the proposed PV integrated DVR system on the overall sustainability and resilience of the distribution network.
- Investigating the potential scalability and applicability of the proposed system in larger distribution grids and industrial settings.
- In intricate and interconnected distribution systems, the necessity arises for the placement of a considerable number of DVRs. Consequently, the formulation of intricate optimization problems becomes imperative to facilitate decentralized voltage restoration. In this context, refining the training of the SARFI optimization and control of DVRs based on the specific system dynamics and operational imperatives becomes crucial. This adaptation must be tailored to accommodate the evolving complexities of the system and the diverse requirements governing its effective operation.
- An in-depth exploration of the power-sharing dynamics between one or more DVRs during voltage sag/swell occurrences is warranted, particularly concerning the implementation of droop control. This study should focus on establishing a framework wherein the DVRs can share active and reactive power in proportion to their individual capacities, thereby facilitating seamless coordination. Such an investigation holds significant promise for enhancing the overall efficiency and reliability of the system during critical voltage fluctuation events.
- Given the prevalence of radial distribution systems, the meticulous management of voltage control in such networks has garnered substantial attention from researchers globally. This attention has been further amplified with the widespread implementation of smart grids and the integration of Inverter-Based Resources (IBRs) within these systems. A crucial aspect to be explored in this context is the operation of PV-based DVRs alongside Distributed Energy Resources (DERs) and inverters. Specifically, an in-depth investigation into the coordinated control mechanisms among these components and their harmonious interaction with other devices is

pivotal as we advance the use of DVRs within modern, intelligent distribution systems.

These recommendations are crucial for advancing the understanding and practical implementation of the outlined research, thereby contributing significantly to the field of Power System Engineering.

REFERENCES

[1] Nepal Electricity Authority. A year in review 2020/2021, 2021,2022

[2] Naeem Abas , (member, IEEE), Saad Dilshad , (graduate student member, IEEE), Adnan Khalid1, Muhammad Shoaib Saleem , and,Nasrullah Khan, (Senior Member, IEEE), Power Quality Improvement Using Dynamic Voltage Restorer,IEEE ,August 27,2020

[3] Zovnomir Klaic,Srete Nikoloslav,Zorislav Kraus,-Voltage Variation Performance Indices in Distribution Network,2018

[4] IEEE POWER ENGINEERING SOCIETY,IEEE 13 Node Test Feeder.

[5] Tiago Davi Curi Busarello; Jose Antenor Pomilio; Marcelo Godoy Simoes, Design Procedure for a Digital Proportional-Resonant Current Controller in a Grid Connected Inverter,2018

[6] M. H. J. Bollen, Understanding Power Quality Problems—Voltage Sags and Interruptions. New York, NY, USA: IEEE Press, 2000.

[7] A. Ghosh and G. Ledwich, Power Quality Enhancement Using Custom Power Devices.

[8] N.G. Hingorani and L Gyugyi, "Understanding FACTS – Concepts and Technology of Flexible AC Transmission Systems", Wiley, 2000.

[9] R. C. Dugan, M. F. McGranaghan, and H. W. Beaty, Electric Power Systems Quality, 2nd edu. New York, NY, USA: McGraw-Hill, 2006.

[10] A. Moreno-Munoz, Power Quality: Mitigation Technologies in a Distributed Environment. London, U.K.: Springer-Verlag, 2007.

[11] K. R. Padiyar, FACTS Controllers in Transmission and Distribution. New Delhi, India: New Age Int., 2007.

[12] IEEE Recommended Practices and Recommendations for Harmonics Control in Electric Power Systems, IEEE Std. 519, 1992.

[13] S. Middlekauff and E. Collins, "System and customer impact," IEEE Trans. Power Del., vol. 13, no. 1, pp. 278–282, Jan. 1998.

[14] M. Vilathgamuwa, R. Purer, S. Choi, and K. Tseng, "Control of energy optimized dynamic voltage restorer," in Proc. IEEE IECON, 1999, vol. 2, pp. 873–878.

[15] J. G. Nielsen, F. Blaabjerg, and N.Mohan, “Control strategies for dynamic voltage restorer compensating voltage sags with phase jump,” in Proc. IEEE APEC, 2001, vol. 2, pp. 1267–1273.

[16] A. Ghosh and G. Ledwich, “Compensation of distribution system voltage using DVR,” IEEE Trans. Power Del., vol. 17, no. 4, pp. 1030–1036, Oct. 2002.

[17] I.-Y. Chung, D.-J. Won, S.-Y. Park, S.-I. Moon, and J.-K. Park, “The DC link energy control method in dynamic voltage restorer system,” Int. J. Elect. Power Energy Syst., vol. 25, no. 7, pp. 525–531, Sep. 2003.

[18] E. C. Aeloíza, P. N. Enjeti, L. A. Morán, O. C. Montero-Hernandez, and S. Kim, “Analysis and design of a new voltage sag compensator for critical loads in electrical power distribution systems,” IEEE Trans. Ind. Appl., vol. 39, no. 4, pp. 1143–1150, Jul./Aug. 2003.

[19] J. W. Liu, S. S. Choi, and S. Chen, “Design of step dynamic voltage regulator for power quality enhancement,” IEEE Trans. Power Del., vol. 18, no. 4, pp. 1403–1409, Oct. 2003

[20] Villalva, Marcelo Gradella, and Jonas Rafael Gazoli. "Comprehensive approach to modeling and simulation of photovoltaic arrays." IEEE Trans. Power Electron. 24.5 (2009): 1198-1208.

[21] Altas, I. H., and A. M. Sharaf. "A photovoltaic array simulation model for matlab-simulink gui environment." International Conference on Clean Electrical Power, ICCEP, IEEE, 2007.

[22] Kawamura, Hajime, et al. "Simulation of I & V characteristics of a pv module with shaded pv cells." Solar Energy Materials and Solar Cells, vol.75, no.3, 2003, pp. 613-621

[23] Ghimire, A., Bhattarai, N. & Motra, L., 2020. Optimal placement of Dynamic Voltage Restorer in Radial Distribution System using Artificial Neural Network Approach. International Research Journal of Engineering and Technology (IRJET), May.07(05).

[24] Khanh Q. Bach, “A Novel Method For Global Voltage Sag Compensation In Ieee 69 Bus Distribution System By Dynamic Voltage Restorers” , 2019

[25] Hanju Cha; Trung-Kien Vu; Jae-Eon Kim, “Design and control of Proportional-Resonant controller based Photovoltaic power conditioning system”,IEEE Conference,2009

[26] Tiago Davi Curi Busarello, Design Procedure for a Digital Proportional-Resonant Current Controller in a Grid Connected Inverter, 4th IEEE Southern Power Electronics Conference, SPEC 2018

[27] Abdul Hameed Soomro , Abdul Sattar Larik , Mukhtiar Ahmed Mahar Anwer Ali Sahito , Amir Mahmood Soomro ,Ghulam Sarwar Kaloi,”Dynamic Voltage Restorer—A comprehensive review”,Energy Report 7 (2021)

[28] Zvonimir klaic,Srete Nikolovski ,Zorilav Kraus,” Voltage Variation Performance Indices in Distribution Network,ISSN

[29] Wei Du;Kevin P. Schneider;Greg P. Wiegand;Francis K. Tuffner;Jing Xie;Orris L.Dent, A Supplemental Control for Dynamic Voltage Restorers to Improve the Primary Frequency Response of Microgrids,IEEE Transactions on Smart Grid,2022

PUBLICATION(S)

The Optimal Placement of a Photovoltaic-integrated Dynamic Voltage Restorer for the Enhancement of Power Quality within the Distribution System: A case Study of 11kV Simara Industrial feeder in Nepal" has been accepted for the Journal of Advanced College of Engineering and Management (JACEM) for Vol.9, 2024.

APPENDIX A: LINE , LOAD AND VOLTAGE DATA OF IEEE-13 NODE TEST FEEDER

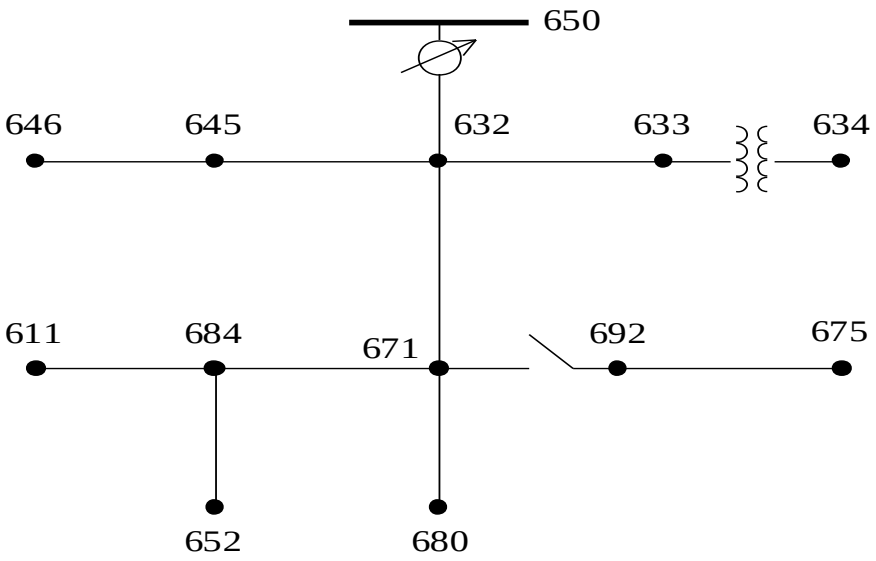

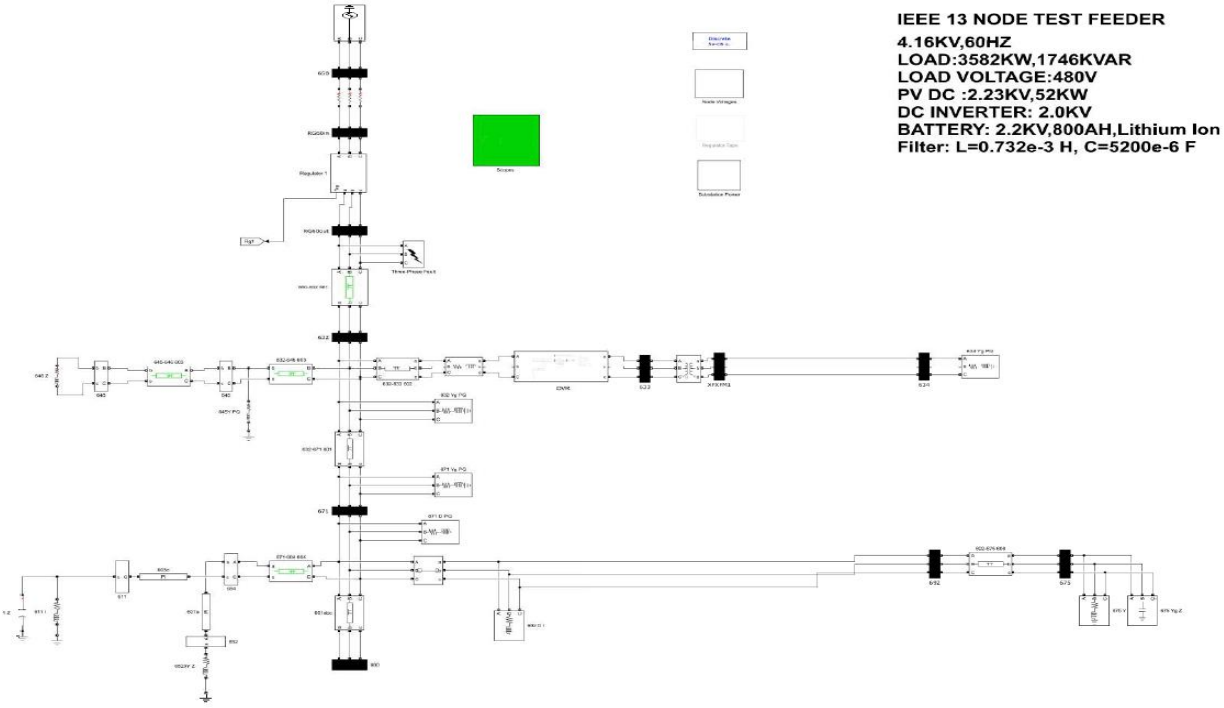

Overhead Line Configuration Data:

Config.	Phasing	Phase	Neutral	Spacing
		ACSR	ACSR	ID
601	B A C N	556,500 26/7	4/0 6/1	500
602	C A B N	4/0 6/1	4/0 6/1	500
603	C B N	1/0	1/0	505
604	A C N	1/0	1/0	505
605	C N	1/0	1/0	510

Underground Line Configuration Data:

Config.	Phasing	Cable	Neutral	Space ID
606	A B C N	250,000 AA, CN	None	515
607	A N	1/0 AA, TS	1/0 Cu	520

Line Segment Data:

Node A	Node B	Length(ft.)	Config.
632	645	500	603
632	633	500	602
633	634	0	XFM-1
645	646	300	603
650	632	2000	601
684	652	800	607
632	671	2000	601
671	684	300	604
671	680	1000	601
671	692	0	Switch
684	611	300	605
692	675	500	606

Transformer Data:

	kVA	kV-high	kV-low	R - %	X - %
Substation:	5,000	115 - D	4.16 Gr. Y	1	8
XFM -1	500	4.16 – Gr.W	0.48 – Gr.W	1.1	2

Capacitor Data:

Node	Ph-A	Ph-B	Ph-C
	kVAr	kVAr	kVAr
675	200	200	200
611			100
Total	200	200	300

Regulator Data:

Regulator ID:	1		
Line Segment:	650 - 632		
Location:	50		
Phases:	A - B -C		
Connection:	3-Ph,LG		
Monitoring Phase:	A-B-C		
Bandwidth:	2.0 volts		
PT Ratio:	20		
Primary CT Rating:	700		
Compensator Settings:	Ph-A	Ph-B	Ph-C
R - Setting:	3	3	3
X - Setting:	9	9	9
Volltage Level:	122	122	122

Spot Load Data:

Node	Load	Ph-1	Ph-1	Ph-2	Ph-2	Ph-3	Ph-3
	Model	kW	kVAr	kW	kVAr	kW	kVAr
634	Y-PQ	160	110	120	90	120	90
645	Y-PQ	0	0	170	125	0	0
646	D-Z	0	0	230	132	0	0
652	Y-Z	128	86	0	0	0	0
671	D-PQ	385	220	385	220	385	220
675	Y-PQ	485	190	68	60	290	212
692	D-I	0	0	0	0	170	151
611	Y-I	0	0	0	0	170	80
	TOTAL	1158	606	973	627	1135	753

Distributed Load Data:

Node A	Node B	Load	Ph-1	Ph-1	Ph-2	Ph-2	Ph-3	Ph-3
		Model	kW	kVAr	kW	kVAr	kW	kVAr
632	671	Y-PQ	17	10	66	38	117	68

Impedances

Configuration 601:

Z (R +jX) in ohms per mile
0.3465 1.0179 0.1560 0.5017 0.1580 0.4236
0.3375 1.0478 0.1535 0.3849
0.3414 1.0348
B in micro Siemens per mile
6.2998 -1.9958 -1.2595
5.9597 -0.7417
5.6386

Configuration 602:

Z (R +jX) in ohms per mile
0.7526 1.1814 0.1580 0.4236 0.1560 0.5017
0.7475 1.1983 0.1535 0.3849
0.7436 1.2112
B in micro Siemens per mile
5.6990 -1.0817 -1.6905
5.1795 -0.6588
5.4246

Configuration 603:

Z (R +jX) in ohms per mile
0.0000 0.0000 0.0000 0.0000 0.0000 0.0000
1.3294 1.3471 0.2066 0.4591
1.3238 1.3569
B in micro Siemens per mile
0.0000 0.0000 0.0000
4.7097 -0.8999
4.6658

Configuration 604:

Z (R +jX) in ohms per mile
1.3238 1.3569 0.0000 0.0000 0.2066 0.4591
0.0000 0.0000 0.0000 0.0000
1.3294 1.3471
B in micro Siemens per mile
4.6658 0.0000 -0.8999
0.0000 0.0000
4.7097

Configuration 605:

Z (R +jX) in ohms per mile
0.0000 0.0000 0.0000 0.0000 0.0000 0.0000
0.0000 0.0000 0.0000 0.0000
1.3292 1.3475
B in micro Siemens per mile
0.0000 0.0000 0.0000
0.0000 0.0000
4.5193

Configuration 606:

Z (R +jX) in ohms per mile
0.7982 0.4463 0.3192 0.0328 0.2849 -0.0143
0.7891 0.4041 0.3192 0.0328
0.7982 0.4463
B in micro Siemens per mile
96.8897 0.0000 0.0000
96.8897 0.0000
96.8897

Configuration 607:

Z (R +jX) in ohms per mile
1.3425 0.5124 0.0000 0.0000 0.0000 0.0000
0.0000 0.0000 0.0000 0.0000
0.0000 0.0000
B in micro Siemens per mile
88.9912 0.0000 0.0000
0.0000 0.0000
0.0000

Power-Flow Results

- **R A D I A L F L O W S U M M A R Y** - DATE: 6-24-2004 AT 15:33: 2 HOURS ---
SUBSTATION: IEEE 13; FEEDER: IEEE 13

SYSTEM INPUT	PHASE (A)	PHASE (B)	PHASE (C)	TOTAL
kW :	1251.398	977.332	1348.461	3577.191
kVAr :	681.570	373.418	669.784	1724.772
kVA :	1424.968	1046.241	1505.642	3971.289
PF :	.8782	.9341	.8956	.9008

LOAD	A-N	A-B	B-N	B-C	C-N	C-A	WYE	DELTA
kW :	785.6	385.0	424.0	625.7	692.5	553.4	1902.1	1564.0
TOT :	1170.563		1049.658		1245.907		3466.128	
kVAr :	393.0	220.0	313.0	358.1	447.9	369.5	1153.9	947.7
TOT :	613.019		671.117		817.450		2101.586	
kVA :	878.4	443.4	527.0	720.9	824.8	665.4	2224.8	1828.7
TOT :	1321.367		1245.865		1490.137		4053.481	
PF :	.8943	.8682	.8045	.8679	.8397	.8316	.8550	.8553
TOT :	.8859		.8425		.8361		.8551	

LOSSES	(A)	(B)	(C)	
kW :	39.107	-4.697	76.653	111.063
kVAr :	152.585	42.217	129.850	324.653
kVA :	157.517	42.478	150.787	343.124

CAPAC	A-N	A-B	B-N	B-C	C-N	C-A	WYE	DELTA
R-kVA:	200.0	.0	200.0	.0	300.0	.0	700.0	.0
TOT :	200.000		200.000		300.000		700.000	
A-kVA:	193.4	.0	222.7	.0	285.3	.0	701.5	.0
TOT :	193.443		222.747		285.276		701.466	

--- **V O L T A G E P R O F I L E** ---- DATE: 6-24-2004 AT 15:33:12 HOURS ----
SUBSTATION: IEEE 13; FEEDER: IEEE 13

NODE	MAG	ANGLE	MAG	ANGLE	MAG	ANGLE	mi.to SR
	A-N		B-N		C-N		
650	1.0000 at	.00	1.0000 at	-120.00	1.0000 at	120.00	.000
RG60	1.0625 at	.00	1.0500 at	-120.00	1.0687 at	120.00	.000
632	1.0210 at	-2.49	1.0420 at	-121.72	1.0174 at	117.83	.379
633	1.0180 at	-2.56	1.0401 at	-121.77	1.0148 at	117.82	.474
XFXFM1	.9941 at	-3.23	1.0218 at	-122.22	.9960 at	117.35	.474
634	.9940 at	-3.23	1.0218 at	-122.22	.9960 at	117.34	.474
645			1.0329 at	-121.90	1.0155 at	117.86	.474
646			1.0311 at	-121.98	1.0134 at	117.90	.530
671	.9900 at	-5.30	1.0529 at	-122.34	.9778 at	116.02	.758
680	.9900 at	-5.30	1.0529 at	-122.34	.9778 at	116.02	.947
684	.9881 at	-5.32			.9758 at	115.92	.815
611					.9738 at	115.78	.871
652	.9825 at	-5.25					.966
692	.9900 at	-5.31	1.0529 at	-122.34	.9777 at	116.02	.852
675	.9835 at	-5.56	1.0553 at	-122.52	.9758 at	116.03	.947

---------- **VOLTAGE REGULATOR DATA** ---- DATE: 6-24-2004 AT 15:33:16 HOURS --
SUBSTATION: IEEE 13; FEEDER: IEEE 13

[NODE]	[VREG]	[SEG]	[NODE]	MODEL	OPT	BNDW
650	RG60	632	632	Phase A & B & C, Wye	RX	2.00

PHASE	LDCTR	VOLT HOLD	R-VOLT	X-VOLT	PT RATIO	CT RATE	TAP
1	122.000	3.000	9.000	20.00	700.00	10	
2	122.000	3.000	9.000	20.00	700.00	8	
3	122.000	3.000	9.000	20.00	700.00	11	

```
- R A D I A L  P O W E R  F L O W  ---  DATE:  6-24-2004 AT 15:33:27 HOURS ---
SUBSTATION:  IEEE 13;   FEEDER:  IEEE 13
--------------------------------------------------------------------------------
  NODE      VALUE         PHASE A         PHASE B         PHASE C     UNT O/L<
                        (LINE A)        (LINE B)        (LINE C)        60.%
---------------------*--------A-------*-------B-------*-------C-------*--------
NODE: 650       VOLTS:   1.000    .00   1.000 -120.00   1.000  120.00 MAG/ANG
kVll   4.160          NO LOAD OR CAPACITOR REPRESENTED AT SOURCE NODE

TO NODE RG60  <VRG>..:  593.30  -28.58  435.61 -140.91  626.92   93.59 AMP/DG <
<RG60  > LOSS=   .000:   (   .000)      (   .000)      (   .000)    kW
---------------------*--------A-------*-------B-------*-------C-------*--------
NODE: RG60      VOLTS:   1.062    .00   1.050 -120.00   1.069  120.00 MAG/ANG
              -LD:    .00    .00    .00    .00    .00    .00 kW/kVR
kVll   4.160      CAP:            .00            .00            .00 kVR

FROM NODE 650   <VRG>:  558.40  -28.58  414.87 -140.91  586.60   93.59 AMP/DG <
<RG60  > LOSS=   .000:   (   .000)      (   .000)      (   .000)    kW
TO NODE 632   .......:  558.40  -28.58  414.87 -140.91  586.60   93.59 AMP/DG <
<632   > LOSS= 59.716:   ( 21.517)      ( -3.252)      ( 41.451)    kW
---------------------*--------A-------*-------B-------*-------C-------*--------
NODE: 632       VOLTS:   1.021   -2.49   1.042 -121.72   1.017  117.83 MAG/ANG
              -LD:    .00    .00    .00    .00    .00    .00 kW/kVR
kVll   4.160      CAP:            .00            .00            .00 kVR

FROM NODE RG60  .....:  558.41  -28.58  414.87 -140.91  586.60   93.59 AMP/DG <
<632   > LOSS= 59.716:   ( 21.517)      ( -3.252)      ( 41.451)    kW
TO NODE 633   .......:   81.33  -37.74   61.12 -159.09   62.70   80.48 AMP/DG
<633   > LOSS=   .808:   (   .354)      (   .148)      (   .306)    kW
TO NODE 645   .......:                  143.02 -142.66   65.21   57.83 AMP/DG <
<645   > LOSS=  2.760:                  (  2.540)      (   .220)    kW
TO NODE 671   .......:  478.29  -27.03  215.12 -134.66  475.50   99.90 AMP/DG <
<671   > LOSS= 35.897:   ( 10.484)      ( -6.169)      ( 31.582)    kW
---------------------*--------A-------*-------B-------*-------C-------*--------
NODE: 633       VOLTS:   1.018   -2.56   1.040 -121.77   1.015  117.82 MAG/ANG
              -LD:    .00    .00    .00    .00    .00    .00 kW/kVR
kVll   4.160      CAP:            .00            .00            .00 kVR

FROM NODE 632   .....:   81.33  -37.74   61.12 -159.09   62.71   80.47 AMP/DG
<633   > LOSS=   .808:   (   .354)      (   .148)      (   .306)    kW
TO NODE XFXFM1.......:   81.33  -37.74   61.12 -159.09   62.71   80.47 AMP/DG <
<XFXFM1> LOSS=  5.427:   (  2.513)      (  1.420)      (  1.494)    kW
---------------------*--------A-------*-------B-------*-------C-------*--------
NODE: XFXFM1    VOLTS:    .994   -3.23   1.022 -122.22    .996  117.35 MAG/ANG
              -LD:    .00    .00    .00    .00    .00    .00 kW/kVR
kVll    .480      CAP:            .00            .00            .00 kVR

FROM NODE 633   .....:  704.83  -37.74  529.73 -159.09  543.45   80.47 AMP/DG <
<XFXFM1> LOSS=  5.427:   (  2.513)      (  1.420)      (  1.494)    kW
TO NODE 634   .......:  704.83  -37.74  529.73 -159.09  543.45   80.47 AMP/DG <
<634   > LOSS=   .000:   (   .000)      (   .000)      (   .000)    kW
```

- **R A D I A L P O W E R F L O W** --- DATE: 6-24-2004 AT 15:33:27 HOURS ---
SUBSTATION: IEEE 13; FEEDER: IEEE 13

```
------------------------------------------------------------------------------
  NODE      VALUE        PHASE A        PHASE B        PHASE C     UNT O/L<
                       (LINE A)       (LINE B)       (LINE C)       60.%
--------------------*--------A-------*-------B-------*-------C-------*--------
NODE: 634       VOLTS:   .994   -3.23   1.022 -122.22    .996  117.34 MAG/ANG
            Y-LD:  160.00  110.00  120.00   90.00  120.00   90.00 kW/kVR
kVll   .480    Y CAP:           .00            .00            .00 kVR

FROM NODE XFXFM1.....:  704.83  -37.74  529.73 -159.09  543.45   80.47 AMP/DG <
<634   > LOSS=   .000:   (   .000)      (   .000)      (   .000)    kW
--------------------*--------A-------*-------B-------*-------C-------*--------
NODE: 645       VOLTS:                 1.033 -121.90   1.015  117.86 MAG/ANG
            Y-LD:               170.00  125.00    .00    .00 kW/kVR
kVll   4.160    Y CAP:                       .00           .00 kVR

FROM NODE 632   .....:               143.02 -142.66   65.21   57.83 AMP/DG <
<645   > LOSS=  2.760:                (  2.540)      (   .220)    kW
TO NODE 646   .......:              65.21 -122.17   65.21   57.83 AMP/DG
<646   > LOSS=   .541:                (   .271)      (   .270)    kW
--------------------*--------A-------*-------B-------*-------C-------*--------
NODE: 646       VOLTS:                 1.031 -121.98   1.013  117.90 MAG/ANG
            D-LD:               240.66  138.12    .00    .00 kW/kVR
kVll   4.160    Y CAP:                       .00           .00 kVR

FROM NODE 645   .....:               65.21 -122.18   65.21   57.82 AMP/DG
<646   > LOSS=   .541:              (   .271)      (   .270)    kW
--------------------*--------A-------*-------B-------*-------C-------*--------
NODE: 671       VOLTS:   .990   -5.30   1.053 -122.34    .978  116.02 MAG/ANG
            D-LD:  385.00  220.00  385.00  220.00  385.00  220.00 kW/kVR
kVll   4.160    Y CAP:           .00            .00            .00 kVR

FROM NODE 632   .....:  470.20  -26.90  186.41 -131.89  420.64  101.66 AMP/DG <
<671   > LOSS= 35.897:   ( 10.484)      ( -6.169)      ( 31.582)    kW
TO NODE 680   .......:    .00    .00    .00    .00    .00    .00 AMP/DG
<680   > LOSS=   .000:   (  -.001)      (   .001)      (   .000)    kW
TO NODE 684   .......:  63.07  -39.12                71.15  121.62 AMP/DG
<684   > LOSS=   .580:   (   .210)                   (   .370)    kW
TO NODE 692   .......:  229.11  -18.18   69.61  -55.19  178.38  109.39 AMP/DG
<692   > LOSS=   .008:   (   .003)      (  -.001)      (   .006)    kW
--------------------*--------A-------*-------B-------*-------C-------*--------
NODE: 680       VOLTS:   .990   -5.30   1.053 -122.34    .978  116.02 MAG/ANG
             -LD:    .00    .00    .00    .00    .00    .00 kW/kVR
kVll   4.160     CAP:           .00            .00            .00 kVR

FROM NODE 671   .....:    .00    .00    .00    .00    .00    .00 AMP/DG
<680   > LOSS=   .000:   (  -.001)      (   .001)      (   .000)    kW
```

```
- R A D I A L  P O W E R  F L O W  ---  DATE:  6-24-2004 AT 15:33:27 HOURS ---
SUBSTATION:  IEEE 13;   FEEDER:  IEEE 13
--------------------------------------------------------------------------------
  NODE      VALUE         PHASE A         PHASE B         PHASE C     UNT O/L<
                        (LINE A)        (LINE B)        (LINE C)        60.%
---------------------*--------A-------*-------B-------*-------C-------*--------
NODE: 684       VOLTS:    .988   -5.32                    .976  115.92 MAG/ANG
              -LD:     .00     .00                   .00     .00 kW/kVR
kVll   4.160      CAP:            .00                          .00 kVR

FROM NODE 671   .....:   63.07  -39.12                  71.15  121.61 AMP/DG
<684   > LOSS=   .580:    (   .210)                    (   .370)    kW
TO NODE 611   .......:                                 71.15  121.61 AMP/DG
<611   > LOSS=   .382:                                 (   .382)    kW
TO NODE 652   .......:   63.07  -39.12                          AMP/DG
<652   > LOSS=   .808:    (   .808)                             kW
---------------------*--------A-------*-------B-------*-------C-------*--------
NODE: 611       VOLTS:                                  .974  115.78 MAG/ANG
              Y-LD:                             165.54   77.90 kW/kVR
kVLL   4.160    Y CAP:                                  94.82 kVR

FROM NODE 684   .....:                                  71.15  121.61 AMP/DG
<611   > LOSS=   .382:                                 (   .382)    kW
---------------------*--------A-------*-------B-------*-------C-------*--------
NODE: 652       VOLTS:    .983   -5.25                           MAG/ANG
              Y-LD:  123.56   83.02                          kW/kVR
kVll   4.160    Y CAP:            .00                           kVR

FROM NODE 684   .....:   63.08  -39.15                          AMP/DG
<652   > LOSS=   .808:    (   .808)                             kW
---------------------*--------A-------*-------B-------*-------C-------*--------
NODE: 692       VOLTS:    .990   -5.31   1.053 -122.34    .978  116.02 MAG/ANG
              D-LD:     .00     .00     .00     .00  168.37  149.55 kW/kVR
kVll   4.160    Y CAP:            .00             .00             .00 kVR

FROM NODE 671   .....:  229.11  -18.18   69.61  -55.19  178.38  109.39 AMP/DG
<692   > LOSS=   .008:    (   .003)       (  -.001)       (   .006)    kW
TO NODE 675   .......:  205.33   -5.15   69.61  -55.19  124.07  111.79 AMP/DG <
<675   > LOSS=  4.136:    (  3.218)       (   .345)       (   .573)    kW
---------------------*--------A-------*-------B-------*-------C-------*--------
NODE: 675       VOLTS:    .983   -5.56   1.055 -122.52    .976  116.03 MAG/ANG
              Y-LD:  485.00  190.00   68.00   60.00  290.00  212.00 kW/kVR
kVll   4.160    Y CAP:          193.44          222.75          190.45 kVR

FROM NODE 692   .....:  205.33   -5.15   69.59  -55.20  124.07  111.78 AMP/DG <
<675   > LOSS=  4.136:    (  3.218)       (   .345)       (   .573)    kW
```

Table 1. Voltage profiles of 13 bus system without and with DVR at bus 632 Total simulation time 0.7sec

Bus no	Voltage in p.u					
	WithoutDVR			WithDVR		
	A	B	C	A	B	C
632	1.0210	1.0420	1.0174	1.042	1.0500	1.0261
633	0.9900	1.0300	0.997	1	1.072	0.99
634	1.0180	1.0401	1.0148	1.0180	1.051	1.0148
650	1.0000	1.0800	1.0000	1	1	1
675	0.9980	1.0529	0.9777	1	1.072	0.9900
692	0.9970	1.0529	0.9777	1	1.072	0.99900
671	1.0210	1.0420	1.0174	1.0312	1.0480	1.0203

Table 2: Results of 13 Node system

Description	Real power loss (kW) at bus 633 during 3 phase fault	Reactive power loss (kVAr) at bus 633 during 3 phase fault	Minimum voltage (p.u.) without Fault	No. of Buses with Under voltage	Rating of DVR
Before DVR installation	30	22	0.99,1.03,0.977 @bus 633,	7	0
After DVR installation	5	3	1,1.072,0.0.99 @bus 633	0	866 kVA

1. **Output Voltages in p.u of different buses(11kv and 0.4kv) obtained from matlab after application of Dvr in optimal loacation during 3 phase, SLG,LLLG,DLG and LL faults.**

Columns 1 through 5

0.049963004064487 0.049963004064487 0.049963004064487 0.049963004064487 0.049963004064487
1.000001343928803 0.999995686679573 1.000006566911841 1.066667670198043 1.052626684369594
1.000001343928707 0.999995686679487 1.000006566911733 1.066667670197875 1.052626684368450

1.000001343928622	0.999995686679390	1.000006566911650	1.066667670197795	1.052626684368359
1.000001343928565	0.999995686679315	1.000006566911572	1.066667670197709	1.052626684368291
1.000001343928451	0.999995686679228	1.000006566911523	1.066667670149597	1.052626684884938
1.000001343928345	0.999995686679133	1.000006566911415	1.066667670149529	1.052626684884876
1.000001343928262	0.999995686679046	1.000006566911315	1.066667670149413	1.052626684884738

Columns 6 through 10

0.049963004064487	0.049963004064487	0.049963004064487	0.049963004064487	0.049963004064487
1.073832088033935	1.021758594134655	1.041536753728872	1.024342981484042	1.018572459254129
1.073832088031596	1.021757934352749	1.041502284711273	1.024301900664814	1.018571736155587
1.073832088031535	1.021757119531654	1.041501873813753	1.024299927064394	1.018570764582672
1.073832088031460	1.021757054968618	1.041497027663477	1.024299168967906	1.018570638157210
1.066673210277756	1.021690349392679	1.041523174614781	1.017437435527106	1.018497445616839
1.066673210277697	1.021690389655418	1.041522730307100	1.017438094303529	1.018497489160958
1.066673210277595	1.021690245295913	1.041524654685609	1.017439659167439	1.018497319597618

Columns 11 through 15

0.049963004064487	0.049963004064487	0.049963004064487	0.049963004064487	0.049963004064487
1.039484374433217	1.022000183196083	0.994804483753133	1.020284611866067	1.003123781602819
1.039447170619416	1.021955746528838	0.994803813417376	1.020248269962336	1.003079680494996
1.039447198336509	1.021953941358151	0.994802841237643	1.020248483544881	1.003078285957442
1.039441731200632	1.021952865535520	0.994802771270172	1.020243402374747	1.003077484592546
1.039468097414690	1.015113127623091	0.994731281374014	1.020269158683185	0.996363986769134
1.039467482897225	1.015113736583028	0.994731344360207	1.020268388219285	0.996364442387598
1.039469459261791	1.015115362584319	0.994731160562013	1.020270379355355	0.996366082854033

Columns 16 through 20

0.049963004064487	0.049963004064487	0.049963004064487	0.049963004064487	0.049963004064487
0.994804483753133	1.020284611866067	1.003123781602819	0	1.031958060060632
0.994803813417376	1.020248269962336	1.003079680494996	0	1.031919440016435
0.994802841237643	1.020248483544881	1.003078285957442	0	1.031919940403378
0.994802771270172	1.020243402374747	1.003077484592546	0	1.031914181248267
0.994731281374014	1.020269158683185	0.996363986769134	0	1.031945554256221
0.994731344360207	1.020268388219285	0.996364442387598	0	1.031944701214163

0.994731160562013	1.020270379355355	0.996366082854033	0	1.031946965004885

Columns 21 through 25

0.049963004064487	0.049963004064487	0.049963004064487	0.049963004064487	0.049963004064487
1.022456370148798	0	1.030221571681869	1.020391189366425	0.992419516929009
1.022409517687469	0	1.030182317502698	1.020343481681619	0.992418857989565
1.022407278196974	0	1.030182945492893	1.020341188337428	0.992418944405209
1.022407450814665	0	1.030177051957945	1.020341530020928	0.992418987076628
1.015558638716062	0	1.030211653240890	1.013501050388878	0.992308961306343
1.015559834700329	0	1.030210715535316	1.013502314448545	0.992309073382258
1.015561928640033	0	1.030213045224833	1.013504514678533	0.992309226581584

Columns 26 through 30

0.049963004064487	0.049963004064487	0.049963004064487	0.049963004064487	0.049963004064487
1.043429133074822	0.986316163705878	0.992422939711715	1.043436713340814	0.986336365331530
1.043427563096120	0.986305161087827	0.992420182318395	1.043432027036049	0.986309650653245
1.043419661169535	0.986299100360527	0.992420133147402	1.043419964654825	0.986297392966625
1.043423439423098	0.986302000366859	0.992420359809022	1.043425349407198	0.986303272336245
1.043495685520363	0.979627452513605	0.992309326627373	1.043494020930062	0.979633999171847
1.043496960620504	0.979624747776789	0.992309497134620	1.043496761701421	0.979627948516512
1.043495528770256	0.979620019910890	0.992309968160190	1.043495843362080	0.979618719619526

Columns 31 through 35

0.049963004064487	0.049963004064487	0.049963004064487	0.049963004064487	0.049963004064487
0.990446244185964	0	0.984367843382037	0	0
0.990443843234799	0	0.984367182856357	0	0
0.990443424559223	0	0.984365520488459	0	0
0.990443314908821	0	0.984366121217444	0	0
0.990328546089272	0	0.977700132883939	0	0
0.990328430536717	0	0.977699594157441	0	0
0.990328295244640	0	0.977698506523450	0	0

Columns 36 through 40

0.049963004064487	0.049963004064487	0.049963004064487	0.049963004064487	0.049963004064487
0.983721448007614	0.988578374097362	0	0	0.992410471117795
0.983723389380661	0.988575343940568	0	0	0.992409812147224
0.983723390212601	0.988574794185403	0	0	0.992409898553070
0.983723390034361	0.988574632623628	0	0	0.992409941222850
0.977060378819161	0.988460095399114	0	0	0.992299914725745
0.977060420139865	0.988459939364509	0	0	0.992300026798907
0.977060420596294	0.988459776053477	0	0	0.992300179995196

Columns 41 through 45

0.049963004064487	0.049963004064487	0.049963004064487	0.049963004064487	0.049963004064487
1.043427892894746	0.986308997516404	0.986491425924872	1.045537467485782	0.984352197693332
1.043426322861760	0.986297994810018	0.986491157225135	1.045539978331251	0.984354106892344
1.043418420944290	0.986291934082696	0.986491157097919	1.045539979621124	0.984354107636217
1.043422199190606	0.986294834088908	0.986491157036192	1.045539978909012	0.984354107119939
1.043494445187120	0.979620326294880	0.986376984398479	1.045609094490024	0.977699738562228
1.043495720286748	0.979617621558368	0.986376999083365	1.045609110329057	0.977699778341110
1.043494288438864	0.979612893693690	0.986376999074175	1.045609110579698	0.977699779002275

APPENDIX B: LINE, LOAD AND VOLTAGE DATA OF 11kV TANAHUSUR FEEDER

Bus No.		Line Data(50Hz)	
From	To	R(Ohms)	L(H)
1	2	1.59	5.01338e-3
2	3	0.959	2.8631e-3
3	4	0.968	2.8705e-3
4	5	0.999	3.00802e-3
5	15	0.968	0.002863
15	16	0.9705	0.002871
2	7	0.6699	0.002005
7	14	0.5755	0.001702
7	8	0.999	0.003008
8	9	0.5679	0.001702
9	10	0.5882	0.001689
10	11	0.61	0.0017911
11	12	0.65	1.90508

Bus No.	Load Data	
	Active Power (kW)	Reactive Power (KVAR)
6	40	0.1
13	80	0.1
17	45	0.1
18	42	20

B.1 For PV-DVR in single location:

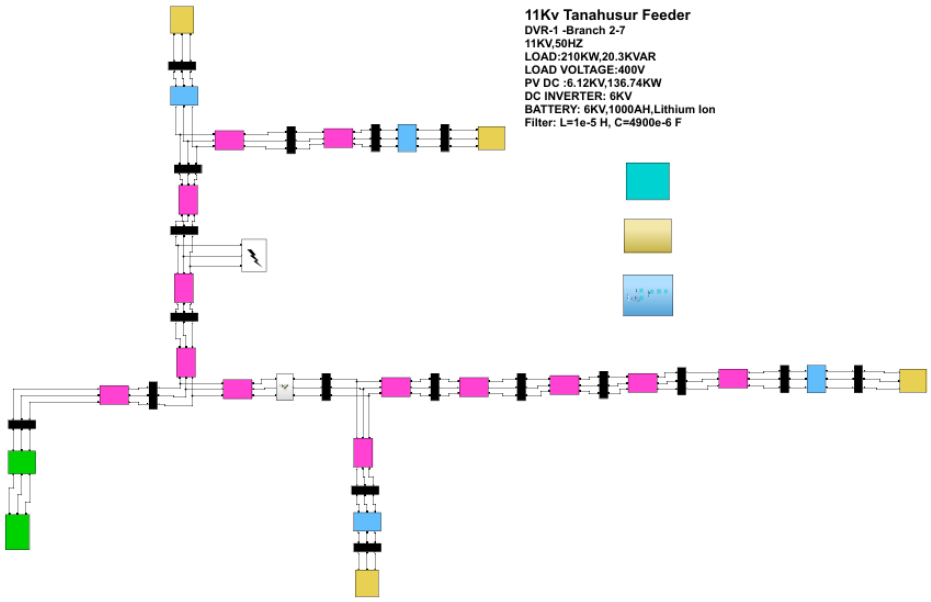

Table 1: Results of 11kV Tanahusur Feeder system during 3phase fault (branch 3-4) conditions

Description	Real power loss (kW) at bus 7	Reactive power loss (kVAr) at bus 7	Minimum voltage (p.u.)	No. of Buses with Under voltage(11kV)	Rating of DVR
Before DVR installation	97.31	49.5	0.51	13	0
After DVR Installation 2-7	0.5	0.42	0.98	6	1040 kVA

Total Real Power and Reactive Power of the system at Normal Conditions: 227.8Kw, 72.1 kVAR

Bus 7 Real power (P) and Reactive Power (Q) at normal condition: 124.8kW, 63.5Kvar

Bus 7 Real power (P) and Reactive Power (Q) at 3 Phase Fault Condition: 27.49kW, 14Kvar

Bus 7 Real power (P) and Reactive Power (Q) at after application of DVR: 124.3kW, 63.08Kvar

Total Real Power and Reactive Power of the system at Normal Conditions: 244.5Kw, 0.815 kVAR

1. **Output Voltages in p.u. of load buses (0.4kV) obtained from matlab after application of Dvr in optimal location during 3 phase, LLLG fault.**

Columns 1 through 5

0.519615242270663	0.519615242270663	0.519615242270663	0.519615242270663	0.519615242270663
0.989493001055666	0.989489656193161	0.989521876621287	0.935691581688815	0.933733596040243
0.989370815303072	0.989367782346572	0.989327936096160	0.917960555836757	0.917179814509589
0.000175149126462	0.000175149126462	0.000175148298875	0.903704450183580	0.902763173073225
0.989267209430034	0.989277346724697	0.989290196256432	0.913767284800693	0.913531607122872
0.989261872034234	0.989284320178526	0.989288586615096	0.908946132269819	0.910330718085456
0.989290761564414	0.989298078514569	0.989263722258113	0.907463671848636	0.906397074948629
0.989293533961861	0.989279669035565	0.989289270005156	0.905597349699540	0.905445124186450

Columns 6 through 10

0.519615242270663	0.519615242270663	0.519615242270663	0.519615242270663	0.519615242270663
0.938553308389589	0.987974366448494	0.987970239752900	0.988003794120047	0.999562627357662
0.918978236337825	0.987851195854053	0.987848389801469	0.987807900901640	0.981067783375697
0.903096502044072	0.000174881027273	0.000174880442200	0.000174880198418	0.966458972547874
0.914681520387025	0.987747893278620	0.987757796619946	0.987770679346293	0.977489035427336
0.910450295206086	0.987742094435921	0.987765055607080	0.987769802388637	0.972292083333395
0.906006461482746	0.987771488685456	0.987779441868662	0.987743915959480	0.970783725299041
0.904907001068104	0.987774663619886	0.987760276344388	0.987770002633912	0.968890108820711

Columns 11 through 12

0.519615242270663	0.519615242270663
0.998791505779905	1.003928865335245
0.981174478424558	0.983152963595343
0.965840596407722	0.966033612371719
0.977283188488256	0.978572673239549
0.974073052290353	0.974033605828658
0.969792785678165	0.969297976970229
0.968523528048042	0.968105038381703

2. **Output Voltages in p.u. of load buses (0.4kV) obtained from matlab after application of Dvr in optimal location during 3 phase, LLL fault.**

Columns 1 through 5

0.519615242270663	0.519615242270663	0.519615242270663	0.519615242270663	0.519615242270663
0.989493001042944	0.989489656188497	0.989521876638856	0.935691585086701	0.933733591582164
0.989370815292090	0.989367782343490	0.989327936112088	0.917960559515322	0.917179811677360
0.000175147422603	0.000175150392175	0.000175151463156	0.903704450743314	0.902763166467833
0.989280435391394	0.989265612422452	0.989281243751908	0.914049930530565	0.913990388803903
0.989280874011186	0.989271279370949	0.989291667573519	0.909452401464159	0.909241768702618
0.989292791261572	0.989284936762161	0.989278736150407	0.907560796550207	0.907076609156501
0.989302006093253	0.989292844592899	0.989272313379219	0.904461843168111	0.904674127408610

Columns 6 through 10

0.519615242270663	0.519615242270663	0.519615242270663	0.519615242270663	0.519615242270663
0.938553302969664	0.987974366436427	0.987970239748215	0.988003794136672	0.999562631014329
0.918978232038435	0.987851195843665	0.987848389798422	0.987807900916699	0.981067787341902
0.903096499451057	0.000174878833236	0.000174882002392	0.000174882636217	0.966458972919201
0.914791544474753	0.987761604212420	0.987746158972181	0.987761796080761	0.977648788784372
0.909970946856250	0.987761812785308	0.987751601615244	0.987772645837095	0.972505842805413
0.906258672289198	0.987774004272021	0.987766142170577	0.987759249612814	0.970816546925603
0.905006943684876	0.987782999047029	0.987773867172021	0.987752793670811	0.967739389458692

Columns 11 through 12

0.519615242270663	0.519615242270663
0.998791501010272	1.003928859526644
0.981174475392141	0.983152958992824
0.965840589107722	0.966033609448201
0.977820372608792	0.978683232719330
0.972560568325258	0.973519226325896
0.970593745530261	0.969559409885872
0.967886958722258	0.968223171763245

3. Output Voltages in p.u. of load buses (0.4kV) obtained from matlab after application of Dvr in optimal location during 3 phase, LL fault.

Columns 1 through 5

0.519615242270663	0.519615242270663	0.519615242270663	0.519615242270663	0.519615242270663
0.989493001042944	0.989489656188497	0.989521876638856	0.935691585086701	0.933733591582164
0.989370815292090	0.989367782343490	0.989327936112088	0.917960559515322	0.917179811677360
0.000175158813802	0.856560410903131	0.856664659378867	0.892088831154648	0.922126066170192
0.989321019502497	0.989271436579478	0.989266150529014	0.911401607627009	0.912249383751410
0.989260132047132	0.989303170197151	0.989282786061720	0.908615261007731	0.906981783834526
0.989295601859413	0.989275738243875	0.989284806419385	0.905556864907648	0.905803620362614
0.989283402933506	0.989294465907685	0.989283201894639	0.903760111114516	0.904353866672891

Columns 6 through 10

0.519615242270663	0.519615242270663	0.519615242270663	0.519615242270663	0.519615242270663
0.938553302969664	0.987974366436427	0.987970239748215	0.988003794136672	0.999562631014329
0.918978232038435	0.987851195843665	0.987848389798422	0.987807900916699	0.981067787341902
0.904821794729596	0.000174890778217	0.855242606273068	0.855346687224843	0.953902775138740
0.910293198294305	0.987802063958436	0.987751808859626	0.987745790399433	0.974682510364854
0.907834993817972	0.987740037116981	0.987784179061255	0.987763385180723	0.972688246253012
0.906582650943122	0.987776196120411	0.987755809004541	0.987765567823176	0.968517850741489
0.905245850613565	0.987764165673087	0.987775222945939	0.987763473573508	0.966950431626740

Columns 11 through 12

0.519615242270663	0.519615242270663
0.998791501010272	1.003928859526644
0.981174475392141	0.983152958992824
0.986628427735989	0.968180781243244
0.975822534343468	0.973904019200346
0.970408092378643	0.971257055758212
0.968670496755433	0.969913309678012
0.967426685635563	0.968478269252195

4. **Output Voltages in p.u. of load buses (0.4kV) obtained from matlab after application of Dvr in optimal location during LLG fault.**

Columns 1 through 5

0.519615242270663	0.519615242270663	0.519615242270663	0.519615242270663	0.519615242270663
0.989493001055666	0.989489656193161	0.989521876621287	0.935691581688815	0.933733596040243
0.989370815303072	0.989367782346572	0.989327936096160	0.917960555836757	0.917179814509589
0.000175150927666	0.572544230774777	0.572648427025791	0.896743823692251	0.914644005360257
0.989273428800522	0.989272887202319	0.989280286916920	0.913146615097868	0.913417300320100
0.989290823958418	0.989276289345571	0.989280009912001	0.908738102255105	0.909621908190843
0.989287649593446	0.989279241859109	0.989289002359565	0.906542076709484	0.906318342591589
0.989288621085800	0.989282337214044	0.989291980071685	0.904830194850197	0.905406728500257

Columns 6 through 10

0.519615242270663	0.519615242270663	0.519615242270663	0.519615242270663	0.519615242270663
0.938553308389589	0.987974366448494	0.987970239752900	0.988003794120047	0.999562627357662
0.918978236337825	0.987851195854053	0.987848389801469	0.987807900901640	0.981067783375697
0.905566156708028	0.000174882928750	0.571663433352849	0.571767461982839	0.959153126228321
0.912646119611228	0.987753541268914	0.987752832009408	0.987760598903871	0.976471307804411
0.908738891143525	0.987771787121352	0.987757003222462	0.987760706549486	0.971880427347318
0.906224687409620	0.987768750370692	0.987760131888965	0.987769987280402	0.969992070330669
0.903443963710705	0.987769533225426	0.987763076489882	0.987772784544702	0.968110507822337

Columns 11 through 12

0.519615242270663	0.519615242270663
0.998791505779905	1.003928865335245
0.981174478424558	0.983152963595343
0.978924829123626	0.968864612626396
0.977025033175185	0.976417868598037
0.973241902531539	0.972207694610716
0.970089503455994	0.969519486606849
0.968763130901752	0.966543216110881

5. **Output Voltages in p.u. of load buses (0.4kV) obtained from matlab after application of Dvr in optimal location during SLG fault.**

Columns 1 through 5

0.519615242270663	0.519615242270663	0.519615242270663	0.519615242270663	0.519615242270663
0.989493001055666	0.989489656193161	0.989521876621287	0.935691581688815	0.933733596040243
0.989370815303072	0.989367782346572	0.989327936096160	0.917960555836757	0.917179814509589
0.571711709568173	0.989242820159374	0.572142823848761	0.908496963142754	0.916354167473148
0.989291802179009	0.989287760376486	0.989284882448383	0.908625569003070	0.909830792088304
0.989300220268199	0.989268973160057	0.989278707085541	0.907289560828694	0.907759849093210
0.989281904062545	0.989288467587537	0.989293414494655	0.904704360075008	0.904929064884355
0.989269688646806	0.989302134024425	0.989303198411773	0.904108382505580	0.903738619484389

Columns 6 through 10

0.519615242270663	0.519615242270663	0.519615242270663	0.519615242270663	0.519615242270663
0.938553308389589	0.987974366448494	0.987970239752900	0.988003794120047	0.999562627357662
0.918978236337825	0.987851195854053	0.987848389801469	0.987807900901640	0.981067783375697
0.901609238294566	0.570833307942477	0.987722149113497	0.571263742743516	0.971137319168398
0.910022733293626	0.987772392423282	0.987768311476525	0.987765344224433	0.972096073149978
0.906723225628233	0.987781229262316	0.987749284569326	0.987758939070577	0.970578845858909
0.904937188820108	0.987762802910661	0.987769330443269	0.987774061741921	0.968063591000005
0.903004260926326	0.987749791185595	0.987782986212681	0.987784359601300	0.967396837753833

Columns 11 through 12

0.519615242270663	0.519615242270663
0.998791505779905	1.003928865335245
0.981174478424558	0.983152963595343
0.980298352256051	0.964593778433227
0.973410778937408	0.973595124187766
0.971277467911783	0.970078453007911
0.968296090921438	0.968138500252514
0.966855809338871	0.966066418301760

B.2 For PV-DVR in Multiple(Two) location:

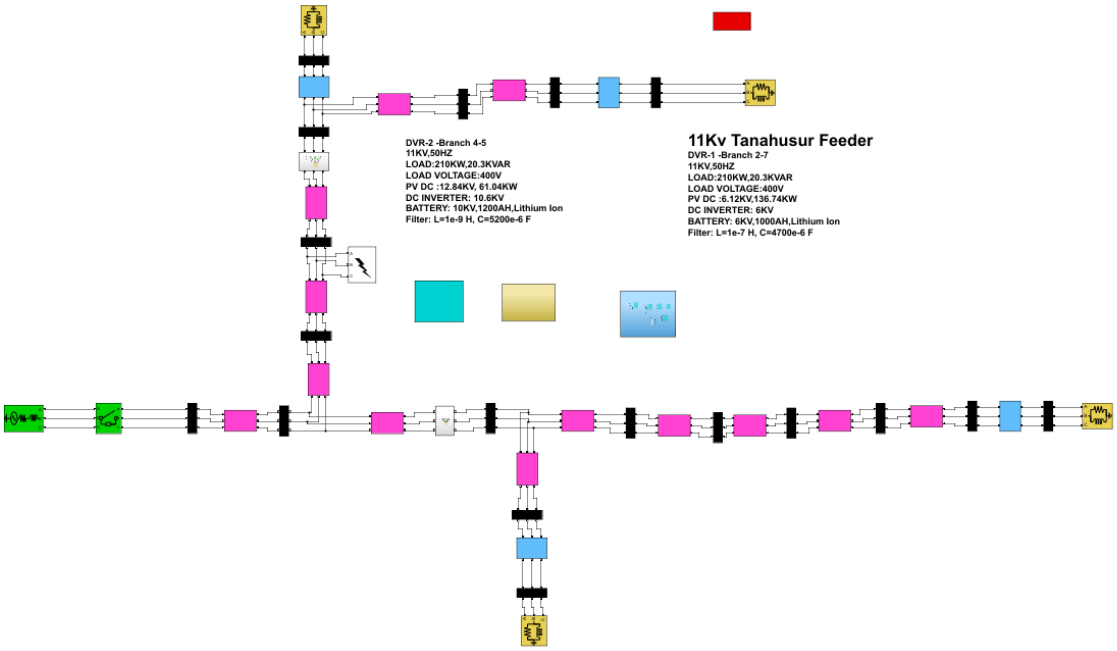

Table 1: Results of 11kV Tanahusur Feeder system during 3 phase fault conditions

Description	Real power loss (kW) at bus 7 and 5	Reactive power loss (kVAr) at bus 7 and 5	Minimum voltage (p.u.)	No. of Buses with Under voltage(11kV)	Rating of DVR
Before DVR installation	97.3@Bus 7 & 102.099@ Bus 5	49.49@Bus 7 & 7.686@Bus 5	0.51	13	0
After DVR Installation at branch 2-7,4-5	0.6@Bus 7 & 0.5@ Bus 5	0.42@Bus 7 & 0.242@Bus 5	0.98	3	1040kVA,1835 kVA

Total Real Power and Reactive Power of the system at Normal Conditions: 227.8Kw, 72.9 kVAR

Bus 7& 5, Real power (P) and Reactive Power (Q) at normal condition: 124.8kW, 63.49Kvar, 102.1kW, 7.687Kvar respectively.

Bus 7& 5, Real power (P) and Reactive Power (Q) at 3 Phase Fault Condition: 27.5kW, 14Kvar,0Kw, 0kVAR respectively

Bus 7& 5, Real power (P) and Reactive Power (Q) at after application of DVR: 124.2kW, 63.07Kvar, 101.6kW, 7.445 Kvar respectively.

Total Real Power and Reactive Power of the system at Normal Conditions: 235.6Kw, 52.69 kVAR

Output Voltages in p.u. of load buses (0.4kV) obtained from matlab after application of two Dvr in optimal locations during 3 phase, LLLG fault.

Columns 1 through 5

0.519615242270663	0.519615242270663	0.519615242270663	0.519615242270663	0.519615242270663
1.027929290143541	1.028348794953315	1.033604341374682	0.934307686316464	0.934759510382397
1.011524194507279	1.011039536944933	1.012240449573434	0.919101380045770	0.917911797145376
0.995116739845474	0.996540051785547	0.996311760820423	0.903423026346964	0.903227412118046
1.013651011282620	1.012415263984780	1.011414651255924	0.913084288884305	0.912864572563293
1.008101185513057	1.007129257191556	1.007396376154236	0.910857122951980	0.909940166779527
1.003905835770913	1.003885278424854	1.003462618221937	0.905364352652042	0.907300432711528
1.000876552826949	1.000971921942571	1.001051135758768	0.904687255006491	0.905690580955001

Columns 6 through 10

0.519615242270663	0.519615242270663	0.519615242270663	0.519615242270663	0.519615242270663
0.939367794778596	1.026345541386305	1.026689651329492	1.031985333746946	0.998829206725443
0.917934791486150	1.009966160941010	1.009444195450241	1.010651403007126	0.982354578378042
0.902415910948298	0.993578413464117	0.994997008500874	0.994779056377750	0.965593601057819
0.913205515543013	1.012067106336164	1.010805503312706	1.009824301628070	0.976730289470505
0.908945913831195	1.006526776368311	1.005523585292060	1.005813733053035	0.974133463326460
0.906451250508241	1.002304112619508	1.002327838492409	1.001887124350699	0.968505005338921
0.904108557517085	0.999327063829246	0.999404805693118	0.999479064851671	0.967680204144048

Columns 11 through 12

0.519615242270663	0.519615242270663
1.000115070216051	1.005082005298043
0.982284303055190	0.982108412431996
0.966114153225525	0.965406422996042
0.976670235382009	0.977138304415047
0.973692524999207	0.972524353495353
0.970878957989324	0.969880809267109
0.968937907753859	0.967386966921190

1. **Output Voltages in p.u. of load buses (0.4kV) obtained from matlab after application of two Dvr in optimal locations during 3 phase, LLL fault.**

Columns 1 through 5

0.519615242270663	0.519615242270663	0.519615242270663	0.519615242270663	0.519615242270663
1.027929284230662	1.028348787590103	1.033604336215785	0.934307686267209	0.934759505182303
1.011524191052142	1.011039532936291	1.012240446714328	0.919101380148000	0.917911792166808
0.995116734610237	0.996540036501260	0.996311736235421	0.903423031069112	0.903227412270518
1.012021795647558	1.013710282782856	1.012733632203004	0.914472572180452	0.913351414129225
1.007812601371882	1.006403472331648	1.006989619176993	0.908789539876225	0.910257938485203
1.001992985330581	1.002317453682890	1.001022622284179	0.906279928192262	0.906223012013152
0.999988310269108	0.999556227806314	0.999684126221672	0.903627229823576	0.905019952115695

Columns 6 through 10

0.519615242270663	0.519615242270663	0.519615242270663	0.519615242270663	0.519615242270663
0.939367798711299	1.026345535480410	1.026689643977707	1.031985328595016	0.998829206674339
0.917934793860882	1.009966157488797	1.009444191446794	1.010651400151980	0.982354578484750
0.902415913794931	0.993578408222327	0.994996993168757	0.994779031746160	0.965593605894194
0.913738773757288	1.010433284227466	1.012132374904446	1.011141741668827	0.978174088705362
0.910428562488672	1.006232206091150	1.004822269903705	1.005408621427899	0.971942916016486
0.906638791626482	1.000395733007491	1.000721213443496	0.999445583767003	0.969596547894247
0.905184687388369	0.998404309894181	0.997997188413667	0.998114256153621	0.966458322653038

Columns 11 through 12

0.519615242270663	0.519615242270663
1.000115064685726	1.005082009504783
0.982284297773167	0.982108414964668
0.966114153582946	0.965406426181621
0.977338490501517	0.977657243631021
0.974138525347784	0.974138386507936
0.969560591413085	0.970094887027642
0.968159488589295	0.968524513364658

2. **Output Voltages in p.u. of load buses (0.4kV) obtained from matlab after application of two Dvr in optimal locations during LLG fault.**

Columns 1 through 5

0.519615242270663	0.519615242270663	0.519615242270663	0.519615242270663	0.519615242270663
1.027929290143541	1.028348794953315	1.033604341374682	0.934307686316464	0.934759510382397
1.011524194507279	1.011039536944933	1.012240449573434	0.919101380045770	0.917911797145376
0.987572807500167	1.013697033909834	0.999223629495914	0.897378095154671	0.915163144079251
1.009371015083249	1.009461880724828	1.010593941196042	0.913472838801107	0.912020580551215
1.004687063062605	1.006265421704000	1.004989483248036	0.908262406224563	0.907977951783968
1.001711406860830	1.001330879656264	1.001801927618058	0.906482382615226	0.904647271786173
0.998776328905670	0.999360257337289	0.999172152990117	0.904359542100763	0.904141408990090

Columns 6 through 10

0.519615242270663	0.519615242270663	0.519615242270663	0.519615242270663	0.519615242270663
0.939367794778596	1.026345541386305	1.026689651329492	1.031985333746946	0.998829206725443
0.917934791486150	1.009966160941010	1.009444195450241	1.010651403007126	0.982354578378042
0.906741943285329	0.986086429442461	1.012130464602359	0.997656149765197	0.959529095186145
0.912018421935765	1.007800252882078	1.007892789636712	1.009008314185711	0.976782386558362
0.909042748731194	1.003099107416488	1.004680541320775	1.003411343125340	0.971278277184616
0.905991385192846	1.000131235328805	0.999776949576265	1.000228189875621	0.970018832855686
0.904552567998967	0.997210379286521	0.997794151050925	0.997602936253518	0.967681100093629

Columns 11 through 12

0.519615242270663	0.519615242270663
1.000115070216051	1.005082005298043
0.982284303055190	0.982108412431996
0.978876628485099	0.970204969485069
0.975695048341734	0.975825261479055
0.971493666189428	0.972660156499924
0.967945377567506	0.969401938834528
0.967480862125550	0.967849275117617

3. **Output Voltages in p.u. of load buses (0.4kV) obtained from matlab after application of two Dvr in optimal locations during LL fault.**

Columns 1 through 5

0.519615242270663	0.519615242270663	0.519615242270663	0.519615242270663	0.519615242270663
1.027929284230662	1.028348787590103	1.033604336215785	0.934307686267209	0.934759505182303
1.011524191052142	1.011039532936291	1.012240446714328	0.919101380148000	0.917911792166808
0.983661076166411	1.021168208468529	1.000151393846799	0.893446937147706	0.921542637307786
1.008261697078368	1.007996349946152	1.007649017833500	0.911719570782550	0.911311917870935
1.003944451134567	1.003104588370750	1.003552963108485	0.907738001846154	0.908461574075215
1.000150279179407	1.000451449846623	1.000846999153422	0.905926191919766	0.905953218506062
0.998720724830212	0.998751898519195	0.999190115698401	0.903317370447536	0.904100401781445

Columns 6 through 10

0.519615242270663	0.519615242270663	0.519615242270663	0.519615242270663	0.519615242270663
0.939367798711299	1.026345535480410	1.026689643977707	1.031985328595016	0.998829206674339
0.917934793860882	1.009966157488797	1.009444191446794	1.010651400151980	0.982354578484750
0.904992996728325	0.982125172730425	1.019561667103448	0.998566870441967	0.955410571910236
0.911705568621995	1.006679781251491	1.006418310698265	1.006064551521435	0.974975944190604
0.908695390390571	1.002369198170271	1.001545517987025	1.001978704441173	0.970757706435453
0.905402020741670	0.998588660014119	0.998870158628606	0.999272979376870	0.969279392574658
0.906159328885303	0.997158279900812	0.997194609341133	0.997622634053318	0.966323111396543

Columns 11 through 12

0.519615242270663	0.519615242270663
1.000115064685726	1.005082009504783
0.982284297773167	0.982108414964668
0.985794017311191	0.968446255684778
0.975057402054090	0.975501232184350
0.971820012271679	0.972275046975239
0.969291701719820	0.968781919625762
0.967522115253911	0.969566846378415

4. **Output Voltages in p.u. of load buses (0.4kV) obtained from matlab after application of two Dvr in optimal locations during SLG fault.**

Columns 1 through 5

0.519615242270663	0.519615242270663	0.519615242270663	0.519615242270663	0.519615242270663
1.027929290143541	1.028348794953315	1.033604341374682	0.934307686316464	0.934759510382397
1.011524194507279	1.011039536944933	1.012240449573434	0.919101380045770	0.917911797145376
1.001670757240787	1.010330036233190	0.990595103171961	0.909259654181454	0.915779053503366
1.004656078712635	1.004141877079060	1.003846339358932	0.909898119179876	0.909634608013725
1.001179439658321	1.001071251240147	1.001055630084884	0.906898935856402	0.906336857735318
0.997654227162169	0.998734585425093	0.999713710313429	0.905114321744045	0.905558739959412
0.998180659316908	0.997189509020048	0.997523023125870	0.902380380172081	0.903813603068369

Columns 6 through 10

0.519615242270663	0.519615242270663	0.519615242270663	0.519615242270663	0.519615242270663
0.939367794778596	1.026345541386305	1.026689651329492	1.031985333746946	0.998829206725443
0.917934791486150	1.009966160941010	1.009444195450241	1.010651403007126	0.982354578378042
0.900611833611180	1.000142606964127	1.008752441767839	0.989039817762433	0.972778807760294
0.909325690898340	1.003071264249112	1.002563323884947	1.002268832966994	0.973779781614492
0.907060598983752	0.999593893203374	0.999488638582251	0.999485075385135	0.970759060863866
0.904082358148650	0.996105719791342	0.997161868822582	0.998145923937083	0.968550087199075
0.902874096871968	0.996600813266464	0.995619695300937	0.995957132901941	0.965386093188173

Columns 11 through 12

0.519615242270663	0.519615242270663
1.000115070216051	1.005082005298043
0.982284303055190	0.982108412431996
0.979874446531180	0.963627661101861
0.973285171110867	0.972941606454153
0.969964315582629	0.970520950832934
0.969153355679941	0.967331815210998
0.966975293723625	0.966047955190291

APPENDIX C: LINE, LOAD AND VOLTAGE DATA OF 11kV SIMARA INDUSTRIAL FEEDER

C.1 Normal Loading

Bus No.	Load Data	
	Active Power (kW)	Reactive Power (kVAR)
7	15	25
9	540	108.6
13	581.28	215.52
16	295.62	84
18	39	6
21	29	10
24	160	91
27	4	3
30	143.21	119
33	199	2
36	664	576
42	11	3
43	1.57	8.4
46	124	2
49	224	1

Bus No.		Line Data(50Hz)	
From	To	R(Ohms)	L(H)
1	2	0.29925	8.203915e-4
3	4	1.1277	3.09158e-3
4	5	0.9705	1.03628e-4
5	6	0.0378	3.09158e-3
6	8	0.0189	5.18142e-5
5	10	0.02205	6.04499e-5
10	11	0.0189	5.18142e-5
11	12	0.04725	1.29567e-4
11	14	0.02205	6.04499e-5
11	19	0.0756	0.0756

Bus No.		Line Data(50Hz)	
From	To	R(Ohms)	L(H)
14	17	3.15e-3	8.6357e-6
14	15	0.02205	6.04499e-5
19	20	9.45e-3	2.59071e-5
19	22	0.02205	6.04499e-5
22	23	0.0252	6.04499e-5
22	25	0.0126	3.45428e-5

25	26	0.0819	2.245e-4
25	28	0.02205	6.04499e-5
28	29	0.0378	1.03628e-4
28	31	6.3e-3	1.72714e-5
31	32	9.45e-3	2.59071e-5
31	34	0.04725	1.295355e-4
34	35	0.08505	2.33163e-4

Bus No.		Line Data(50Hz)	
From	To	R(Ohms)	L(H)
34	37	6.3e-3	1.72714e-5
37	38	0.02205	6.04499e-5
37	39	0.04725	1.2953e-4
39	40	0.02835	7.77213e-5
40	41	6.3e-3	1.72714e-5
39	44	0.10395	2.849781e-4
44	45	0.0378	1.0362e-4
44	47	0.0126	3.45428e-5
47	48	0.04095	1.122641e-4
47	50	0.02205	6.04499e-5

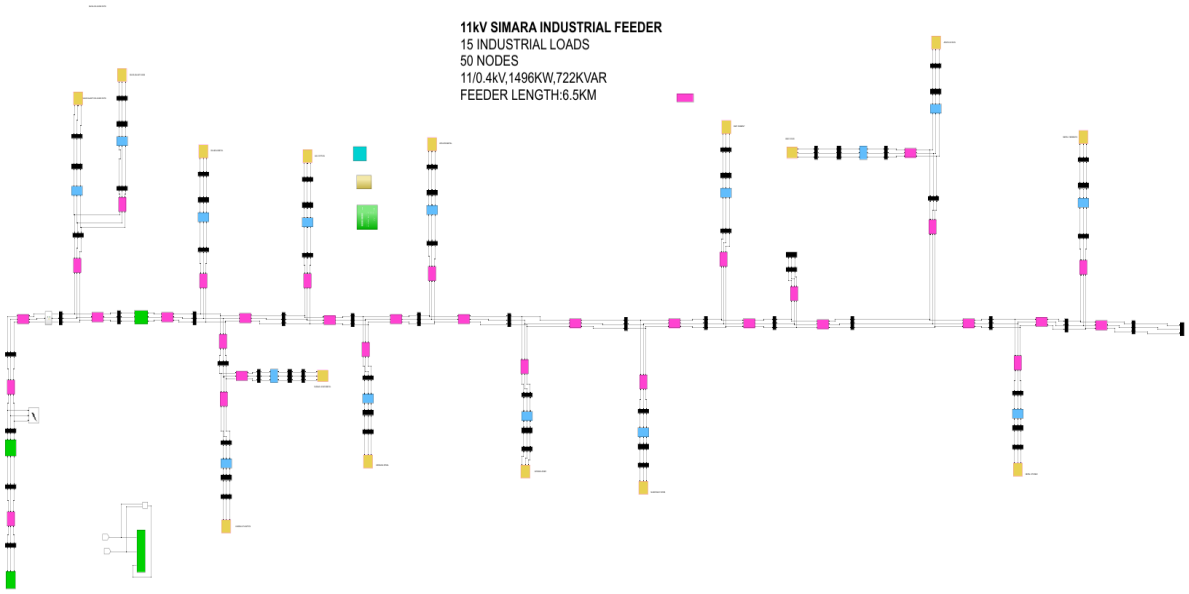

Table 1. Voltage profiles load buses of simara without and with DVR at Branch 3-4 for time Total simulation time 0.7sec

Bus no	Voltage in p.u	
	Without DVR	With DVR
7	0.9171	0.9892
9	0.9208	0.9927
13	0.9830	0.9732
16	0.9742	0.9834
18	0.9681	0.9990
21	0.9964	0.9989
24	0.9861	0.9968
27	0.9714	0.9951
30	0.9752	0.9894
33	0.9697	0.9808
36	0.9783	0.9796
42	0.9862	0.9885
43	0.9608	0.9899
46	0.9599	0.9902
49	0.9576	0.9992

Table 2: Results of simara feeder

Description	**Real power loss (kW) at bus 5 during SLG Fault**	**Reactive power loss (kVAr) at bus 5 during SLG fault**	**Minimum voltage (p.u.)**	**No. of Buses with Under voltage**	**Rating of DVR**
Before DVR installation	881.1	384.7	0.9171 @bus 7	48	0
After DVR Installation at branch 4-5	1.6	1.7	0.9732 @bus 13	2	2600 kVA

Total Real Power and Reactive Power of the system at Normal Conditions: 1512Kw, 705.4 kVAR

Bus 5 Real power (P) and Reactive Power (Q) at normal condition: 1508.9kW, 698Kvar

Bus 5 Real power (P) and Reactive Power (Q) at 3 Phase Fault Condition: 690.8kW, 313.6Kvar

Bus 5 Real power (P) and Reactive Power (Q) at after application of DVR: 1507.3kW, 696.3Kvar

Total Real Power and Reactive Power of the system at Normal Conditions: 1510.9Kw, 704.2 kVAR

1. **Output Voltages in p.u. of load buses (0.4kV) obtained from matlab after application of Dvr in optimal locations during 3 phase, LLLG fault**

Columns 1 through 5

0.519615242270663	0.519615242270663	0.519615242270663	0.519615242270663	0.519615242270663
0.999036983755894	0.995800299193566	1.006196761971451	0.987757321662850	0.985941661543499
0.998779916904186	0.995388079423548	1.006793663006801	0.987497172452190	0.985315962777656
0.994221081229461	0.990496992213837	1.001014113472019	0.983011047660137	0.980627305689379
1.002526236866509	0.997277027407535	1.007197597495180	0.991246948761934	0.987419901905344
0.999103043458661	0.998104126574016	1.005992742004876	0.987717404855818	0.988057157826745
0.998082320842038	0.994523665078827	1.004535114010085	0.986689539654563	0.984635251409796
0.999285992167998	0.993902125973155	1.002412185651016	0.988044000278219	0.984127250590205

Columns 6 through 10

0.519615242270663	0.519615242270663	0.519615242270663	0.519615242270663	0.519615242270663
0.993076176915396	0.997037845237848	0.994020034645856	1.004312466377469	0.993473261565005
0.993548328665493	0.996782607567762	0.993581525701624	1.004898502801644	0.993218623049265
0.987998636110766	0.992233420295572	0.988717515389058	0.999145043519392	0.988689897336570
0.994005517794205	1.000528414859248	0.995502033689161	1.005309122979348	0.996960641482290
0.992847283419478	0.997089796051437	0.996296758481580	1.004107970995419	0.993500863850146
0.991488466787558	0.996067843561228	0.992744301073940	1.002658710258513	0.992477774545168
0.989320191182766	0.997291447043008	0.992140972998576	1.000536044797730	0.993735100962899

Columns 11 through 15

0.519615242270663	0.519615242270663	0.519615242270663	0.519615242270663	0.519615242270663
0.993591165607320	1.004149260105172	0.988370665877917	0.984861734982142	0.995702005733156
0.993001214927641	1.004686524936421	0.988124986999114	0.984339999475561	0.996240136696415
0.988268620510918	0.998999920565232	0.983614726194951	0.979578342027797	0.990596353495235
0.995074505010336	1.005116663439775	0.991850597160480	0.986345983426181	0.996668384475867
0.995758786485602	1.003935395692956	0.988381564321988	0.987048079528280	0.995488726586671
0.992275077310586	1.002515664737208	0.987358250004954	0.983586936088280	0.994083136205325
0.991733086276967	1.000354790004134	0.988636910519628	0.983039667365168	0.991951623749134

Columns 16 through 20

0.519615242270663	0.519615242270663	0.519615242270663	0.519615242270663	0.519615242270663
0.977660836749115	0.978617312563196	0.986823425073168	0.992224898025291	0.985704137055679
0.977443155288391	0.978159043264200	0.987354639837057	0.991978368040344	0.985286387253322
0.972958154020881	0.973380811879996	0.981768219953351	0.987444024076573	0.980449583320887
0.981117257397328	0.980110106312632	0.987782473496371	0.995702811898097	0.987188651232416
0.977666282796195	0.980831908803963	0.986612256727652	0.992275344372800	0.987973108699062
0.976648457555353	0.977375858705524	0.985222648571116	0.991258255137871	0.984451095808762
0.977923944891254	0.976814300923549	0.983110730098015	0.992477001418835	0.983852452817410

Columns 21 through 25

0.519615242270663	0.519615242270663	0.519615242270663	0.519615242270663	0.519615242270663
0.997299353667174	0.997268428597674	0.993688097910569	1.004646774701890	0.984788157767225
0.997884876319653	0.997006268945573	0.993272620733612	1.005242918589783	0.984557904588510
0.992171550963624	0.992460654381573	0.988397560277643	0.999473844255824	0.980044703387003
0.998290091264018	1.000753703466546	0.995169091649533	1.005648097978533	0.988241108263001
0.997097536216359	0.997330640700015	0.995981666554999	1.004444658853906	0.984845651968067
0.995656302893255	0.996314685763916	0.992417391766959	1.002988454399556	0.983840693177358
0.993549033350582	0.997518774091885	0.991801200237519	1.000870426950311	0.985036498050252

Columns 26 through 30

0.519615242270663	0.519615242270663	0.519615242270663	0.519615242270663	0.519615242270663
0.981642324067977	0.993125094862156	0.995753615433954	0.992901852148437	1.003986355336612
0.981226550233263	0.993718765877305	0.995407102775537	0.992398468136375	1.004582675423317
0.976410604279397	0.988017665950593	0.990955279132603	0.987656566949744	0.998855362918709
0.983126429662430	0.994112507275017	0.999270935252536	0.994545215082296	1.004981440303450
0.983901381014818	0.992925390846037	0.995708087009956	0.995090671148821	1.003796571087000
0.980397219984909	0.991483641817811	0.994767652977055	0.991700859689746	1.002348690429850
0.979803279584226	0.989387070500736	0.996044393612965	0.991160087753108	1.000217925471460

Columns 31 through 35

0.519615242270663	0.519615242270663	0.519615242270663	0.519615242270663	0.519615242270663
0.968028520661296	0.965193688123971	0.978874302289759	0.995868994095510	0.991158778044849
0.967840047476162	0.964785510506602	0.979466285461301	0.995603375310258	0.990743621838315

0.963371026031144	0.960047169170970	0.973846749656315	0.991067688263994	0.985883358544751
0.971438648208570	0.966676221125109	0.979844720598008	0.999349993024842	0.992638959532847
0.968078207113438	0.967413818138727	0.978677561138030	0.995928755546867	0.993445304279173
0.967087484909104	0.963980950856633	0.977253438990510	0.994915806379367	0.989892461223907
0.968274155254502	0.963410004451175	0.975183870399606	0.996119967086931	0.989278814648548

Columns 36 through 40

0.519615242270663	0.519615242270663	0.519615242270663	0.519615242270663	0.519615242270663
1.004977658492324	0.985971976976335	0.982508458444008	0.993680136961871	0.995295306850905
1.005613815222356	0.985712534737484	0.982096612497339	0.994276139920771	0.994963360550605
0.999812553298324	0.981216775967667	0.977278684061590	0.988566877950769	0.990489071428791
1.006000588647097	0.989416900960875	0.983974773423668	0.994671012432423	0.998813529964258
1.004787619375640	0.986030152336560	0.984774882322844	0.993481088813875	0.995304997771968
1.003319880077668	0.985027699468294	0.981252350721388	0.992041739628383	0.994356382724215
1.001222079260458	0.986217986164241	0.980643942078593	0.989945692423502	0.995569912662990

Columns 41 through 45

0.519615242270663	0.519615242270663	0.519615242270663	0.519615242270663	0.519615242270663
0.991554874037999	1.003043835839854	0.995251174236017	0.991682954212575	1.003121505658313
0.991076399869162	1.003680607808437	0.994930319005458	0.991230573774187	1.003756499399236
0.986317636217080	0.997917318674871	0.990448019987883	0.986438898211029	0.997987472255579
0.993183997979776	1.004062338718669	0.998759986129776	0.993277539563479	1.004140079367891
0.993762215456327	1.002860650795844	0.995265983325647	0.993918269289317	1.002935768709154
0.990354919636797	1.001405480518930	0.994306123996852	0.990469424409927	1.001479546160581
0.989802979554411	0.999302595216465	0.995521589428614	0.989899645372326	0.999377757619889

2. **Output Voltages in p.u. of load buses (0.4kV) obtained from matlab after application of Dvr in optimal locations during 3 phase, LLL fault**

Columns 1 through 5

0.519615242270663	0.519615242270663	0.519615242270663	0.519615242270663	0.519615242270663
0.999036980656539	0.995800306583764	1.006196768779996	0.987757318577334	0.985941668830366
0.998779916643002	0.995388090452080	1.006793671567699	0.987497172159383	0.985315973715135
0.994208853920649	0.990481057698102	1.001042904086821	0.982998930516115	0.980611585191020
1.002946427349128	1.001018912631717	1.008841101857184	0.991609445768061	0.990861127139069
1.000281236863585	0.996675334749337	1.007482289372783	0.988920344202642	0.986418342028789
0.999466708398062	0.997596513977208	1.006545439071513	0.988030353247714	0.987608164201236
0.997390698836687	0.992460795074204	1.004434924961825	0.986183891507601	0.982670731088323

Columns 6 through 10

0.519615242270663	0.519615242270663	0.519615242270663	0.519615242270663	0.519615242270663
0.993076183533179	0.997037845692480	0.994020042143701	1.004312474896361	0.993473262032055
0.993548337034010	0.996782610853488	0.993581536838964	1.004898513072420	0.993218626333996
0.988027018967392	0.992221310844226	0.988701591343232	0.999173804192361	0.988677825197925
0.995545102466257	1.000938741490242	0.999193509890523	1.006937999844653	0.997357103965323
0.994250747047092	0.998268924495903	0.994838072273887	1.005590034275619	0.994684251977830
0.993480029484937	0.997446675600343	0.995797803787431	1.004665772090200	0.993846036169989
0.991322514164427	0.995403160628390	0.990694541145973	1.002553765017699	0.991857296403082

Columns 11 through 15

0.519615242270663	0.519615242270663	0.519615242270663	0.519615242270663	0.519615242270663
0.993591173042856	1.004149268611845	0.988370666357824	0.984861742409166	0.995702014188076
0.993001226019464	1.004686535201137	0.988124990280041	0.984340010530054	0.996240146895724
0.988252738310225	0.999028662816502	0.983602710577559	0.979562589243031	0.990624855867720
0.998616839866056	1.006713006982316	0.992234016113979	0.989877074605974	0.998252604189098

0.994170829145654	1.005379086005451	0.989562246423702	0.985502860096599	0.996936507392437
0.995312779612485	1.004538485689889	0.988717495699522	0.986573656875538	0.996074615069735
0.990301191090548	1.002385298465647	0.986776310176112	0.981584603728580	0.993953884777531

Columns 16 through 20

0.519615242270663	0.519615242270663	0.519615242270663	0.519615242270663	0.519615242270663
0.977660837236631	0.978617319913466	0.986823433431196	0.992224898508708	0.985704144488887
0.977443158538558	0.978159054213409	0.987354649924555	0.991978371339338	0.985286398295416
0.972946264658730	0.973365147145128	0.981796466252551	0.987431972464499	0.980433790185276
0.981487743075339	0.983648926153943	0.989345612520308	0.996109461255583	0.990841086869723
0.978829779609597	0.979339874341615	0.988048281960076	0.993447820638198	0.986532182382087
0.977997014331532	0.980343354291626	0.987194241729946	0.992630597033549	0.987472359909298
0.976100658437054	0.975365731346080	0.985092732113994	0.990603168809149	0.982415046278603

Columns 21 through 25

0.519615242270663	0.519615242270663	0.519615242270663	0.519615242270663	0.519615242270663
0.997299362154892	0.997268429065346	0.993688105406871	1.004646783233982	0.984788158232307
0.997884886545852	0.997006272247887	0.993272631861837	1.005242928873143	0.984557907847420
0.992200111430963	0.992448546206747	0.988381634864974	0.999502617378459	0.980032743221299
0.999907375395853	1.001171780725904	0.998887946828322	1.007280138552248	0.988650712889540
0.998570682787429	0.998508387923789	0.994549056581898	1.005927640214705	0.986008363942166
0.997652546246642	0.997692311259967	0.995479457080309	1.004998811181327	0.985204028996144
0.995555094021247	0.995624908297040	0.990365364561218	1.002890385563007	0.983183270779419

Columns 26 through 30

0.519615242270663	0.519615242270663	0.519615242270663	0.519615242270663	0.519615242270663
0.981642331454042	0.993125103301291	0.995753615837154	0.992901859544064	1.003986363856326
0.981226561213481	0.993718776045492	0.995407106009208	0.992398479183283	1.004582685703784

0.976394876838416 0.988046108693660 0.990943170064510 0.987640677798018 0.998884101241682

0.986755248169925 0.995730864024508 0.999666194542268 0.997926923446823 1.006512503670760

0.982463635575960 0.994394587580644 0.996946009582170 0.993517201732642 1.005197959337669

0.983403328030148 0.993477564843846 0.996031249848576 0.994675069003802 1.004428519129321

0.978372316604090 0.991390431746906 0.994148997101830 0.989828693710590 1.002278533454133

Columns 31 through 35

0.519615242270663 0.519615242270663 0.519615242270663 0.519615242270663 0.519615242270663

0.968028521149292 0.965193695397241 0.978874310616852 0.995868994584833 0.991158785505049

0.967840050703175 0.964785521317331 0.979466295489371 0.995603378630108 0.990743632920933

0.963359264543033 0.960031709132554 0.973874783757549 0.991055597078937 0.985867473591595

0.971835682780861 0.970203409561254 0.981446456486219 0.999766768111007 0.996343850073898

0.969220665045749 0.965982790952035 0.980129199839106 0.997105904384412 0.992015029997833

0.968431348254536 0.966919836809489 0.979227199837381 0.996288778766586 0.992946180773813

0.966475505766275 0.961992328793547 0.977166958072870 0.994227612615319 0.987849055989054

Columns 36 through 40

0.519615242270663 0.519615242270663 0.519615242270663 0.519615242270663 0.519615242270663

1.004977667025375 0.985971977793428 0.982508465850348 0.993680145730346 0.995295307453809

1.005613825509175 0.985712538357273 0.982096623494434 0.994276150422389 0.994963363983193

0.999841338453335 0.981204812536676 0.977262937566619 0.988595345808683 0.990476985164651

1.007601521752310 0.989830962537068 0.987647947956920 0.996287747223021 0.999217812412918

1.006260700321220 0.987195962947191 0.983357317241840 0.994948224026013 0.996500621120414

1.005350139002232 0.986387196906415 0.984279852738426 0.994032909658798 0.995638899040093

1.003252182080564 0.984348422195761 0.979227032289723 0.991947802157163 0.993679119800241

Columns 41 through 45

0.519615242270663	0.519615242270663	0.519615242270663	0.519615242270663	0.519615242270663
0.991554881484636	1.003043844342487	0.995251174670042	0.991682961793180	1.003121514159011
0.991076410958711	1.003680618070020	0.994930322268783	0.991230584992814	1.003756509656498
0.986301763500015	0.997946036654481	0.990435930144723	0.986423018259799	0.998016196805351
0.996606110716146	1.005586654092458	0.999166868074804	0.996780801598330	1.005686410712419
0.992215213667303	1.004277346337655	0.996461740904643	0.992407353504545	1.004369516151844
0.993334290312141	1.003479539617373	0.995605387433360	0.993470191474665	1.003538301650518
0.988459402737948	1.001357216144709	0.993629781388167	0.988529828192022	1.001423694289308

3. **Output Voltages in p.u. of load buses (0.4kV) obtained from matlab after application of Dvr in optimal locations during LL fault**

Columns 1 through 5

0.519615242270663	0.519615242270663	0.519615242270663	0.519615242270663	0.519615242270663
0.999036980656539	0.995800306583764	1.006196768779996	0.987757318577334	0.985941668830366
0.998779916643002	0.995388090452080	1.006793671567699	0.987497172159383	0.985315973715135
0.991113675496798	0.990546413034063	1.009558935299966	0.979820011184275	0.980704784914290
0.999539285943246	0.997055779319557	1.004084997452841	0.988196623756132	0.986884769829403
0.997314372716126	0.993830130802339	1.003450398636377	0.985976486928331	0.983892267939278
0.998286535150829	0.992927945662280	1.004106506825722	0.986989627271527	0.982817987736826
0.999082134719874	0.994133933933073	1.003858982583481	0.987748019984248	0.984203420355641

Columns 6 through 10

0.519615242270663	0.519615242270663	0.519615242270663	0.519615242270663	0.519615242270663
0.993076183533179	0.997037845692480	0.994020042143701	1.004312474896361	0.993473262032055
0.993548337034010	0.996782610853488	0.993581536838964	1.004898513072420	0.993218626333996

0.996481534368101	0.989113211984820	0.988771982248991	1.007677209767468	0.985553392041087
0.990861099599589	0.997533470182413	0.995231148199534	1.002192749716946	0.993953824367272
0.990310252667579	0.995309909377029	0.992043457632257	1.001566371513599	0.991733225166567
0.990901240040017	0.996282926981328	0.991113648428411	1.002216580224262	0.992715275145239
0.990804232138054	0.997076992192786	0.992349241192141	1.001985196310391	0.993500462340646

Columns 11 through 15

0.519615242270663	0.519615242270663	0.519615242270663	0.519615242270663	0.519615242270663
0.993591173042856	1.004149268611845	0.988370666357824	0.984861742409166	0.995702014188076
0.993001226019464	1.004686535201137	0.988124990280041	0.984340010530054	0.996240146895724
0.988328228257935	1.007554681279406	0.980471847358685	0.979648655894752	0.999071568512737
0.994628733504178	1.001977940700575	0.988842050387580	0.985929603538022	0.993548828421604
0.991545127888716	1.001379416773184	0.986627234877649	0.982866288499938	0.992956747447083
0.990539960175346	1.002005163056039	0.987610066983254	0.981856658847296	0.993581827807718
0.991836410458631	1.001834815854785	0.988390880979059	0.983178200533999	0.993410178006052

Columns 16 through 20

0.519615242270663	0.519615242270663	0.519615242270663	0.519615242270663	0.519615242270663
0.977660837236631	0.978617319913466	0.986823433431196	0.992224898508708	0.985704144488887
0.977443158538558	0.978159054213409	0.987354649924555	0.991978371339338	0.985286398295416
0.969833211842256	0.973449894051508	0.990167960827256	0.984334761026815	0.980505390548201
0.978132210473065	0.979748633344905	0.984683687425386	0.992720122936896	0.986922112658514
0.975933958890446	0.976668966910758	0.984100263407909	0.990505722053256	0.983757034611974
0.976900153193435	0.975692288360286	0.984719627609564	0.991471829615256	0.982836161710033
0.977682461333779	0.976978732429969	0.984557202156054	0.992264601222348	0.984060886140058

Columns 21 through 25

0.519615242270663	0.519615242270663	0.519615242270663	0.519615242270663	0.519615242270663
0.997299362154892	0.997268429065346	0.993688105406871	1.004646783233982	0.984788158232307
0.997884886545852	0.997006272247887	0.993272631861837	1.005242928873143	0.984557907847420
1.000642577026142	0.989353752046635	0.988446963538626	1.008010004388043	0.976966139572975
0.995195326404699	0.997768487058761	0.994937467633563	1.002538418339027	0.985286674301090
0.994571375551810	0.995549471486110	0.991724465992540	1.001905285344280	0.983088329649903
0.995219396446538	0.996518586471947	0.990821500197813	1.002559025521242	0.984045659519973
0.994990167625053	0.997311957170079	0.992025511492316	1.002315608672822	0.984833292552308

Columns 26 through 30

0.519615242270663	0.519615242270663	0.519615242270663	0.519615242270663	0.519615242270663
0.981642331454042	0.993125103301291	0.995753615837154	0.992901859544064	1.003986363856326
0.981226561213481	0.993718776045492	0.995407106009208	0.992398479183283	1.004582685703784
0.976466691221595	0.996451723523144	0.987751337954938	0.987709665444379	1.007457756506765
0.982855492105626	0.991039044944377	0.996196664221088	0.994117001375585	1.001868555833722
0.979705773566132	0.990410483157306	0.994006334105383	0.990995300111631	1.001241019923342
0.978787628156572	0.991060620755648	0.995011634553161	0.990080169308198	1.001881680075298
0.980007985940047	0.990822057176091	0.995737935831441	0.991235454019377	1.001689278032109

Columns 31 through 35

0.519615242270663	0.519615242270663	0.519615242270663	0.519615242270663	0.519615242270663
0.968028521149292	0.965193695397241	0.978874310616852	0.995868994584833	0.991158785505049
0.967840050703175	0.964785521317331	0.979466295489371	0.995603378630108	0.990743632920933
0.960328483966224	0.960108785775961	0.982155672115441	0.987962753956544	0.985932338236954

0.968524348907589	0.966374739042026	0.976817523834063	0.996366713636005	0.992405926063012
0.966353690140929	0.963296219711695	0.976193893021328	0.994152011549206	0.989201662025517
0.967294438322060	0.962373604076191	0.976839787153420	0.995120387875913	0.988302515433170
0.968075013164436	0.963598127306282	0.976605189089815	0.995911260015290	0.989500801302170

Columns 36 through 40

0.519615242270663	0.519615242270663	0.519615242270663	0.519615242270663	0.519615242270663
1.004977667025375	0.985971977793428	0.982508465850348	0.993680145730346	0.995295307453809
1.005613825509175	0.985712538357273	0.982096623494434	0.994276150422389	0.994963363983193
1.008376636681760	0.978145073690469	0.977327703030722	0.997011441681794	0.987319276137336
1.002902622762087	0.986462540167840	0.983743980797215	0.991598944668626	0.995763438948464
1.002252112325879	0.984269523484444	0.980567659007375	0.990969839300069	0.993588478206986
1.002917407403280	0.985232080142066	0.979677073061508	0.991619477447538	0.994560154499009
1.002657969060863	0.986013246199632	0.980864501925173	0.991375168352135	0.995315888353704

Columns 41 through 45

0.519615242270663	0.519615242270663	0.519615242270663	0.519615242270663	0.519615242270663
0.991554881484636	1.003043844342487	0.995251174670042	0.991682961793180	1.003121514159011
0.991076410958711	1.003680618070020	0.994930322268783	0.991230584992814	1.003756509656498
0.986369947731931	1.006518674476820	0.987289790059317	0.986489892919443	1.006573206304681
0.992787123994063	1.000964877834700	0.995722550032251	0.992927892302709	1.001042379305659
0.989655394648370	1.000320734281803	0.993539187265970	0.989774573908612	1.000397788836565
0.988749359348540	1.000975373414787	0.994513323087878	0.988874235848527	1.001054838346436
0.989904308803199	1.000753968199251	0.995273911220574	0.990039147163704	1.000825080266259

4. **Output Voltages in p.u. of load buses (0.4kV) obtained from matlab after application of DVR in optimal locations during LLG fault**

Columns 1 through 5

0.519615242270663	0.519615242270663	0.519615242270663	0.519615242270663	0.519615242270663
0.999036983755894	0.995800299193566	1.006196761971451	0.987757321662850	0.985941661543499
0.998779916904186	0.995388079423548	1.006793663006801	0.987497172452190	0.985315962777656
0.993428540376468	0.915810600415842	1.086328282208642	0.982143843231750	0.906701126313980
1.001845016670978	0.994995724393734	1.006975031449639	0.990289999780655	0.984970518078568
0.995470852561177	0.995470760846550	1.005022689400467	0.984185747249551	0.985450600503914
0.999895434825404	0.996105728930435	1.005415044084492	0.988544723410696	0.986075904116323
0.998856268679262	0.992477160170524	1.004302088763175	0.987423834709242	0.982554521134839

Columns 6 through 10

0.519615242270663	0.519615242270663	0.519615242270663	0.519615242270663	0.519615242270663
0.993076176915396	0.997037845237848	0.994020034645856	1.004312466377469	0.993473261565005
0.993548328665493	0.996782607567762	0.993581525701624	1.004898502801644	0.993218623049265
1.072218734373025	0.991431468542827	0.914167537959520	1.084300750514457	0.987871396253130
0.993894648072964	0.999804105050366	0.993194214670604	1.005092085249027	0.996173040117604
0.991764040814230	0.993474496929894	0.993669898314835	1.003127174767002	0.989911173071631
0.992290508462804	0.997884410213946	0.994301364508546	1.003532141532831	0.994302126257685
0.991247500708549	0.996835399042651	0.990689894336789	1.002422808460833	0.993236055418473

Columns 11 through 15

0.519615242270663	0.519615242270663	0.519615242270663	0.519615242270663	0.519615242270663
0.993591165607320	1.004149260105172	0.988370665877917	0.984861734982142	0.995702005733156
0.993001214927641	1.004686524936421	0.988124986999114	0.984339999475561	0.996240136696415
0.913739389274929	1.084151564074174	0.982785044777465	0.905727245998889	1.075026364003496
0.992643507737546	1.004953060593996	0.991011218803034	0.983972357908910	0.996492978574476

0.993138186624451	1.002895077383809	0.984820582079342	0.984445411200674	0.994467445252917
0.993772192323553	1.003357136672223	0.989182274941633	0.985068598495057	0.994924872557815
0.990188093702459	1.002281440399238	0.988108077266897	0.981523801719035	0.993843578431852

Columns 16 through 20

0.519615242270663	0.519615242270663	0.519615242270663	0.519615242270663	0.519615242270663
0.977660836749115	0.978617312563196	0.986823425073168	0.992224898025291	0.985704137055679
0.977443155288391	0.978159043264200	0.987354639837057	0.991978368040344	0.985286387253322
0.972125656750933	0.899991840356001	1.065444108702010	0.986641875427290	0.906519285428388
0.980243366587049	0.977779407914494	0.987608273876191	0.994971252878234	0.984896549544245
0.974152251258046	0.978248121651790	0.985593955195435	0.988680759542683	0.985370550723241
0.978453948437684	0.978864620805621	0.986054762109929	0.993066209136530	0.985994520373569
0.977388783749161	0.975323761429077	0.984980951567182	0.992021357503663	0.982406020712113

Columns 21 through 25

0.519615242270663	0.519615242270663	0.519615242270663	0.519615242270663	0.519615242270663
0.997299353667174	0.997268428597674	0.993688097910569	1.004646774701890	0.984788157767225
0.997884876319653	0.997006268945573	0.993272620733612	1.005242918589783	0.984557904588510
1.076730975075736	0.991666782433018	0.913865763473884	1.084659599687772	0.979247243250650
0.998071877237942	1.000065307586031	0.992878603742844	1.005424884911979	0.987531991547514
0.996121674113847	0.993709948733477	0.993359091875627	1.003472036262334	0.981276258014401
0.996524413189567	0.998125595030394	0.993988346986062	1.003864150420014	0.985632613089207
0.995421581658047	0.997083850549022	0.990365685529594	1.002753572217760	0.984600290915967

Columns 26 through 30

0.519615242270663	0.519615242270663	0.519615242270663	0.519615242270663	0.519615242270663
0.981642324067977	0.993125094862156	0.995753615433954	0.992901852148437	1.003986355336612
0.981226550233263	0.993718765877305	0.995407102775537	0.992398468136375	1.004582675423317

0.902782475402115	1.072222492579084	0.990046943862946	0.913083132491797	1.084016142344920
0.980836313709294	0.993891134458859	0.998373403730078	0.991930159781203	1.004808058508446
0.981311668535642	0.991959517795905	0.992210833310030	0.992583184015323	1.002736041648692
0.981931462059344	0.992351651848580	0.996625826533279	0.993122049975534	1.003154678412485
0.978355557728010	0.991253462406965	0.995461901761886	0.989427647199549	1.002103580696755

Columns 31 through 35

0.519615242270663	0.519615242270663	0.519615242270663	0.519615242270663	0.519615242270663
0.968028520661296	0.965193688123971	0.978874302289759	0.995868994095510	0.991158778044849
0.967840047476162	0.964785510506602	0.979466285461301	0.995603375310258	0.990743621838315
0.962568230933339	0.887650128783409	1.056839126882891	0.990272969327213	0.911538822728009
0.970697148321935	0.964398611426989	0.979625878107336	0.998658158423029	0.990348728392515
0.964578949179548	0.964868748127938	0.977721360581790	0.992315388916188	0.990831724937509
0.968854188242542	0.965476918737738	0.978111576579875	0.996724936148088	0.991457685252005
0.967833660854037	0.961958967707127	0.977029361817620	0.995682177993613	0.987842196913369

Columns 36 through 40

0.519615242270663	0.519615242270663	0.519615242270663	0.519615242270663	0.519615242270663
1.004977658492324	0.985971976976335	0.982508458444008	0.993680136961871	0.995295306850905
1.005613815222356	0.985712534737484	0.982096612497339	0.994276139920771	0.994963360550605
1.085038593958350	0.980426550707835	0.903583402798055	1.072821679533598	0.989614919250745
1.005761795770749	0.988734197266630	0.981704184599751	0.994452927548298	0.997999546821644
1.003818487594566	0.982451241191804	0.982183422638004	0.992519382219434	0.991776004611392
1.004182009407146	0.986818991615036	0.982804535319774	0.992905082221494	0.996173843898376
1.003071111638927	0.985787827799282	0.979220510010588	0.991809468654159	0.995065550061951

Columns 41 through 45

0.519615242270663	0.519615242270663	0.519615242270663	0.519615242270663	0.519615242270663
0.991554874037999	1.003043835839854	0.995251174236017	0.991682954212575	1.003121505658313
0.991076399869162	1.003680607808437	0.994930319005458	0.991230573774187	1.003756499399236
0.911856068276963	1.083002002810376	0.989587559448756	0.911990267365688	1.083071695117145
0.990612169045873	1.003858066858691	0.997966560396126	0.990781564509166	1.003926293275040
0.991248528020352	1.001832285998456	0.991722198526306	0.991379312394021	1.001924796353326
0.991792061877753	1.002215940114808	0.996124907284082	0.991941976483453	1.002305019690299
0.988107480161911	1.001145518394650	0.995026336632214	0.988273320792370	1.001222045556062

5. **Output Voltages in p.u. of load buses (0.4kV) obtained from matlab after application of DVR in optimal locations during SLG fault**

Columns 1 through 5

0.519615242270663	0.519615242270663	0.519615242270663	0.519615242270663	0.519615242270663
0.999036983755894	0.995800299193566	1.006196761971451	0.987757321662850	0.985941661543499
0.998779916904186	0.995388079423548	1.006793663006801	0.987497172452190	0.985315962777656
0.914762546916125	1.001396582634666	1.080674041723657	0.904345467772758	0.990961371477046
0.998139208159983	0.994319712485242	1.005672345707006	0.986798865477408	0.984370277736729
0.997505434078897	0.994534194011411	1.002726274812218	0.986188314291330	0.984603561661639
0.996779057035996	0.993617804198992	1.004313381888218	0.985288673557428	0.983561324442408
0.995702684267187	0.991692140946708	1.002439395130869	0.984440891572397	0.981872415021923

Columns 6 through 10

0.519615242270663	0.519615242270663	0.519615242270663	0.519615242270663	0.519615242270663
0.993076176915396	0.997037845237848	0.994020034645856	1.004312466377469	0.993473261565005

0.993548328665493	0.996782607567762	0.993581525701624	1.004898502801644	0.993218623049265
1.066423034748654	0.912916831842572	0.999528430311758	1.078633206943648	0.909632997565098
0.992543690482697	0.996128896539928	0.992526937008258	1.003787887116665	0.992548540445094
0.989632909985338	0.995500859511266	0.992744095200432	1.000849057468204	0.991927341031344
0.991253946730324	0.994749302678935	0.991811083098743	1.002435311507018	0.991138058744860
0.989384199228353	0.993708461877060	0.989922144331195	1.000565794615240	0.990151021734217

Columns 11 through 15

0.519615242270663	0.519615242270663	0.519615242270663	0.519615242270663	0.519615242270663
0.993591165607320	1.004149260105172	0.988370665877917	0.984861734982142	0.995702005733156
0.993001214927641	1.004686524936421	0.988124986999114	0.984339999475561	0.996240136696415
0.998776570530247	1.078388983933267	0.904944158952533	0.990084052042023	1.069326514497505
0.992087550865886	1.003607398192455	0.987427884700442	0.983328335115617	0.995178317581036
0.992289955200614	1.000671464021919	0.986816207629402	0.983557996307483	0.992261588136088
0.991255604928108	1.002290995878884	0.986004910482412	0.982577065068061	0.993855944537060
0.989489674446534	1.000407822282637	0.985062523659662	0.980805695071121	0.991994698782447

Columns 16 through 20

0.519615242270663	0.519615242270663	0.519615242270663	0.519615242270663	0.519615242270663
0.977660836749115	0.978617312563196	0.986823425073168	0.992224898025291	0.985704137055679
0.977443155288391	0.978159043264200	0.987354639837057	0.991978368040344	0.985286387253322
0.895124567395117	0.983896832064063	1.059785736939589	0.908505881204077	0.991170797815137
0.976698362563498	0.977114774869687	0.986305503787693	0.991315408248043	0.984228582634572
0.976101462532976	0.977344088512423	0.983414682497365	0.990690798088646	0.984446869381056
0.975297087393379	0.976395115557481	0.984995462379996	0.989943313295756	0.983523567713845
0.974388723743210	0.974599880261666	0.983152531516598	0.988912038279344	0.981649571694617

Columns 21 through 25

0.519615242270663	0.519615242270663	0.519615242270663	0.519615242270663	0.519615242270663
0.997299353667174	0.997268428597674	0.993688097910569	1.004646774701890	0.984788157767225
0.997884876319653	0.997006268945573	0.993272620733612	1.005242918589783	0.984557904588510
1.071102930969008	0.913137555119719	0.999254112024355	1.079002284958030	0.901703912042063
0.996776127178988	0.996381132059566	0.992217567817826	1.004118034881289	0.983891010176335
0.993858467404827	0.995745309762930	0.992426536146621	1.001180821401616	0.983266961705651
0.995436274319326	0.995009291256006	0.991507216754689	1.002766497444658	0.982545009091916
0.993579647869380	0.993940737589020	0.989592719581587	1.000897578681675	0.981503148242413

Columns 26 through 30

0.519615242270663	0.519615242270663	0.519615242270663	0.519615242270663	0.519615242270663
0.981642324067977	0.993125094862156	0.995753615433954	0.992901852148437	1.003986355336612
0.981226550233263	0.993718765877305	0.995407102775537	0.992398468136375	1.004582675423317
0.987077046410212	1.066632290147145	0.911649445002137	0.998076026362806	1.078207419543148
0.980175785882946	0.992599958831651	0.995044911767652	0.991629680325640	1.003364177103495
0.980392340868357	0.989694691473808	0.994305856576900	0.991711545419742	1.000471137511211
0.979470463061416	0.991269307873505	0.993380656627225	0.990679103719720	1.002133245887890
0.977607640293367	0.989418273093823	0.992424356161100	0.988901789900358	1.000263549229709

Columns 31 through 35

0.519615242270663	0.519615242270663	0.519615242270663	0.519615242270663	0.519615242270663
0.968028520661296	0.965193688123971	0.978874302289759	0.995868994095510	0.991158778044849
0.967840047476162	0.964785510506602	0.979466285461301	0.995603375310258	0.990743621838315

0.886347282222793	0.970483220534515	1.051333829456485	0.911853545900891	0.996706426839714
0.967116877118490	0.963741466120400	0.978352934872479	0.994987695799530	0.989696936418663
0.966509189589558	0.963965621567470	0.975487261461744	0.994350444078940	0.989902419902507
0.965802753025834	0.963047218654009	0.977048601189442	0.993610234972580	0.988984253351167
0.964800501165065	0.961239131776516	0.975219468563212	0.992545836813256	0.987075488346057

Columns 36 through 40

0.519615242270663	0.519615242270663	0.519615242270663	0.519615242270663	0.519615242270663
1.004977658492324	0.985971976976335	0.982508458444008	0.993680136961871	0.995295306850905
1.005613815222356	0.985712534737484	0.982096612497339	0.994276139920771	0.994963360550605
1.079368042452150	0.902791806212456	0.988007751564711	1.067231326674891	0.911250997827815
1.004413197152948	0.985095785936875	0.981058988383937	0.993154139114057	0.994583416149420
1.001494137555037	0.984462027936561	0.981262530926674	0.990247524986931	0.993853519655590
1.003100226714511	0.983738125937752	0.980352837991366	0.991823792936437	0.993011599363895
1.001238346482788	0.982679524196029	0.978460107440418	0.989972475952903	0.991982151565516

Columns 41 through 45

0.519615242270663	0.519615242270663	0.519615242270663	0.519615242270663	0.519615242270663
0.991554874037999	1.003043835839854	0.995251174236017	0.991682954212575	1.003121505658313
0.991076399869162	1.003680607808437	0.994930319005458	0.991230573774187	1.003756499399236
0.996790971838088	1.077230606060165	0.911225225155666	0.997019605584679	1.077331267739795
0.990267220264967	1.002413987672870	0.994505845442842	0.990351864335597	1.002512716239252
0.990361051766917	0.999529859230724	0.993793801241739	0.990473648771095	0.999618543279238
0.989355233945749	1.001189557680677	0.992966623953469	0.989499573162266	1.001262475110689
0.987553708056509	0.999330072312514	0.991934894690813	0.987661538100935	0.999402269025765

C.2 Over-Loading

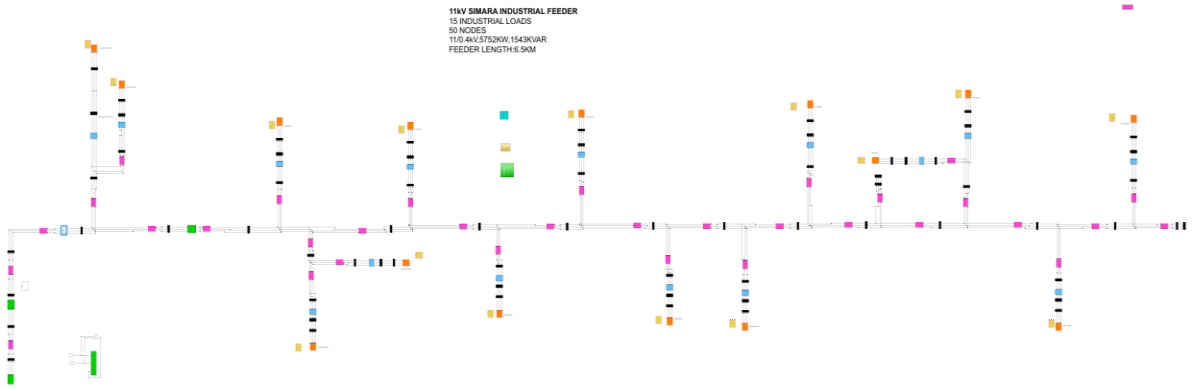

Bus no.	Load	
	Real Power kW	Reactive Power kVAR
7	266	172.89
9	463	108.6
13	556	215.52
16	70	6.36
18	390	84.78
21	30.75	11.35
24	534	91.6
27	286	4
30	606	120.77
33	368	3
36	545	577.62
42	598.5	12
43	1.57	8.4

46	124.2	2
49	214	1

Table 1: Voltage profiles load buses of simara without and with DVR in overloading at Branch 3-4 .Total simulation time 0.7sec

Busno	Voltage in p.u	
	WithoutDVR	WithDVR
7	0.8464	0.978
9	0.862	1.003
13	0.8825	0.9899
16	0.8765	0.988
18	0.8628	0.990
21	0.8809	0.985
24	0.8914	1.0008
27	0.8859	0.986
30	0.8796	0.982
33	0.8795	0.985
36	0.8836	0.996
42	0.8866	0.9923
43	0.8774	0.996
46	0.8846	0.9921
49	0.8549	0.9920

Table 2: Results of simara feeder During Overload Condition

Description	**Real power loss at bus 5 (kW)**	**Reactive power loss at bus 5 (kVAr)**	**Minimum voltage (p.u.)**	**No. of Buses with Under voltage**	**Rating of DVR**
Before DVR installation	2727.93	641.408	0.8464	48	0
After DVR Installation at branch 4-5	23.34	7.1	0.978	2	2600 kVA

Feeder connected load: P=5752kW,Q=1543kW

Real Power(P) and Reactive Power(Q) at bus 5 at overloading condition: 3024.07kW,901.5927kVar

Real Power(P) and Reactive Power(Q) at bus 5 at after installation of DVR: 5728.66kW,1535.9kW

1. **Output Voltages in p.u. of load buses (0.4kV) obtained from matlab after application of Dvr in optimal locations during Normal Loading Conditions.**

Columns 1 through 11

0.4619	0.4619	0.4619	0.4619	0.4619	0.4619	0.4619	0.4619	0.4619	0.4619	0.4619
0.8586	0.8519	0.8628	0.8855	0.8792	0.8889	0.8915	0.8846	0.8962	0.8867	0.8836
0.8503	0.8447	0.8536	0.8770	0.8717	0.8795	0.8828	0.8767	0.8867	0.8782	0.8759
0.8553	0.8474	0.8566	0.8821	0.8745	0.8825	0.8878	0.8796	0.8898	0.8833	0.8788
0.8534	0.8451	0.8533	0.8802	0.8722	0.8792	0.8859	0.8772	0.8864	0.8814	0.8764
0.8535	0.8464	0.8546	0.8803	0.8734	0.8805	0.8860	0.8786	0.8877	0.8815	0.8776
0.8521	0.8460	0.8549	0.8788	0.8731	0.8809	0.8846	0.8782	0.8881	0.8800	0.8773
0.8512	0.8444	0.8534	0.8779	0.8714	0.8793	0.8836	0.8765	0.8866	0.8791	0.8756

Columns 12 through 22

0.4619	0.4619	0.4619	0.4619	0.4619	0.4619	0.4619	0.4619	0.4619	0.4619	0.4619
0.8945	0.8833	0.8759	0.8876	0.8731	0.8699	0.8796	0.8840	0.8739	0.8868	0.8847
0.8851	0.8748	0.8684	0.8782	0.8648	0.8623	0.8703	0.8754	0.8663	0.8774	0.8760
0.8881	0.8799	0.8712	0.8812	0.8698	0.8651	0.8733	0.8806	0.8692	0.8804	0.8813
0.8847	0.8780	0.8689	0.8778	0.8679	0.8628	0.8700	0.8787	0.8669	0.8771	0.8795
0.8860	0.8781	0.8701	0.8791	0.8680	0.8641	0.8713	0.8787	0.8681	0.8784	0.8794
0.8864	0.8766	0.8698	0.8796	0.8665	0.8637	0.8717	0.8773	0.8677	0.8788	0.8780
0.8849	0.8757	0.8681	0.8780	0.8656	0.8621	0.8702	0.8764	0.8661	0.8773	0.8770

Columns 23 through 33

0.4619	0.4619	0.4619	0.4619	0.4619	0.4619	0.4619	0.4619	0.4619	0.4619	0.4619

0.8775	0.8898	0.8751	0.8681	0.8807	0.8856	0.8785	0.8904	0.8620	0.8552	0.8695
0.8700	0.8806	0.8668	0.8607	0.8714	0.8769	0.8709	0.8812	0.8536	0.8478	0.8602
0.8730	0.8835	0.8719	0.8636	0.8744	0.8821	0.8739	0.8841	0.8586	0.8506	0.8632
0.8707	0.8801	0.8700	0.8613	0.8711	0.8802	0.8715	0.8807	0.8567	0.8483	0.8600
0.8716	0.8813	0.8700	0.8624	0.8724	0.8802	0.8726	0.8819	0.8568	0.8495	0.8612
0.8714	0.8818	0.8686	0.8621	0.8728	0.8788	0.8723	0.8824	0.8554	0.8492	0.8616
0.8697	0.8803	0.8677	0.8605	0.8713	0.8778	0.8706	0.8809	0.8545	0.8475	0.8601

Columns 34 through 44

0.4619	0.4619	0.4619	0.4619	0.4619	0.4619	0.4619	0.4619	0.4619	0.4619	0.4619
0.8857	0.8773	0.8916	0.8783	0.8711	0.8830	0.8866	0.8790	0.8913	0.8866	0.8792
0.8770	0.8696	0.8823	0.8696	0.8632	0.8736	0.8778	0.8713	0.8820	0.8778	0.8714
0.8821	0.8725	0.8853	0.8746	0.8660	0.8767	0.8829	0.8741	0.8850	0.8829	0.8742
0.8802	0.8701	0.8819	0.8727	0.8637	0.8733	0.8810	0.8718	0.8816	0.8810	0.8718
0.8803	0.8713	0.8832	0.8728	0.8650	0.8746	0.8811	0.8730	0.8829	0.8811	0.8731
0.8789	0.8710	0.8836	0.8714	0.8647	0.8750	0.8797	0.8727	0.8833	0.8797	0.8728
0.8778	0.8693	0.8821	0.8705	0.8630	0.8735	0.8787	0.8709	0.8818	0.8787	0.8711

Column 45

0.4619
0.8914
0.8820
0.8850
0.8817
0.8829
0.8834
0.8818

2. **Output Voltages in p.u. of load buses (0.4kV) obtained from matlab after application of Dvr in optimal locations during OverLoading Conditions.**

Columns 1 through 5

0.519615242270663	0.519615242270663	0.519615242270663	0.519615242270663	0.519615242270663
0.958337055994112	0.941348200164612	0.942628491056065	0.988425012024178	0.971448057015390
0.961002738459608	0.943081485183710	0.942971500692470	0.991126606536670	0.973126807877502
0.962126151352591	0.941836803285773	0.942286568110837	0.992257622955322	0.971774928634237
0.962974529796910	0.946616460350282	0.949479525558297	0.993074739338321	0.976743351196399
0.966270769926574	0.946995062178042	0.947994027219260	0.996488955920504	0.977238946232248
0.966682498536397	0.952057457373641	0.951596661532099	0.997070424160037	0.982715146374757
0.960750573922218	0.944365206064857	0.946445024912248	0.990860328933116	0.974496456121180

Columns 6 through 10

0.519615242270663	0.519615242270663	0.519615242270663	0.519615242270663	0.519615242270663
0.971178264957562	0.995731361580536	0.977971596752388	0.979883769164902	0.990308813742439
0.971522621717151	0.998360772125441	0.979609718603568	0.980248710254724	0.992942241159396
0.970860163488662	0.999674375062202	0.978356360671976	0.979573638042888	0.994102855829981
0.978348399421026	1.000700551815061	0.983491423349614	0.987022800880261	0.994765427973359
0.976765322243075	1.003879347637729	0.983692964092410	0.985474462909895	0.998299366864825
0.980479151247008	1.004545716654692	0.989239442948537	0.989221629521670	0.998964776178047
0.975223399474057	0.998344282536260	0.981003586863282	0.983895906670301	0.992633701749890

Columns 11 through 15

0.519615242270663	0.519615242270663	0.519615242270663	0.519615242270663	0.519615242270663
0.976740103586612	0.977608252576908	0.986435876779542	0.968247004396905	0.970072411834659

0.978193917724759	0.977971126344271	0.989120258303221	0.969919482890324	0.970410794800470
0.977043128873614	0.977352023274691	0.990261689269030	0.968578477480405	0.969761506162590
0.981802162903243	0.985055840018728	0.991077301317682	0.973535295773131	0.977290201286239
0.982471276978588	0.983354425206023	0.994477556995925	0.974016662443893	0.975679569145850
0.988261217016160	0.987156869372685	0.995069526366143	0.979466240935082	0.979402358972385
0.979722494914540	0.981897164797720	0.988866913994984	0.971284625701042	0.974160850998017

Columns 16 through 20

0.519615242270663	0.519615242270663	0.519615242270663	0.519615242270663	0.519615242270663
0.975255469877229	0.961690288175257	0.961618968561513	0.987467469863941	0.966234175102005
0.977941826838904	0.963366568502346	0.961969026404697	0.990092222079488	0.967877030042866
0.979055102582066	0.962095150626092	0.961303614567716	0.991260267686428	0.966546350328137
0.979882277119403	0.967058183891976	0.968691673165280	0.991949774099885	0.971454316900554
0.983251092271781	0.967397714448710	0.967141064595433	0.995443889711665	0.971987742211022
0.983762838082078	0.972733480710224	0.970809803695982	0.996106627598354	0.977473747335847
0.977681010486167	0.964713831105839	0.965603952656305	0.989807382732266	0.969256384440240

Columns 21 through 25

0.519615242270663	0.519615242270663	0.519615242270663	0.519615242270663	0.519615242270663
0.969461182376053	0.988707640443013	0.970936331146162	0.972885377846848	0.977928136001047
0.969802518976469	0.991031142013947	0.972061974257569	0.973285576555824	0.980598521222745
0.969154064677393	0.992376856154800	0.971199723684959	0.972720965183682	0.981686236333042
0.976676696519852	0.992566158324656	0.975412082600111	0.980539647792136	0.982399404107312
0.975066439227751	0.996459611301717	0.976644907195578	0.978757439165667	0.985874589639611
0.978790909279679	0.997266817173617	0.982649345841117	0.982581256549659	0.986451945148993
0.973551003414208	0.990705026061959	0.973843972379048	0.977394876104723	0.980266150341969

Columns 26 through 30

0.519615242270663	0.519615242270663	0.519615242270663	0.519615242270663	0.519615242270663
0.960250637942588	0.963122500975995	0.989692151054810	0.972135432779457	0.973706695165346
0.961897459479116	0.963459911011426	0.991983580593207	0.973157916580286	0.974131058867699
0.960553133773843	0.962818253240734	0.993414621091771	0.972406992309311	0.973534574751363
0.965391380570669	0.970309861705562	0.993747514293962	0.976642209147020	0.981299791222147
0.966001274996060	0.968702644886960	0.997482187345367	0.977787944938198	0.979567468988351
0.971429817633165	0.972399529986175	0.998302130241146	0.983774442356126	0.983367093996756
0.963267425515905	0.967201796653424	0.991791156345382	0.974978527705602	0.978167566119518

Columns 31 through 35

0.519615242270663	0.519615242270663	0.519615242270663	0.519615242270663	0.519615242270663
0.964016570300716	0.946837737886033	0.951870250520624	0.989875188030014	0.970559613930990
0.966581642569098	0.948438035402334	0.952219950051015	0.992207694272458	0.971905362162647
0.967841659558143	0.947257761962087	0.951544774239951	0.993676126632528	0.970871696025470
0.968761275493742	0.952133816753398	0.958809325171533	0.994256016850978	0.975553565444650
0.971932670476495	0.952398240503598	0.957303278137808	0.997753171315705	0.976214886823491
0.972511121096994	0.957713110535139	0.960957763581061	0.998552087805141	0.981993643677452
0.966485548927800	0.949790728659649	0.955748085470336	0.992152276458277	0.973481802236446

Columns 36 through 40

0.519615242270663	0.519615242270663	0.519615242270663	0.519615242270663	0.519615242270663
0.975329230765236	0.981283070376178	0.963308156977798	0.965898173966212	0.990736730401110
0.975755544232961	0.983835301883127	0.964872805357211	0.966263013512533	0.993154082437617

0.975100623564667	0.985172682418188	0.963682291828320	0.965594275260057	0.994603452796040
0.982720157786128	0.986172404345394	0.968716749763917	0.972955303102960	0.995382502711800
0.981090092926066	0.989294374275414	0.968915311529001	0.971422048041445	0.998710523385217
0.984846921479918	0.989990672621581	0.974431508484257	0.975126013271109	0.999474238550665
0.979606084548402	0.983848213042910	0.966272983616234	0.969863989604058	0.993165878613850

Columns 41 through 45

0.519615242270663	0.519615242270663	0.519615242270663	0.519615242270663	0.519615242270663
0.972503757240086	0.975011514610281	0.990667406322000	0.972554118328615	0.975093714092697
0.973783077917958	0.975416984185541	0.993113072678699	0.973913900375008	0.975492070449817
0.972823264057514	0.974745965473241	0.994542626452141	0.972888502759586	0.974819483220444
0.977536773051908	0.982268105931575	0.995361709910328	0.977705024281253	0.982318076669570
0.978118916958073	0.980685005817682	0.998658427098756	0.978179204422951	0.980744960195975
0.983857755094359	0.984424578512441	0.999411878670926	0.983871283553014	0.984482064850302
0.975382335544525	0.979161316064320	0.993123611406150	0.975461316683991	0.979211691707549

APPENDIX D: PR CONTROLLER SOURCE CODE

```
close all
clear all
clc
format long

%Sampling Paramters
fa = 2000; %Sampling frequency in Hz
Ta = 1/fa;  %Samping period
wa = 2*pi*fa; %Sampling angular frequency

%Grid-Connected Inverter and System Parameters
Linv = 10e-3; %Output filter inductor [H]
Rinv = 0.5e-3; %Output filter resistance [ohm]
Vdc = 220; %Total DC-Link Voltage [V]
Vp = 480; %Peak voltage of the grid [V]
fg = 60; %Grid frequency [Hz]
wg = 2*pi*fg; %Angular grid frequency [rad/s]
Hi = 1/10; %Current sensor gain [A/A]
fsw = 30e3; %Switching frequency [Hz]
Pnom = 1000; %Inverter nominal power [W]

%Desired Parameters of the Proportional-Resonant Controller
fr = 60; %Desired resonant frequency [Hz]
wr = 2*pi*fr; %Desired resonant angular frequency [rad/s]
qsi = 0.95; %Damping factor
Bs = 1.5; %Desired resonant frequency bandwidth [Hz]
Br = 2*pi*Bs; %Desired resonant angular frequency bandwidth [rad/s]

%Design of the proportional and resonant gains
alpha = 2*qsi + 1;
Kp =……; %Desgined proportional gain
Ki =……; %Deesigned resonant gain

%Design of the resonant filter
kr = 1; %Gain of the resonant filter - not including the Ki
Cte =……; %Defined constant for simplicity

b0 = kr*Br*Ta;
b1 = (-kr*Br*(exp(-0.5*Br*Ta))*cos(Ta*sqrt((wr^2)-0.25*(Br^2)))-Cte)*Ta;
b2 = 0;

a0 = 1;
a1 = -2*(exp(-0.5*Br*Ta))*cos(Ta*sqrt((wr^2)-0.25*(Br^2)));
a2 = exp(-Br*Ta);

b = [b0,b1,b2];
a = [a0,a1,a2];

TFz = tf(b,a,fa); %Defining the transfer function in z-domina
s = tf('s');
z = (2+Ta*s)/(2-Ta*s); %Bilinear transformation for mapping z-domain in w-domain
```

```
TFw = (b0 + b1*z^-1 + b2*z^-2)/(a0 + a1*z^-1 + a2*z^-2); %Transfer function in w-domain
TFPRw = TFw*Ki+Kp;

opts = bodeoptions('cstprefs');
opts.FreqUnits = 'Hz';
figure
bode(TFw,opts)
title('Frequency response in w-domain of the resonant part');
grid


figure
bode(TFPRw,opts)
title('Frequency response in w-domain of the PR controller');
grid

%Desired Parameters of the Proportional-Resonant Controller for the second
%resonant part - subscript 2 means second controller

fr2 = 300; %Desired resonant frequency [Hz]
wr2 = 2*pi*fr2; %Desired resonant angular frequency [rad/s]
qsi2 = 0.95; %Damping factor
Bs2 = 1.5; %Desired resonant frequency bandwidth [Hz]
Br2 = 2*pi*Bs2; %Desired resonant angular frequency bandwidth [rad/s]

%Design of the proportional and resonant gains
alpha2 = 2*qsi2 + 1;
Kp2 =……..; %Desgined proportional gain
Ki2 =……..; %Deesigned resonant gain

%Design of the resonant filter
kr2 = 1; %Gain of the resonant filter - not including the Ki
Cte2 =……..; %Defined constant for simplicity

b02 = kr2*Br2*Ta;
b12= (-kr2*Br2*(exp(-0.5*Br2*Ta))*cos(Ta*sqrt((wr2^2)-0.25*(Br2^2)))-Cte2)*Ta;
b22 = 0;

a02 = 1;
a12 = -2*(exp(-0.5*Br2*Ta))*cos(Ta*sqrt((wr2^2)-0.25*(Br2^2)));
a22 = exp(-Br2*Ta);

b2 = [b02,b12,b22];
a2 = [a02,a12,a22];

TFz2 = tf(b2,a2,fa); %Defining the transfer function in z-domina

TFw2 = (b02 + b12*z^-1 + b22*z^-2)/(a02 + a12*z^-1 + a22*z^-2); %Transfer function in w-domain
TFPRw2 = TFw2*Ki2+Kp2;

TF = TFw + TFw2;

figure
bode(TF,opts)
title('Frequency response in w-domain of the resonant parts combined');
```

```
grid

open_system(['TestIEEE13working.slx'])
```

APPENDIX E: OPTIMAL LOCATION SOURCE CODE AND CALCULATED SARFI VALUES ALL THREE TEST SYSTEMS.

```
% Load the Simulink model
simulink_model = 'simarafeederdvrbalanced';
open_system(simulink_model);

% Define candidate locations for placing the DVR (bus numbers)
candidate_locations = [14,15,10,19,12,23,34,39,44,49,54,66,63,70,75]; % Example bus numbers, modify as needed
voltage_locations=[v10,v12,v18,v25,v22,v30,v35,v40,v45,v50,v55,v65,v67,v72,v77];
% Initialize variables to store SARFI values and optimal location
optimal_location = [];
min_sarfi = inf;

% Initialize a vector to store SARFI values for each location
sarfi_values = zeros(size(candidate_locations));
% Simulate the system for each candidate location
for i = 1:length(candidate_locations)
    % Set the DVR location in the model
    dvr_location = candidate_locations(i);
     set_param([simulink_model '/DVR'],'location',[_,_,_,_]);
    % Simulate the model
    sim_time = 0.7; % Simulation time in seconds
    simout = sim(simulink_model, 'stoptime', num2str(sim_time));

    % Extract voltage data from simulation results
    voltage_data(i) =voltage_locations(i) ;
    rmsVoltages(i) = sqrt(mean(voltage_data.^2));

    % Calculate SARFI for the current location
    sag_indices = rmsVoltages(i) < 207; % Define voltage sag threshold
    swell_indices = rmsVoltages(i) > 253; % Define voltage swell threshold
    sarfi = ((sum(sag_indices) + sum(swell_indices)) / (numload)); % Modify the frequency deviation term as needed

    % Store the calculated SARFI value
    sarfi_values(i) = 100*sarfi;

    % Check if the current SARFI is the lowest
    if sarfi < min_sarfi
        min_sarfi = sarfi;
        optimal_location = dvr_location;
    end
     set_param([simulink_model '/DVR'],'location',[_,_,_,_);
end

% Display SARFI values at each location
for i = 1:length(candidate_locations)
    disp(['SARFI at Bus ' num2str(candidate_locations(i)) ': ' num2str(sarfi_values(i))]);
end

% Display optimal location and minimum SARFI value
disp(['Optimal DVR Location: Bus ' num2str(optimal_location)]);
disp(['Minimum SARFI Value: ' num2str(100*min_sarfi)]);
% Plot DVR location vs SARFI values
```

```
figure;
plot(candidate_locations, sarfi_values, 'bo-', 'LineWidth', 2);
bar(candidate_locations, sarfi_values, 0.5, 'b');
xlabel('DVR Location (Bus Number)');
ylabel('SARFI Value (%)');
title('DVR Location vs SARFI');
grid on;

% Highlight the optimal location on the plot
hold on;
plot(optimal_location, 100*min_sarfi, 'ro', 'MarkerSize', 10, 'MarkerFaceColor', 'r');
hold off;
legend('SARFI Values', 'Optimal Location', 'Location', 'Best');
```

Busno	SARFI VALUES – IEEE 13 NODE TEST SYSYTEM
611	8.33
632	7.14
633	6.66
634	7.69
645	8.33
646	12.5
650	11.11
652	9.09
671	10
675	6.67
680	7.14
684	2.22
692	10

Busno	SARFI VALUES – SIMARA FEEDER
1	14.52
2	13.6
3	13.66
4	10.77
5	8.2
6	11.5
8	11.89
10	10.09
11	10.8
12	9.11
14	10.4
17	11.14
19	9.42
20	9.5
22	10.3
23	9.99
25	11.2
26	10.6
28	13.66
29	10.77
31	11.2
32	12.5
34	11.69
35	10.99
37	10.55
38	12.11
39	11.4
40	12.14
41	10.42
44	9.85
45	10.43
47	12.99
48	11.35
50	10.6

Busno	SARFI VALUES - TANAHUSUR FEEDER
1	9.52
2	8.6
3	7.66
4	7.77
5	7.2
15	8.5
16	9.89
7	6.09
14	10
18	9.66
8	8.14
9	9.22
10	8.5
11	8.3
12	7.99

The Optimal Placement of a Photovoltaic-integrated Dynamic Voltage Restorer for the enhancement of Power Quality within the Distribution System. A Case Study of 11kV Tanahusur Radial Distribution Feeder and 11kV Simara Industrial Feeder

ORIGINALITY REPORT

19%
SIMILARITY INDEX

PRIMARY SOURCES

1	ethesis.nitrkl.ac.in Internet	181 words — 1%
2	dspace.unza.zm Internet	164 words — 1%
3	Viswaprakash Babu, Dr K. Shafeeque Ahmed, Dr Y. Mohamed Shuaib, Dr.M. Manikandan. "Power Quality Enhancement using Dynamic Voltage Restorer (DVR) Based Predictive Space Vector Transformation (PSVT) with Proportional Resonant (PR)-controller", IEEE Access, 2021 Crossref	140 words — 1%
4	research.ijcaonline.org Internet	136 words — 1%
5	journals.pen2print.org Internet	110 words — 1%
6	Lakshmi Lakshmi Kumari, Uma Vani Uma Vani. "Dynamic Voltage Restorer for Sag and Swell Issues in Power System", Indonesian Journal of Electrical Engineering and Computer Science, 2018	109 words — 1%

"Adaptive fuzzy gain scheduling PID controller for maximum power point tracking of photovoltaic system", Renewable Energy, 2013.
Crossref

125 P. Jayaprakash. "Current mode control of Dynamic Voltage restorer for power quality improvement in distribution system", 2008 IEEE 2nd International Power and Energy Conference, 12/2008 — 6 words — < 1%
Crossref

126 epdf.pub — 6 words — < 1%
Internet

127 trace.tennessee.edu — 6 words — < 1%
Internet

128 umpir.ump.edu.my — 6 words — < 1%
Internet

129 www.freepatentsonline.com — 6 words — < 1%
Internet

EXCLUDE QUOTES	ON	EXCLUDE SOURCES	OFF
EXCLUDE BIBLIOGRAPHY	ON	EXCLUDE MATCHES	< 6 WORDS

Gmail **prabin dhakal <prbndhkl@gmail.com>**

Paper for publication

jacem advanced <jacem@acem.edu.np> Mon, Nov 20, 2023 at 10:56 AM
To: prabin dhakal <prbndhkl@gmail.com>

Dear Author
Your Journal Paper titled “
The Optimal Placement of a Photovoltaic-integrated Dynamic Voltage Restorer for the Enhancement of Power Quality within the Distribution System: A case Study of 11kV Simara Industrial feeder in Nepal
”has been accepted for the Journal of Advanced College of Engineering and Management (JACEM) for Vol.9, 2024. However, there are some minor changes that need to be done. Please look at the website for the format. We will contact you for further changes.
Regards,
Prem Chandra Roy
Editor-In-Chief
9851198671
Laxmi Prasad Bhatt
Editorial Board
9848811288
jacem

[Quoted text hidden]